Distribution Agreement

In presenting this thesis or dissertation as a partial fulfillment of the requirements for an advanced degree from Emory University, I hereby grant to Emory University and its agents the non-exclusive license to archive, make accessible, and display my thesis or dissertation in whole or in part in all forms of media, now or hereafter known, including display on the world wide web. I understand that I may select some access restrictions as part of the online submission of this thesis or dissertation. I retain all ownership rights to the copyright of the thesis or dissertation. I also retain the right to use in future works (such as articles or books) all or part of this thesis or dissertation.

Signature:

_____ _____

Lisa Mariko Giles Date

Molecular Pathogenesis of DYT1 Dystonia

By

Lisa Mariko Giles
Doctor of Philosophy

Graduate Division of Biological and Biomedical Science
Neuroscience Graduate Program

Lih-Shen Chin, Ph.D. Advisor	Lian Li, Ph.D. Advisor
Victor Faundez, M.D., Ph.D. Committee Member	E. Chris Muly, M.D., Ph.D. Committee Member
Yoland Smith, Ph.D. Committee Member	Bruce Wainer, M.D., Ph.D. Committee Member

Accepted:

Lisa A. Tedesco, Ph.D.
Dean of the Graduate School

Date

Molecular Pathogenesis of DYT1 Dystonia

By

Lisa Mariko Giles

B.A., Johns Hopkins University, 2002

Advisors: Lih-Shen Chin, Ph.D.

Lian Li, Ph.D.

An Abstract of

A dissertation submitted to the Faculty of the Graduate

School of Emory University in partial fulfillment

of the requirements for the degree of

Doctor of Philosophy

Graduate Division of Biomedical and Biological Sciences

Neuroscience Graduate Program

2008

Abstract

Molecular Pathogenesis of DYT1 Dystonia

By Lisa Mariko Giles

Early onset-generalized torsion dystonia (DYT1) has been linked to two mutations in the C-terminal tail of the protein torsinA. The most common mutation is a 3-bp in-frame deletion that results in the loss of one of a pair of glutamate residues at position 302 or 303 (torsinA ΔE). The second mutation, identified in a single family, is an 18-bp in-frame deletion that results in the loss of six amino acids from position 323-328 (torsinA Δ323-8). It is unclear why torsinA mutations result in a neuronal phenotype despite widespread expression in multiple tissues.

Here we report a neuronal cell-type specific nuclear envelope (NE) preference for torsinA. Further, ATP-bound and dystonia-associated mutant torsinA display an enhanced NE preference compared to WT and ATP-unbound torsinA. We find that the N-terminal portion of torsinA is sufficient for oligomerization, and that dystonia-associated mutations do not disrupt oligomerization. We also demonstrate that, while torsinA WT is a long-lived protein that is processed through the autophagy-lysosomal pathway, both dystonia-associated mutations destabilize torsinA protein and result in premature degradation through the ubiquitin proteasome pathway and the autophagy-lysosome pathway.

We conducted a yeast-two hybrid screen for torsinA-interacting proteins and identified a novel protein, which we named printor (protein interactor of torsinA). Printor co-distributes with torsinA in brain and other tissues, and exists in both cytosolic and membrane-associated pools. Printor co-localizes with torsinA at the endoplasmic reticulum (ER), however, unlike torsinA, printor shows a distinct ER preference. Printor shows reduced co-localization with ATP-bound and dystonia-associated mutant torsinA, and does not interact with ATP-bound torsinA or torsinA ΔE. Together, our findings demonstrate a neuronal cell-type specific phenotype for torsinA and implicates premature degradation as a possible mechanism for mutant torsinA loss of function. Further, our findings suggest that printor is a novel component of the DYT1 pathogenic pathway.

Molecular Pathogenesis of DYT1 Dystonia

By

Lisa Mariko Giles

B.A., Johns Hopkins University, 2002

Advisors: Lih-Shen Chin, Ph.D.

Lian Li, Ph.D.

.

A dissertation submitted to the Faculty of the Graduate

School of Emory University in partial fulfillment

of the requirements for the degree of

Doctor of Philosophy

Graduate Division of Biological and Biomedical Sciences

Neuroscience Graduate Program

2008

Acknowledgments

First and foremost, I would like to thank my advisors, Dr. Lian Li and Dr. Lih-Shen Chin. Without their patience and mentorship, I would not be where I am today. They have shaped me as a scientist and helped to hone my skills and sharpen my mind and for that I am grateful. I would also like to thank the members of my committee, Dr. Victor Faundez, Dr. Chris Muly, Dr. Yoland Smith and Dr. Bruce Wainer. They have encouraged me, provided me with insight and challenged me to be the best scientist that I could be and I have benefitted so much from their support.

I would also like to thank a multitude of fellow students and lab mates who helped me troubleshoot when things were rough and kept me sane when my sanity seemed to hang by a thread. My fellow Li lab grad students past and present, James Olzmann, Elizabeth Webber, James Lee, Brandi Whatley, Jue Chen, Sammy Lee, Jeanne McKeon, have helped me with advice, taught me techniques, and let me beg, borrow and steal equipment and especially glassware without which I never would have made it. My friends Jill Glausier, Heather Ross, Karen Rommelfanger, and Jenn Wilhelm, have kept me sane, healthy and inebriated when necessary. I would like to thank my friends outside of Emory for understanding that I did not fall off the face of the earth; I was just working trying to earn my degree.

Of course, there is my family, without whom I would not be who I am today. My parents, Tom and Hami Imboden instilled in me a desire to learn and I appreciate their support in all that I do. My sisters, Emily and Sarah have always supported my decisions and provided me with laughter and perspective when I needed it. I would also like to thank my aunts, Ginny, Edie and Connie, my grandmother, Beryle, and my uncle Ken, for coming to be with me and for supporting me and encouraging me in all that I do. I also thank my husband's family for accepting me as one of their own and for understanding the times when work came first. Finally, I would like to thank my husband Steve. His patience, understanding, love and support have helped me make it this far. I cannot imagine having been through the last four years without him by my side.

TABLE OF CONTENTS

CHAPTER III. PRINTOR, A NOVEL TORSINA-INTERACTING PROTEIN IMPLICATED IN DYSTONIA PATHOGENESIS

LIST OF FIGURES

CHAPTER I. INTRODUCTION AND BACKGROUND

CHAPTER II, DYSTONIA-ASSOCIATED MUTATIONS CAUSE PREMATURE DEGRADATION OF TORSINA PROTEIN AND CELL-TYPE SPECIFIC MISLOCATION TO THE NUCLEAR ENVELOPE

CHAPTER III. PRINTOR, A NOVEL TORSINA-INTERACTING PROTEIN IMPLICATED IN DYSTONIA PATHOGENESIS

CHAPTER IV. DISCUSSION AND CONCLUSIONS

LIST OF TABLES

CHAPTER I. INTRODUCTION AND BACKGROUND

CHAPTER I

INTRODUCTION AND BACKGROUND

Opening Remarks

Dystonia is a movement disorder characterized by involuntary movements and prolonged muscle contraction, resulting in twisting body motions, tremor, and abnormal posture (Bressman et al. 2001). The most common and severe form of dystonia, early-onset generalized torsion dystonia (DYT1), has been linked to two mutations in the protein torsinA: an in-frame 3-bp (GAG) deletion which results in the loss of a glutamate residue at position 302 or 303 (torsinA ΔE) (Ozelius et al. 1997), and an in-frame 18-bp deletion resulting in the loss of amino acids F323-Y328 (torsinA Δ323-8) (Leung et al. 2001). TorsinA has been shown to be ubiquitously expressed in multiple tissue types (Shashidharan et al. 2000), however, torsinA mutations manifest mainly as a neurological phenotype. Discerning the effects of mutations on torsinA protein behavior is fundamental to understanding the molecular mechanisms of DYT1 dystonia. Identification of differences in torsinA behavior between non-neuronal and neuronal cells is also key to understanding what makes neurons more susceptible to torsinA mutations. Although torsinA has been identified to be a member of the AAA^+ (ATPases associated with a variety of cellular activities) superfamily of ATPases (Beyer 1997; Ozelius et al. 1997; Ozelius et al. 1998), its exact function remains a mystery. A growing and important area of torsinA research has focused on identifying interacting proteins in an effort to discover potential substrates and regulators of torsinA activity, as well as to ascertain how torsinA mutations alter or disrupt the interactions.

The studies described in the following chapters explore the effect of dystonia-associated mutations on localization, oligomerization and degradation of torsinA and the

identification of a novel torsinA-interacting protein, named printor (protein interactor of torsinA), as well as the functional significance of this interaction.

Dystonia

The term dystonia covers a broad spectrum of movement disorders that are all characterized by sustained muscle contractions that produce repetitive twisting movements and abnormal postures due to concurrent contractions of agonist and antagonist muscles (de Carvalho Aguiar and Ozelius 2002; Albanese 2003; Albanese et al. 2006). Dystonia can either be genetically inherited or sporadic. There are currently 17 known genetically inherited dystonic loci that are referred to as DYT1 to DYT17 (Table I-1). Dystonias can be separated into a number of subcategories depending on the phenotype, and each genetically defined dystonia is associated with a well-characterized phenotype. The main subgroups are primary dystonia, dystonia-plus, secondary dystonia, and heredodegenerative.

Primary Dystonia

Primary dystonia refers to syndromes in which dystonia is the main phenotypic manifestation. Primary dystonias are unassociated with any prior brain injuries and are generally not responsive to levadopa treatments (de Carvalho Aguiar and Ozelius 2002; Klein and Ozelius 2002). Primary dystonias often have a genetic basis and can be further subdivided into early onset, which has a median age of onset of 9 years, and late onset, which has a median age of 45 years (de Carvalho Aguiar and Ozelius 2002; Klein and

Ozelius 2002). Early onset primary dystonias tend to be more generalized, starting in a leg or arm and spreading to other limbs and trunk, while late onset primary dystonias tend to remain more focal, especially in the upper part of the body (de Carvalho Aguiar and Ozelius 2002; Klein and Ozelius 2002). DYT1, 2, 4, 6, 7, 13 and 17 are primary forms of dystonia (Parker 1985; Gimenez-Roldan et al. 1988; Almasy et al. 1997; Leube et al. 1997; Ozelius et al. 1997; Valente et al. 2001; de Carvalho Aguiar and Ozelius 2002; Klein and Ozelius 2002). Most primary dystonias are autosomal dominant, with the exception of DYT2 and DYT 17 which are both autosomal recessive (de Carvalho Aguiar and Ozelius 2002; Klein and Ozelius 2002; Chouery et al. 2008). Although the likely genetic loci of DYT6, 7, 13 and 17 have been identified, the only primary dystonia gene that has been identified is the *DYT1* gene, which is located on 9q34 and encodes the protein torsinA (Ozelius et al. 1997; de Carvalho Aguiar and Ozelius 2002; Klein and Ozelius 2002). As of now, the genetic loci for DYT2 and DYT4 are unknown (de Carvalho Aguiar and Ozelius 2002; Klein and Ozelius 2002).

Dystonia-plus

Dystonia-plus dystonia refers to dystonias that are accompanied by other symptoms, and include DYT5, 11, 14, 15 and 16 (Zimprich et al. 2001; Han et al. 2007; Camargos et al. 2008; Wider et al. 2008). DYT5 and DYT16 are both accompanied by Parkinsonism (Zimprich et al. 2001; Camargos et al. 2008), as is DYT14, which was recently recharacterized as a novel mutation in DYT5 (Wider et al. 2008). DYT5, which is L-dopa responsive, has been linked to dominantly inherited mutations in the protein GTP Cyclohydrolase 1, which is a rate limiting enzyme in required for the synthesis of BH4, a

co-factor required for the synthesis of aromatic amino acids including tyrosine, a dopamine precursor (Rao and Cotlier 1985; Jarman et al. 1997). DYT16, which is not L-dopa responsive, has been linked to mutations in the protein PRKRA, an interferon-inducible, double stranded RNA dependent protein kinase (Camargos et al. 2008). DYT11 and DYT15 are accompanied by myoclonic jerks (Zimprich et al. 2001; Han et al. 2007). DYT11 has been linked to a loss-of-function mutations in the protein ε-sarcoglycan (Zimprich et al. 2001); however, the causative mutation for DYT15 is currently unknown.

Secondary dystonia

Secondary dystonias describe a subgroup that is associated with other brain injuries. Lesions of the putamen and thalamus can often present with dystonic symptoms. Acquired diseases, such as demyelinating and neoplastic diseases can also result in dystonic phenotypes.

Heredodegenerative dystonia

Heredodegenerative dystonias are generally associated with and secondary to other movement disorders. Parkinson's disease patients often display dyskinesias, and almost 15% of Parkinson's disease patients display focal dystonias (de Carvalho Aguiar and Ozelius 2002; Klein and Ozelius 2002). Dystonia is a frequent finding in early-onset Parkinson's patients, as well as in patients with corticobasal degeneration. Spinocerebellar ataxia type 3 is also associated with dystonic symptoms, and the severity

of the symptoms can be related to the length of the trinucleotide repeat (de Carvalho Aguiar and Ozelius 2002; Klein and Ozelius 2002).

Treatment

The current treatment options for dystonia vary based on the dystonic phenotype. For instance, patients with dopa-responsive-dystonia (DYT5) can be treated with levodopa; however levodopa does not improve most dystonias, and in some cases, can even worsen symptoms (de Carvalho Aguiar and Ozelius 2002; Klein and Ozelius 2002). In these forms of dystonia, anticholinergics, benzodiazepines, dopamine depleters and GABA-ergic drugs are often used (de Carvalho Aguiar and Ozelius 2002; Klein and Ozelius 2002). Patients with focal dystonias often respond well to focal injections of botulinum toxin (de Carvalho Aguiar and Ozelius 2002; Klein and Ozelius 2002). Generalized dystonias can be treated with deep brain stimulation or selective lesioning of the globus pallidus (de Carvalho Aguiar and Ozelius 2002; Klein and Ozelius 2002).

DYT1 and the Identification of TorsinA

Torsion dystonia is a primary dystonia characterized by sustained muscle contractions that often cause painful twisting and repetitive movements. Idiopathic torsion dystonia has been linked to at least six different autosomal genes, and each has a distinct set of symptoms (Ozelius et al. 1997). The gene DYT underlies early-onset generalized dystonia, the most severe and common form of hereditary dystonia. Symptoms general begin in an arm or leg at an early age (approximately 12 years, though the range runs

from 4 to 44) and spreads to other limbs within five years. The prevalence of DYT1 is similar in all ethnic profiles; however Ashkenazi Jews have the highest prevalence due to a founder mutation. DYT1 follows an autosomal dominant inheritance, but it has a reduced penetrance of 30-40%. The DYT1 gene has been mapped to chromosome 9q34 (Ozelius et al. 1997), and the identified protein was named torsinA.

TorsinA transcripts were analyzed to identify dystonia-linked mutations. While a number of variations were found in the coding sequence, only two mutations had an effect on the protein sequence: aspartic acid 174 to histidine (D174H) and the deletion of one of a pair of glutamic acid residues at positions 302/303 due to a GAG in frame deletion. The D174H was confirmed as a polymorphism by the presence in control samples, however, all of the DYT1 samples analyzed contained the GAG deletion (Ozelius et al. 1997). When further samples were analyzed, they found that all of the analyzed affected and unaffected gene carriers of the 64 families studied were heterozygous for the deletion, but the deletion never appeared in control samples and never appeared in the homozygous state (Ozelius et al. 1997). Allelic analysis suggested that the GAG deletion has arisen multiple times, and is not the result of a single common founder mutation (Ozelius et al. 1997).

A second mutation in the DYT1 gene was identified by Leung et al. (Leung et al. 2001) during a search for individuals that displayed both early onset dystonia and some other neurological features such as monoclonus or Parkinsonism. In one patient with early onset dystonia and myoclonic features, an 18 base pair deletion was identified near the stop codon. The deletion resulted in the loss of the amino acids between positions 323 and 328 (FTKLDY) in the carboxy terminus of torsinA. This deletion had not been

identified in over 1,800 samples from dystonic individuals or 482 controls that were analyzed by Leung et al. Analysis of the patient's family found the same deletion in the patient's brother, mother and maternal grandfather. The other family members displayed neurological features related to dystonia and myoclonus (Leung et al. 2001). It was later found that the patient, brother and father also had a mutation in the epsilon-sarcoglycan gene, which is the underlying gene for myoclonic dystonia (Klein et al. 2002). Because of this concomitant mutation, it remains to be established whether the Δ323-8 torsinA mutation contributes to the pathogenesis of dystonia.

TorsinA is expressed in a variety of tissues, including liver, heart, kidney and brain, where it is neuron specific (Shashidharan et al. 2000). It is unclear why mutations to torsinA result in a neurological disease, despite widespread expression, though one possible explanation would be that torsinA interacts with a different subset of proteins in the neuron. TorsinA also displays a widespread expression pattern in the brain, with enriched expression in the cerebral cortex, caudate-putamen, globus pallidus, hippocampal formation, thalamus, substantia nigra and molecular cell layer of the cerebellar cortex (Shashidharan et al. 2000; Konakova and Pulst 2001; Walker et al. 2001; Walker et al. 2002; Augood et al. 2003; Rostasy et al. 2003; Xiao et al. 2004), and histochemical studies reveal staining of cytoplasm, proximal processes and terminals (Shashidharan et al. 2000; Konakova and Pulst 2001; Walker et al. 2001; Walker et al. 2002; Augood et al. 2003; Rostasy et al. 2003; Xiao et al. 2004). There have been some reports of torsinA immunoreactivity in neuronal nuclei (Shashidharan et al. 2000; Walker et al. 2001; Walker et al. 2002), although that is not observed in all studies. In most studies, post-mortem examination of DYT1 positive brain tissue shows no obvious

changes in the pattern of immunoreactivity (Walker et al. 2002; Rostasy et al. 2003) at the light microscope level. However, one group identified ubiquitin and torsinA positive inclusions in brainstem nuclei of post-mortem DYT1 positive brain tissues but not controls (McNaught et al. 2004). These inclusions were associated with the nuclear envelope (NE) and were found in brainstem nuclei known to participate in motor control pathways. It is still unclear what role, if any, these inclusions play in the development of dystonia.

TorsinA is Localized to the ER

TorsinA has a 20 amino-acid endoplasmic reticulum (ER) signal sequence, that is thought to be cleaved (Hewett et al. 2003; Liu et al. 2003), followed by a 20-amino acid hydrophobic domain. Through immunocytochemical experiments and subcellular fractionation, torsinA has been shown to localize with various ER marker proteins (Kustedjo et al. 2000; O'Farrell et al. 2002; Kustedjo et al. 2003; Bragg et al. 2004; Gonzalez-Alegre and Paulson 2004; Goodchild and Dauer 2004; Naismith et al. 2004). Assessments of glycosylation (Kustedjo et al. 2003; Bragg et al. 2004) and protection from proteases (Hewett et al. 2003; Kustedjo et al. 2003) suggest that torsinA has an ER lumenal orientation. However, an intriguing finding is that a number of the identified torsinA-interacting proteins are cytoplasmic, including kinesin light chain (Kamm et al. 2004) and vimentin (Hewett et al. 2006). This suggests either that a population of torsinA on the ER faces the cytoplasm or that a cytosolic pool of torsinA exists that is able to interact with these cytosolic proteins.

TorsinA ΔE has been reported to form cytoplasmic, often perinuclear, inclusions (Hewett et al. 2000; Kustedjo et al. 2000; O'Farrell et al. 2002; Bragg et al. 2004; Bragg et al. 2004) that often co-localize with nuclear envelope (NE) marker proteins (Bragg et al. 2004; Gerace 2004; Gonzalez-Alegre and Paulson 2004; Goodchild and Dauer 2004; Naismith et al. 2004). Closer examination of these inclusions by electron microscopic analysis reveals them to include membranous structures that appear to be derived from the perinuclear membrane (Hewett et al. 2000; Gonzalez-Alegre and Paulson 2004; Misbahuddin et al. 2005). However, these inclusions are not seen in DYT1 patient tissues and it has been reported that these inclusions are only present at high levels of mutant torsinA overexpression (Bragg et al. 2004). It is therefore likely that these inclusions are artifacts of overexpression, and it is unclear whether they play any part in DYT1 pathogenesis. At lower levels of expression, torsinAΔE reportedly localizes to the NE over the ER (Kustedjo et al. 2000; Gonzalez-Alegre and Paulson 2004; Goodchild and Dauer 2004; Naismith et al. 2004) (Bragg et al. 2004; Goodchild and Dauer 2004). However, torsinA WT can be found in both ER and NE, which represent contiguous subdomains of the same membrane, and like many ER and NE proteins can move between the two subdomains with relative ease (Ellenberg et al. 1997; Goodchild and Dauer 2005). In addition, the relative ratio of visible NE and ER can vary greatly depending on the microscopic plane of focus and cell type. Because a quantitative analysis of the relative NE to ER distribution of torsinA WT and torsinA ΔE has never been performed, it is difficult to assess the significance of the reported shift in localization.

Although torsinA Δ323-8 has been reported to display a normal pattern of subcellular distribution (O'Farrell et al. 2002), this mutant form of torsinA has received little study and, therefore, not much is known about the effects of the Δ323-8 mutation.

TorsinA Belongs to the AAA$^+$ Superfamily and has Molecular Chaperone Activity

Though the specific function of torsinA is currently unknown, sequence analysis reveals torsinA to be a member of the AAA$^+$ (ATPases associated with a variety of cellular activities) superfamily of Walker type ATPases (Beyer 1997; Ozelius et al. 1997; Ozelius et al. 1998). Like all Walker type ATPases, torsinA contains a WalkerA ATP binding domain, and a WalkerB ATP hydrolyzing domain (Ozelius et al. 1997). TorsinA has been shown to bind ATP (Shashidharan et al. 2000) and has ATPase activity (Kustedjo et al. 2003; Konakova and Pulst 2005). The effect of dystonia-associated mutations on torsinA ATPase activity has been examined by two groups, however, one group reported no effect (Kustedjo et al. 2003), while the other group reported a disruption in ATPase activity (Konakova and Pulst 2005).

Disruption of ATP binding or hydrolysis changes the subcellular localization of torsinA in transfected cells (Goodchild and Dauer 2004; Naismith et al. 2004; Torres et al. 2004). A well-characterized glutamate (E) to glutamine (Q) mutation at position 171 (torsinA E171Q) in the WalkerB motif disrupts ATP hydrolysis, resulting in a constitutively ATP-bound form of torsinA. TorsinAE171Q has a strikingly similar pattern of distribution to torsinA ΔE, with a shift from the ER to the NE (Gerace 2004; Goodchild and Dauer 2004; Naismith et al. 2004), suggesting that the ΔE mutation may

be affecting torsinA ATPase activity. Additionally, a second well characterized lysine (K) to alanine (A) mutation at position 108 (torsinA K108A) in the WalkerA motif that disrupts ATP binding restores torsinAΔE localization to a wild-type like pattern (Goodchild and Dauer 2004; Torres et al. 2004).

AAA^+ proteins often form oligomeric ring formations (Patel and Latterich 1998; Neuwald et al. 1999; Vale 2000; Maurizi and Li 2001; Ogura and Wilkinson 2001; Lupas and Martin 2002). Although several groups have examined whether or not torsinA also oligomerizes, the results have been controversial, with some showing that torsinA exists in a monomeric form (Kustedjo et al. 2003) and others showing that torsinA oligomerizes (Torres et al. 2004; Pham et al. 2006).The two dystonia-associated mutations of torsinA occur in the C-terminus, which is thought to be important for substrate recognition and oligomerization (Ogura and Wilkinson 2001). However, the effect of dystonia-associated torsinA ΔE and torsinA Δ323-8 mutations on the oligomerization of torsinA protein remains unclear.

Because many AAA^+ family members facilitate changes in protein conformation (Neuwald et al. 1999; Ogura and Wilkinson 2001), it has been hypothesized that torsinA may function as a chaperone protein (Shashidharan et al. 2000; Sharma et al. 2001; McLean et al. 2002; Caldwell et al. 2003; Walker et al. 2003; Caldwell and Caldwell 2004). TorsinA shares homology with the Hsp100/ClpB family of molecular chaperones (Ozelius et al. 1998), and several studies display a chaperone-like activity in torsinA that is disrupted by the ΔE mutation. Overexpression of wild type torsinA, but not mutant torsinA, has been shown to reduce the number of polyglutamine repeat aggregates in C. elegans (Caldwell et al. 2003; Caldwell et al. 2004), and torsinA immunoreactivity has

been found in inclusion bodies of trinucleotide repeat diseases (Walker et al. 2003), such as Huntington's disease, and spinocerebellar ataxia III, which is consistent with previous observations of chaperone proteins found in trinucleotide repeat aggregates (Cummings et al. 1998). In addition, overexpressed wild type torsinA, but not mutant torsinA, has been shown to suppress α-synuclein aggregation to a similar degree as known chaperones HDJ-1, HDJ-2 and Hsp70 (McLean et al. 2002). Like other chaperone proteins, torsinA may protect against cell death induced by proteasomal inhibition, oxidative stress and trophic withdrawal (Kuner et al. 2003; Shashidharan et al. 2004). Protein aggregates such as Lewy bodies tend to contain many known chaperone proteins, such as Hsp70 and Hsp40 (Auluck et al. 2002). TorsinA immunoreactivity has been identified in Lewy bodies in post-mortem tissue from sporadic Parkinson's disease patients (Shashidharan et al. 2000) as well as in tissue from patients with diffuse Lewy body disease (Sharma et al. 2001). In addition, torsinA was shown to increase the degradation of mutant form of ε-sarcoglycan that developed ER-localized aggregates (Esapa et al. 2007). However, *in vitro* evidence of chaperone activity has not yet been shown, and no interaction between torsinA and α-synuclein or trinucleotide repeat proteins has been demonstrated. It is not known how torsinA chaperone activity is utilized in the cell, and ε-sarcoglycan, is the only possible endogenous substrate identified.

TorsinA is involved in neurite extension and plays a role in the secretory pathway

Although torsinA is generally thought to be an ER lumenal protein, torsinA has been identified in neurites of brain slices and cultured neurons (Augood et al. 2003; Rostasy et al. 2003; Kamm et al. 2004). The presence of torsinA in the growth cones of cultured

neurons (Kamm et al. 2004) has led some to question whether torsinA plays a role in neurite extension. Although torsinA overexpression does not appear to have an effect on neurite length, siRNA mediated knock-down of torsinA resulted in an increase in neurite length (Ferrari-Toninelli et al. 2004). In contrast, overexpression of ΔE torsinA appears to inhibit neurite extension (Hewett et al. 2006). However, the mechanisms through which torsinA effects neurite length is still unknown and it is not clear what effect this may have on the development of dystonia.

All secretory proteins must first pass through the ER before entering the secretory pathway. There is evidence to suggest that torsinA may play a role in the secretory pathway, although the mechanism by which torsinA affects the secretory pathway is currently unknown. TorsinA has been seen in the cytoplasm, proximal processes and terminals of neurons in patient samples (Shashidharan et al. 2000; Konakova and Pulst 2001; Walker et al. 2001; Walker et al. 2002; Augood et al. 2003; Rostasy et al. 2003; Xiao et al. 2004), as well as in cultured cells (Hewett et al. 2000; Kamm et al. 2004). Additionally, torsinA has been shown to localize with what appear to be secretory granules in cultured cells (Granata et al. 2008), and torsinA ΔE inclusion formations have been shown to contain proteins involved with exocytosis (Misbahuddin et al. 2005; Granata et al. 2008). Overexpression of torsinA WT has been shown to have a negative effect on the plasma-membrane expression levels of polytopic membrane bound proteins, such as the dopamine transporter and the norepinephrine transporter (Torres et al. 2004), as well as a reduced level of synaptic vesicle marker synaptotagmin presentation on the plasma membrane (Granata et al. 2008). Hewett et al. demonstrated that the secretion of exogenously expressed *Gaussia* luciferase was reduced in DYT1 patient fibroblasts

compared to controls, suggesting either a function in secretory protein processing or exocytosis, however it is not clear which (Hewett et al. 2007). Conversely, Granata et al. reported a decrease in endocytosis in cells overexpressing torsinA WT and increase in endocytosis in cells overexpressing torsinA ΔE with no effect on exocytosis rates (Granata et al. 2008). Although these data seem to support a possible role for torsinA in the secretory pathway, it is not clear at what stage in the secretory pathway torsinA might be having an effect. In addition, there is no obvious deficit in DYT1 patients that would imply secretory pathway disruption.

TorsinA transgenic animals reveal loss of function phenotype

TorsinA null mice die within 48 hours of birth, despite a lack of obvious developmental abnormalities (Goodchild et al. 2005). TorsinA null mice display normal neocortical layering and spinal cord development, normal levels of synapsin which suggest that synaptic development is comparable to WT mice, and further examination of the nigrostriatal dopaminergic system demonstrated no change in striatal projections compared to WT mice (Goodchild et al. 2005). Upon closer examination it was revealed that the NE ultrastructure of torsinA null mice was abnormal, containing NE membrane derived vesicles not found in wild-type (WT) animals (Goodchild et al. 2005). Interestingly, these NE abnormalities were only found in neurons, and were absent from astrocytes, oligodendrocytes and cells associated with the blood-brain barrier (Goodchild et al. 2005). Like torsinA null mice, mice homogeneously expressing the ΔE torsinA mutation die within 48 hours of birth and have NE abnormalities, which has led to the suggestion that the ΔE torsinA mutation is a loss of function mutation (Goodchild et al.

2005). Their heterozygous litter mates show no obvious structural abnormalities (Goodchild et al. 2005).

Many different labs have also created transgenic mice expressing human WT or ΔE torsinA in mice, with varying results. Although the different mouse models vary in the number of abnormalities reported, as well as in the degree of severity, there are few commonly reported phenotypes. Several groups have reported gait abnormalities and difficulties with beam walking tests, as well as impaired motor learning (Dang et al. 2005; Sharma et al. 2005; Shashidharan et al. 2005; Grundmann et al. 2007; Zhao et al. 2008). Another common feature appears to be alterations in dopamine levels, release or turnover (Shashidharan et al. 2005; Balcioglu et al. 2007; Grundmann et al. 2007; Zhao et al. 2008). Alterations in dopamine uptake and turnover have also been reported in DYT1 patients (Otsuka et al. 1992; Augood et al. 2002). Finally, several groups have reported torsinA or ubiquitin positive inclusions in the brainstem, similar to what was reported in human patients (McNaught et al. 2004; Dang et al. 2005; Shashidharan et al. 2005; Grundmann et al. 2007). In an inducible torsinA knock-down model, mice displayed a similar phenotype to knock-in models, further supporting the idea that ΔE torsinA is a loss of function mutation (Dang et al. 2006)

In a *Drosophila* model of DYT1, flies overexpressing human ΔE torsinA showed severe motor impairments when exposed to high temperatures (Koh et al. 2004). In these flies, ΔE torsinA was found in aggregates associated with endosomes and the NE (Koh et al. 2004). The structural defects associated with ΔE torsinA were similar to those seen in mutations that disrupt the TGF-β signaling pathway, and overexpression of certain transcriptional effectors of the TGF-β pathway were able to rescue motor impairment

(Koh et al. 2004). Although this suggests a potential role for torsinA in the TGF-β pathway, there is no evidence of TGF-β signaling deficits in DYT1 patients or other torsinA animal models.

Torsin Family Proteins

Human torsinA family members

The human genome contains four torsin family proteins (Ozelius et al. 1997; Ozelius et al. 1999; Hewett et al. 2004), comprised of torsinA (TOR1A), torsinB (TOR1B), torp2A (TOR2A) and torp3A (TOR3A). Very little is known about torp2A or torp3A and both proteins remain to be characterized. TorsinB has 70% homology with torsinA, with a predicted size of 38kD (Ozelius et al. 1997; Ozelius et al. 1999). The genes encoding torsinA and torsinB are found adjacent to each other on chromosome 9, but they have opposite orientations (Ozelius et al. 1999). TorsinB, like torsinA, also has an N-terminal signal sequence, as well as an ATP binding site and a hydrophobic domain (Ozelius et al. 1997; Hewett et al. 2004). Although the glutamate pair that is affected by the GAG deletion in torsinA is also conserved in torsinB (Ozelius et al. 1997; Baptista et al. 2004), no mutations in torsinB have been reported.

TorsinA and torsinB share a similar pattern of protein expression in mouse, rat and human brains (Augood et al. 1999; Konakova and Pulst 2001; Bahn et al. 2006; Vasudevan et al. 2006). TorsinB also shares a similar pattern of intracellular localization with torsinA, and co-localizes with NE and ER marker proteins (Hewett et al. 2004; O'Farrell et al. 2004). In cells overexpressing both proteins, torsinB is able to complex

with torsinA (Hewett et al. 2004), though it is not clear whether this interaction occurs endogenously. Of key interest are the ways these two proteins differ. When overexpressed at high levels, torsinB forms perinuclear inclusions similar to those seen when ΔE torsinA is overexpressed, and when both torsinB and ΔE torsinA are overexpressed, the two proteins co-localize in similar inclusion bodies (Hewett et al. 2004). However, the significance of this effect is difficult to assess as these inclusion bodies are likely artifacts of overexpression that are not seen in patients. Another intriguing difference is that unlike torsinA, torsinB is not detected in Lewy bodies, which may point to differing functions (O'Farrell et al. 2004). Although torsinA and torsinB appear to be well placed to complex and perhaps provide functional redundancy, the current body of research is too sparse to reach any conclusions.

TorsinA orthologues

The *Caenorhabditis elegans* protein OOC-5 is a torsinA related protein that also localizes to the endoplasmic reticulum (Basham and Rose 2001). OOC-5 appears to be involved in establishing polarity in the two cell embryo of *C. elegans*, although the mechanism is unclear (Basham and Rose 2001; Toninelli et al. 2003). The ability of OOC-5 to bind ATP and ADP is redox-dependent (Zhu et al. 2008). Whether torsinA functions in a similar manner to OOC-5 is not known.

The *Drosophila melanogaster* protein torp4a is another torsinA related protein which is also localized to the ER and NE (Muraro and Moffat 2006). Targeted down-regulation of torp4a in the eye results in progressive retinal degeneration, while up-regulation appears to protect from age-related retinal degeneration (Muraro and Moffat

2006). In *Drosophila*, torp4a is likely involved in microtubule and actin based intracellular movement and the biogenesis of lysosome-related organelles (Muraro and Moffat 2006). It is unclear whether torsinA and torp4a serve similar functions. Unlike mammals, *Drosophila* contain only one torsin protein, and the C-terminal region, where both dystonia-associated mutations are found, is not well conserved.

TorsinA-interacting Proteins

Kinesin light chain1 (KLC1)

Kamm et al. identified kinesin light chain 1 (KLC1) as an interactor of torsinA using yeast-two hybrid screens of an adult human brain cDNA library using the c-terminus of torsinA as bait (Kamm et al. 2004). Additionally, they identified two alternatively spliced isoforms of KLC1, KCL1-B and KLC1-C (Kamm et al. 2004). They found that torsinA co-localizes with KLC-1 in cell bodies and neurites, with concentrations at the neuronal growth cones (Kamm et al. 2004). Their studies suggested that torsinA and kinesin-1 exist in a complex, and that some population of torsinA is present on the cytoplasmic face of vesicles (Kamm et al. 2004).

Dopamine Transporter (DAT)

Because dopamine imbalances may play a role in DYT1 pathology, Torres et al. sought to examine the effect of torsinA on dopamine reuptake (Torres et al. 2004). They demonstrated that overexpression of torsinA WT reduced dopamine transporter (DAT) levels on the cell surface, and resulted in an increase in DAT levels in cellular

compartments (Torres et al. 2004). They further demonstrated that torsinA could be co-immunoprecipitated when using anti-DAT antibody. Although they observed a similar effect on other polytopic membrane-bound proteins, including the norepinephrine transporter (NET), subunits of G protein-coupled receptors, and a subunit of a potassium channel, they did not show evidence of any interaction between these proteins and torsinA (Torres et al. 2004). The mechanism through which torsinA regulates DAT membrane levels is currently unclear.

Lamina-Associated Polypeptide 1 (LAP)/ Lumenal Domain Like Lap1 (LULL1)

Based on the assumption that overexpressing a NE torsinA-interacting protein would increase the level of torsinA at the NE, Goodchild and Dauer overexpressed a number of NE proteins with lumenal domains and identified Lamina-associated polypeptide 1 (LAP1) as a potential torsinA binding partner (Goodchild and Dauer 2005). Using deletion constructs, they established that the lumenal domain of LAP1 was the torsinA-interacting region (Goodchild and Dauer 2005). A search for proteins with a similar lumenal domain led to the identification of Lumenal domain Like LAP1 (LULL1), an ER localized protein (Goodchild and Dauer 2005). Interaction analysis revealed that both LAP1 and LULL1 interacted more strongly with ATP-bound torsinA E171Q than with torsinA WT, suggesting that both proteins may be substrates of torsinA, however, the function of both interactions remains unknown (Goodchild and Dauer 2005).

Vimentin

Hewett et al. reported the formation of a vimentin ring around the nucleus of DYT1 patient fibroblasts that was not present in control fibroblasts (Hewett et al. 2006). Further investigation showed that disrupting vimentin structure using nocodazole to collapse microtubule structure resulted in a redistribution of torsinA to vimentin aggregates in both control and DYT1 lines (Hewett et al. 2006). TorsinA was found to co-fractionate with cytoskeletal elements and co-immunoprecipitate with vimentin, as well as other cytoskeletal elements, such as kinesin, α-tubulin and actin (Hewett et al. 2006). Mutant torsinA was found to delay cell adhesion and restrict neurite extension, both of which require vimentin (Hewett et al. 2006). Their studies suggest that torsinA is either restricted to a portion of the ER that interacts with vimentin, or that vimentin interacts with a population of torsinA that presents on the cytoplasmic face of the ER (Hewett et al. 2006).

Snapin

Granata et al. identified snapin as an interactor of torsinA using yeast-two hybrid screen of an adult human brain cDNA library using full-length torsinA WT and torsinA ΔE (Granata et al. 2008). Snapin was able to bind both torsinA WT and torsinA ΔE in *in vitro* and *in vivo* binding assays, and snapin co-localizes with torsinA in secretory organelles (Granata et al. 2008). In addition, they demonstrated that overexpression of torsinA WT impaired synaptic vesicle recycling, but that overexpression of torsinA ΔE and knockdown of torsinA WT resulted in increased levels of synaptic vesicle recycling, suggesting that torsinA ΔE might represent a loss of function mutation (Granata et al.

2008). However, the exact function of torsinA in synaptic vesicle recycling remains unclear.

ε-Sarcoglycan

ε-sarcoglycan is the product of the gene associated with DYT11 (Zimprich et al. 2001). The family found with the torsinA Δ323-8 mutation also has a mutation in ε-sarcoglycan (Klein et al. 2002). Although WT e-sarcoglycan is found on the plasma membrane, mutant forms of e-sarcoglycan are retained in the ER (Esapa et al. 2007). Interestingly, Esapa et al. demonstrated that torsinA WT and torsinA ΔE interact with mutant ε-sarcoglycan, although they were unable to demonstrate an interaction with WT ε-sarcoglycan (Esapa et al. 2007). Overexpression of torsinA WT resulted in increased degradation of both WT and mutant ε-sarcoglycan, although the effect seems stronger for the mutant (Esapa et al. 2007). They hypothesized that torsinA may assist in clearing misfolded ε-sarcoglycan from the ER (Esapa et al. 2007).

Mechanisms of Protein Quality Control in the ER

A major unstudied area in the torsinA field is the effect of mutation on torsinA stability and turnover. As previously stated, torsinA is considered to be an ER resident protein. The ER has specialized processes for handling the degradation of both normal and misfolded proteins. Below is a review of these processes.

Unfolded Protein Response (UPR)

The ER is one of the primary sites for protein translation and assembly. Proteins bound for the secretory pathway and membrane proteins are co-translationally translocated into the ER lumen, where they are properly folded, modified, and assembled (Shen et al. 2004; Zhang and Kaufman 2004). The ER is home to many resident molecular chaperone proteins, such as BiP, whose primary function is to enhance protein folding by preventing protein aggregation and preventing proteins from getting stuck in low-energy, non-functional states (Zhang and Kaufman 2004). A number of events can prevent a protein from folding correctly, including oxidative damage, mutations, lack of assembly partners or simple chance. The accumulation of unfolded proteins triggers a process known as the unfolded protein response (UPR) (Shen et al. 2004; Kincaid and Cooper 2007).

The major components of the UPR are inostitol-requiring transmembrane kinase and endonuclease 1 (IRE1), protein kinase-like ER kinase (PERK), and activating transcription factor 6 (ATF6), all of which are regulated by the molecular chaperone BiP (Shen et al. 2004; Zhang and Kaufman 2004; Kincaid and Cooper 2007). BiP binds to IRE1, PERK and ATF6, preventing them from interacting with each other (Zhang and Kaufman 2004). As unfolded protein levels in the ER increase, BiP is recruited away to aid in folding, which activates the UPR (Zhang and Kaufman 2004).

Upon release from BiP, IRE1 dimerizes and autophosphorylates, activating its RNAse activity, which acts to activate a transcriptional activator that increases expression of UPR genes (Zhang and Kaufman 2004; Kincaid and Cooper 2007). Simultaneously, ATF6 is transported to the Golgi where it is cleaved to generate a transcriptional activator that enhances transcription of ER-resident molecular chaperones (Zhang and Kaufman 2004; Kincaid and Cooper 2007). Release from BiP activates the kinase activity of

PERK, which phosphorylates the translation-initiation factor eIF2α (Zhang and Kaufman 2004; Kincaid and Cooper 2007). Phosphorylation of eIF2a prevents the formation of the ternary translation initiation complex, which leads to attenuation of general translation, reducing ER load (Zhang and Kaufman 2004; Kincaid and Cooper 2007). However, phosphorylated eIF2a is able to selectively promote translation of a subset of genes necessary for UPR (Zhang and Kaufman 2004; Kincaid and Cooper 2007). Thus the UPR consists of a concerted effort to reduce the load on the ER by reducing translation of most proteins, and increasing the transcription and translation of molecular chaperone proteins to aid in protein folding.

ER-Associated Degradation (ERAD)

Another way that the ER deals with unfolded or misfolded proteins is to remove them from the ER and target them for degradation in a process known as ER-associated degradation (ERAD) (Kleizen and Braakman 2004; Meusser et al. 2005; Kincaid and Cooper 2007). During ERAD, unfolded proteins are retrotranslocated to the cytoplasm, where they are ubiquitinated and targeted for degradation by the proteasome (Kleizen and Braakman 2004; Meusser et al. 2005; Kincaid and Cooper 2007). ER resident molecular chaperones, including BiP, play a role in ERAD by preventing aggregation of misfolded proteins and delivering them to the translocon for delivery to the cytosol (Nishikawa et al. 2005). .

Ubiquitin Proteasome System

There are two major sites of protein clearance and degradation in the cell: the lysosome and the proteasome. The 26S proteasome complex consists of a 19S cap that recognizes substrates and unfolds them for passage through the narrow 20S protealytic core (Pickart 1997). Degradation by the proteasome is considered ubiquitin-dependent, and proteins conjugated to a chain of at least 4 ubiquitin molecules have a greater affinity for the proteasome than proteins with shorter chains or unubiquitinated proteins (Pickart 1997; Pickart and Fushman 2004). Ubiquitin is a highly conserved 76-amino-acid protein found in all eukaryotes (Pickart and Eddins 2004). Attachment of an ubiquitin molecule to a protein target is a reversible covalent reaction which requires the sequential activation of three enzymes (Fig I-1). The E1 ubiquitin activating enzyme adenylates an ubiquitin monomer, which is then covalently bound to an E1 cysteine residue through a thiol-ester bond (Wilkinson 2000; Pickart and Eddins 2004). The E1 then recruits an E2 ubiquitin conjugating enzyme, and the ubiquitin monomer is then transferred to a cysteine residue within the E2 (Wilkinson 2000; Pickart and Eddins 2004). Finally, an E3 ubiquitin ligase recruits both the ubiquitination substrate and an E2 and facilitates the transfer of ubiquitin to a lysine residue within the target protein (Pickart and Eddins 2004). There is a single E1 in each cell, that recruits and transfers ubiquitin to all the E2 enzymes, of which there are little more than a dozen currently known (Wilkinson 2000; Pickart and Eddins 2004). Each E2 is dedicated to just a few E3 enzymes, which are, in turn, dedicated to just a few protein substrates (Wilkinson 2000; Pickart and Eddins 2004). Some E3s have been shown to interact with multiple E2 enzymes, and the different combinations could impact substrate selection, therefore, it is thought to be the combination of E2 and E3 that conveys substrate specificity (Pickart and Eddins 2004).

Although ubiquitination is most classically associated with proteasomal degradation, ubiquitin is also involved in a number of signaling pathways. Mono-ubiquitination is a targeting signal for membrane receptor internalization, and can modulate the activity of transcription factors (Wilkinson 1999). The formation of a poly-ubiquitin chain involves the conjugation of further ubiquitin monomers to lysine residues within the initial substrate bound ubiquitin (Pickart 1997; Wilkinson 1999; Pickart and Fushman 2004). Ubiquitin contains 11 lysine residues, and increasing evidence suggests that which lysine is used to originate the poly-ubiquitin chain can determine the fate of the substrate (Wilkinson 1999; Pickart and Fushman 2004). Ubiquitin chains that are formed through linkage to K48 are the primary proteasome degradation signal, although K29 linkage is also associated with proteasome degradation (Pickart 1997; Wilkinson 1999; Pickart and Fushman 2004). In contrast, K63 linkage is associated with a number of non-proteasomal signaling pathways, including DNA repair and protein trafficking, and has recently been implicated in aggresome formation (Wilkinson 1999; Pickart and Fushman 2004; Olzmann et al. 2007).

ERAD II

Recently, a secondary ERAD pathway, referred to as ERAD II, was discovered that leads to the autophagy-lysosome pathway (hereafter referred to as autophagy) and selectively targets unfolded or aggregated proteins for degradation (Fujita et al. 2007; Yorimitsu and Klionsky 2007). ERAD II is thought to be activated in the event of proteasome disruption, ERAD failure, or when aggregates in the ER lumen are unable to be

retrotranslocated to the cytosol (Fujita et al. 2007; Yorimitsu and Klionsky 2007). The signaling mechanisms that initiate ERAD II are not clear.

Autophagy

The second major pathway for protein clearance and degradation is the autophagy-lysosome pathway which is generally considered to be a bulk, non-selective pathway for clearing cytoplasmic proteins, however recent evidence has demonstrated that autophagy can also mediate the selective removal of damaged protein aggregates and organelles (Wang and Klionsky 2003; Cuervo 2004; Yang et al. 2005; Yorimitsu and Klionsky 2005). There are three types of autophagy. Chaperone mediated autophagy involves the export of a cytosolic protein directly into the lysosome, microautophagy involves the direct engulfment of cytosolic proteins and organelles at the surface of the lysosome by protrusions or invaginations of the lysosomal membrane, and macroautophagy requires the sequestration of cytosolic proteins or organelles into a double-membrane vesicle referred to as the autophagosome (Cuervo 2004; Yorimitsu and Klionsky 2005). The focus of this section will be macroautophagy, hereafter referred to as autophagy.

Autophagy has been thoroughly studied in yeast, and many autophagy-associated genes (ATG) and their encoded proteins (Atg) have been identified, some of which are well conserved in mammalian cells (Wang and Klionsky 2003; Cuervo 2004; Yang et al. 2005; Yorimitsu and Klionsky 2005). Autophagy is best characterized as a starvation response, wherein the cell recycles non-essential proteins to free up resources for the synthesis of essential proteins in the absence of nutrients (Wang and Klionsky 2003; Cuervo 2004; Yang et al. 2005; Yorimitsu and Klionsky 2005). Tor (target of rapamycin)

kinase is thought to be the nutrient sensor that controls the induction of autophagy (Wang and Klionsky 2003; Cuervo 2004; Yang et al. 2005; Yorimitsu and Klionsky 2005). Under nutrient rich conditions, Tor kinase hyperphosphorylates Atg13, preventing its interaction with Atg1 (Wang and Klionsky 2003; Cuervo 2004; Yang et al. 2005; Yorimitsu and Klionsky 2005). Under starvation conditions, Atg13 is dephosphorylated allowing it to interact with Atg1, which activates Atg1 kinase activity, although it is not clear whether Atg1 kinase activity is necessary for autophagosome formation or whether the Atg1-Atg13 complex performs a structural role (Wang and Klionsky 2003; Cuervo 2004; Yang et al. 2005; Yorimitsu and Klionsky 2005).

Autophagosome membrane formation is thought to be a *de novo* event that occurs at a poorly characterized organelle known as the phagophore or pre-autophagosomal structure (PAS), although the source of the autophagosomal membranes is not clear (Wang and Klionsky 2003; Cuervo 2004; Yang et al. 2005; Yorimitsu and Klionsky 2005). Interestingly, two ubiquitin-like conjugation systems are necessary for autophagosome formation (Wang and Klionsky 2003; Yang et al. 2005; Yorimitsu and Klionsky 2005). Although Atg8 and Atg12 have no significant sequence homology to ubiquitin, both follow similar conjugation pathways, requiring activation by E1-homolog Atg7 and transfer to an E2- like protein (Wang and Klionsky 2003; Yang et al. 2005; Yorimitsu and Klionsky 2005). Atg8 is first cleaved by Atg4, exposing a glycine residue that can then be conjugated to an internal cysteine residue of Atg7 (Wang and Klionsky 2003; Yang et al. 2005; Yorimitsu and Klionsky 2005). Atg8 is then transferred to an internal cysteine residue of Atg3, an E2-like protein that mediates the conjugation of Atg8 to phosphatidylethanolamine (PE). Atg8-PE can be found at the PAS, in

autophagosomes and autophagic bodies, and is thought to be a structural component of the autophagosome, making it an ideal marker of autophagy (Wang and Klionsky 2003; Yang et al. 2005; Yorimitsu and Klionsky 2005). There are three known Atg8 homologues in mammals: Microtubule-associated protein 1 light chain 3 (LC3), γ-aminobutyric acid type A receptor-associated protein (GABARAP), and Golgi-associated ATPase enhancer of 16 kDa (GATE-16) (Wang and Klionsky 2003; Yang et al. 2005; Yorimitsu and Klionsky 2005).

Similar to Atg8, Atg12 is activated by Atg7 and transferred to E2-like protein Atg10, which mediates the conjugation of Atg12 to an internal lysine residue of Atg5 (Wang and Klionsky 2003; Yang et al. 2005; Yorimitsu and Klionsky 2005). The Atg12-Atg5 complex then binds Atg16 through a direct interaction between Atg16 and Atg5, and Atg16 self-oligomerizes forming a large Atg12-Atg5-Atg16 complex of 350 kDa in yeast and 800 kDa in mammals (Wang and Klionsky 2003; Yang et al. 2005; Yorimitsu and Klionsky 2005). The Atg12-Atg5-Atg16 complex is necessary for autophagosome membrane elongation, however the complex is not present on the complete autophagosome and it is thought to mediate expansion and curvature of the membrane (Wang and Klionsky 2003; Yang et al. 2005; Yorimitsu and Klionsky 2005).

Phosphatidylinostital 3-phosphate (PI3) plays an important role in autophagosome formation, although the exact role is unclear (Wang and Klionsky 2003; Yang et al. 2005; Yorimitsu and Klionsky 2005). However, inhibition of PI3 kinase by 3-methyladenine (3-MA) or wortmannin results in inhibition of autophagosome formation (Wang and Klionsky 2003; Yang et al. 2005; Yorimitsu and Klionsky 2005). The yeast PI3 kinase, Vps34, can be found in two complexes: complex I, which consists of Vps34, Vps15,

Atg6 and Atg14, regulates autophagy and is localized primarily at the PAS; complex II, which consists of Vps34, Vps15, Atg6 and Vps38, is involved in endocytosis (Wang and Klionsky 2003; Yang et al. 2005; Yorimitsu and Klionsky 2005). There are 3 classes of PI3 kinases in mammalian cells, of which class III is a functional orthologue of Vps34 (Wang and Klionsky 2003; Yang et al. 2005; Yorimitsu and Klionsky 2005). The mammalian orthologue of Vps15 is p150, and the mammalian orthologue of Atg6 is beclin-1, which has been identified as a tumor suppressor gene (Wang and Klionsky 2003; Yang et al. 2005; Yorimitsu and Klionsky 2005). The PI3 kinase complex is thought to be necessary to recruit both Atg8-PE and Atg12-Atg5-Atg16 to the PAS (Wang and Klionsky 2003; Yang et al. 2005; Yorimitsu and Klionsky 2005).

The autophagosome and its contents are transported to the lysosome, where they are degraded by hydrolytic enzymes contained in the lysosomal lumen (Wang and Klionsky 2003; Cuervo 2004; Yang et al. 2005; Yorimitsu and Klionsky 2005). The constitutive clearance of damaged proteins through the autophagy pathway has also been shown to be essential to proper neuronal function, as mice lacking necessary autophagy-associated proteins develop motor deficits and abnormal reflexes and ubiquitin-positive inclusion bodies accumulate in their neurons (McCray and Taylor 2008; Mizushima et al. 2008). Autophagy thought to be responsible for clearing proteinaceous aggregates associated with neurodegenerative diseases, such as the Lewy bodies found in Parkinson's Disease, and an age-related decline in autophagy may be responsible for the increased susceptibility to age-related disease (Levine and Kroemer 2008; McCray and Taylor 2008; Mizushima et al. 2008). Ubiquitin may also play a role in clearance of protein aggregates through the autophagy pathway. K63 ubiquitin linkage has been

shown to direct proteins to the aggresome (Olzmann et al. 2007; Olzmann et al. 2008), and p62/sequestosome-1 has both an LC3-binding domain and an ubiquitin-binding domain, which may allow it to mediate autophagosome formation around ubiquitinated protein aggregates (Huang and Klionsky 2007; Levine and Kroemer 2008; McCray and Taylor 2008).

Hypotheses and Organizational Overview

The finding that mutations in torsinA are linked to the development of DYT1 dystonia was a major development in understanding the pathogenesis of dystonia (Ozelius et al. 1997). Although a great deal of research has been focused on determining the underlying mechanisms that lead to disease, a number of unanswered questions remain. It is still unclear why torsinA mutations result in a purely neurological phenotype, despite torsinA being a ubiquitously expressed protein (Shashidharan et al. 2000). Determining whether there are neuron-specific properties of torsinA is critical to evaluate current research and establish physiologically significant models of torsin-associated pathogenesis. In addition, the effect of dystonia-associated mutations on torsinA stability and turnover is also a largely unexplored area of torsinA research. To address these issues, in Chapter II, we characterized the localization of torsinA in non-neuronal and neuronal cells and also examined the effect of the dystonia-associated mutations on torsinA localization. We also tested the hypothesis that dystonia-associated mutations may destabilize torsinA and result in premature degradation. Our findings demonstrate that torsinA has a neuron-specific NE preference that is enhanced by the dystonia-associated mutations.

Furthermore, we provide the first direct evidence that torsinA is a long-lived protein that is degraded through autophagy, and that the dystonia-associated mutations destabilize the protein and result in premature degradation mediated by the UPS.

A major goal in the field of torsinA research has been to find interacting partners. Although a number of proteins have been identified (Kamm et al. 2004; Torres et al. 2004; Goodchild and Dauer 2005; Hewett et al. 2006; Granata et al. 2008), none of the known interactions are affected by the dystonia-associated mutations, making their role in the pathogenesis of DYT1 dystonia unclear. In an effort to identify novel torsinA-interacting partners, we performed a yeast two-hybrid screen of a rat hippocampal/cortical cDNA library using full length torsinA WT and torsinAΔ40, which lacks the N-terminal signal sequence and hydrophobic domains, as bait. Three of the positive clones in this screen encoded a novel protein, which we named printor for protein interactor of torsinA. In Chapter III, we characterize the localization of this novel protein and establish that it co-localizes and interacts with torsinA. We also examined the effect of dystonia-associated mutation of torsinA on the interaction and report for the first time, an interacting partner that interacts with torsinA WT but not torsinA ΔE.

Together the findings in this dissertation indicate that torsinA may have a neuron-specific function that makes neurons more vulnerable to mutation. In addition, our data demonstrate that dystonia-associated mutation results in premature degradation through the proteasome, indicative of folding perturbation and possible loss of function. We have also identified a novel interacting protein named printor that co-distributes with torsinA. Finally, we are able to show that printor preferentially interacts with torsinA WT, but not

torsinA ΔE. These findings have significant implications for understanding the pathogenic mechanisms that lead to the development of DYT1 dystonia.

Locus	Location	Inheritance Pattern	Protein	Putative Function	Reference
DYT1	9q34	AD	TorsinA	Molecular chaperone, ATPase	(Ozelius et al. 1997)
DYT2	Unknown	AR	Unknown	Unknown	(Gimenez-Roldan et al. 1988)
DYT3	Xq13.1	XR	TAF1	Transcription	(Graeber and Muller 1992)
DYT4	Unknown	AD	Unknown	Unknown	(Parker 1985)
DYT5 / DYT14	14q22.1-q22.2	AD	GCH1	Enzyme necessary for DA synthesis	(Jarman et al. 1997)
DYT6	8p21-8q22	AD	Unknown	Unknown	(Almasy et al. 1997)
DYT7	18p11.3	AD	Unknown	Unknown	(Leube et al. 1997)
DYT8	2q33-q35	AD	MR-1	Unknown	(Rainier et al. 2004)
DYT9	1p13.3-p21	AD	Unknown	Unknown	(Auburger et al. 1996)
DYT10	16p11-q21	AD	Unknown	Unknown	(Kikuchi et al. 2007)
DYT11	7q21-q31	AD	ε-sarcoglycan	Muscle sarcoglycan complex component	(Zimprich et al. 2001)
DYT12	19q13	AD	ATP1A3	Na+/K+ ATPase subunit	(de Carvalho Aguiar et al. 2004)
DYT13	1p36.13	AD	Unknown	unknown	(Valente et al. 2001)
DYT15	18p11	AD	Unknown	Unknown	(Han et al. 2007)
DYT16	2q31.2	AR	PRKRA	Kinase	(Camargos et al. 2008)
DYT17	20p12.1-q13.12	AR	Unknown	Unknown	(Chouery et al. 2008)

Table I-1. Identified genes and proteins associated with dystonia disease. *AD*, autosomal dominant; *AR*, autosomal recessive; *XR*, X-linked recessive; *DA*, dopamine.

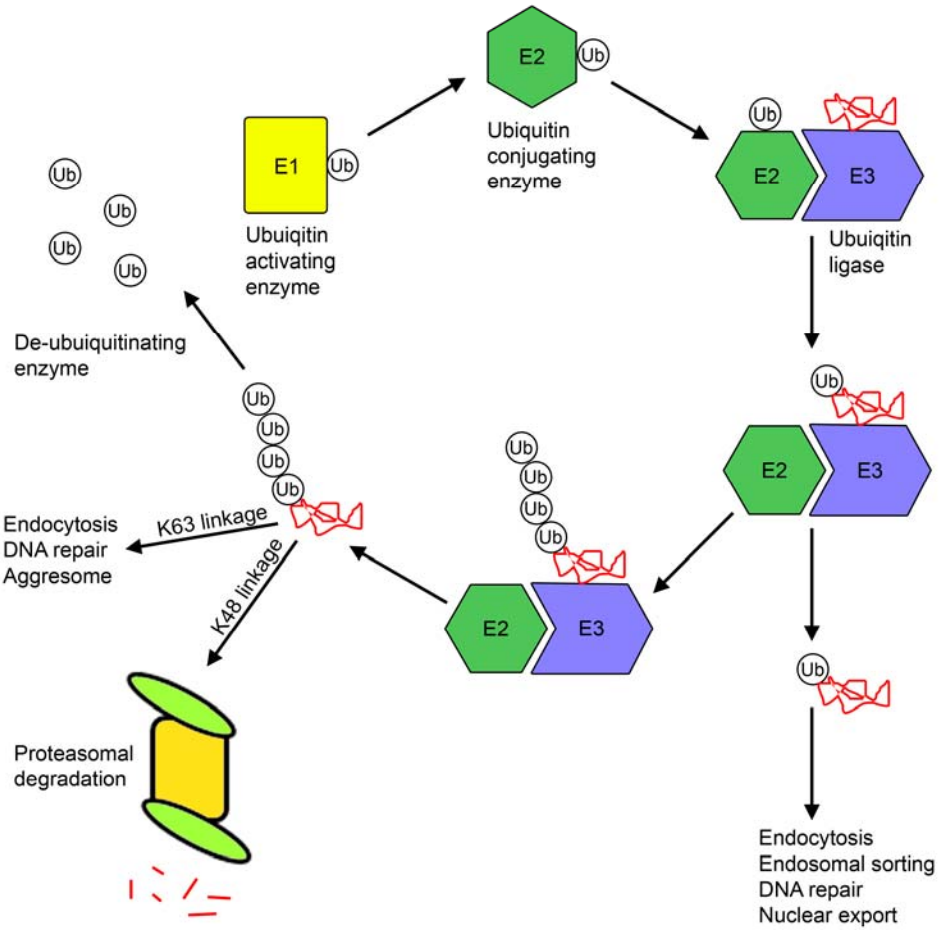

Figure I-1. Schematic of the ubiquitin proteasome system. The E1 ubiquitin activating enzyme activates an ubiquitin monomer, which is then covalently bound to an E1 cysteine residue through a thiol-ester bond. The E1 then recruits an E2 ubiquitin conjugating enzyme, and the ubiquitin monomer is then transferred to a cysteine residue within the E2. Finally, an E3 ubiquitin ligase recruits both the ubiquitination substrate and an E2 and facilitates the transfer of ubiquitin to a lysine residue within the target protein. Proteins can either leave the cycle with a single ubiquitin moiety attached, or it can go through several rounds of ubiquitination and acquire a poly-ubiquitin chain, in which subsequent ubiquitin monomers are conjugated to internal lysine residues of

already conjugated ubiquitin. Depending on the internal lysine residue used to build the chain, polyubiquitination can target the protein for different fates. Proteins can also be de-ubiquitinated by a de-ubiquitinating enzyme.

CHAPTER II

DYSTONIA-ASSOCIATED MUTATIONS CAUSE PREMATURE DEGRADATION OF TORSINA PROTEIN AND CELL TYPE-SPECIFIC MISLOCALIZATION TO THE NUCLEAR ENVELOPE

Part of the work described in this chapter has been published:

Giles, L.M., Chen, J., Li, L. and Chin, L.S. (2008) Dystonia-associated mutations cause premature degradation of torsinA protein and cell type-specific mislocalization to the nuclear envelope. *Hum. Mol. Genet.* **17** (17), 2712-22.

ABSTRACT

An in-frame 3-bp deletion in the torsinA gene resulting in the loss of a glutamate residue at position 302 or 303 (torsinA ΔE) is the major cause for early-onset torsion dystonia (DYT1). In addition, an 18-bp deletion in the torsinA gene resulting in the loss of residues 323–328 (torsinA Δ323-8) has also been associated with dystonia. Here we report that torsinA ΔE and torsinA Δ323-8 mutations cause neuronal cell type-specific mislocalization of torsinA protein to the nuclear envelope without affecting torsinA oligomerization. Furthermore, both dystonia-associated mutations destabilize torsinA protein in dopaminergic cells. We find that wild-type torsinA protein is degraded primarily through the macroautophagy-lysosome pathway. In contrast, torsinA ΔE and torsinA Δ323-8 mutant proteins are degraded by both the proteasome and macroautophagy-lysosome pathways. Our findings suggest that torsinA mutation-induced premature degradation may contribute to the pathogenesis of dystonia via a loss-of-function mechanism, and underscore the importance of both the proteasome and macroautophagy in the clearance of dystonia-associated torsinA mutant proteins.

INTRODUCTION

Dystonia is a movement disorder characterized by involuntary movements and prolonged muscle contraction, resulting in twisting body motions, tremor, and abnormal posture (Bressman et al. 2001). Early-onset generalized torsion dystonia (DYT1) is the most common and severe form of hereditary dystonia. DYT1 is autosomal dominant with a 30-40% penetrance and the disease onset usually occurs between 1 to 28 years of age (Bressman et al. 2001). Most cases of DYT1 dystonia are caused by an in-frame 3-bp (GAG) deletion in the gene encoding protein torsinA, which results in the loss of a glutamate residue at position 302 or 303 (torsinA ΔE) (Ozelius et al. 1997). In addition, an in-frame 18-bp deletion in the torsinA gene resulting in the loss of amino acids F323-Y328 (torsinA Δ323-8) was found in three members of a single family with dystonia (Leung et al. 2001). Because of a concomitant mutation in the myoclonic dystonia (DYT11)-linked protein epsilon-sarcoglycan in two of these patients (Klein et al. 2002), it remains to be established whether the torsinA Δ323-8 mutation contributes to the pathogenesis of dystonia.

TorsinA is a 332-amino-acid protein that is expressed in brain and multiple other tissues (Shashidharan et al. 2000). It is unclear why mutations in torsinA manifest mainly as a neurological phenotype. TorsinA contains an N-terminal 20-amino-acid endoplasmic reticulum (ER) signal sequence (Hewett and Breakefield 2003; Liu et al. 2003), followed by a 20-amino-acid hydrophobic domain. Immunohistochemical studies in neurons reveal the presence of torsinA in the cytoplasm, neuronal processes and synaptic terminals (Shashidharan et al. 2000; Konakova and Pulst 2001; Walker et al. 2001; Walker et al.

2002; Augood et al. 2003; Rostasy et al. 2003; Xiao et al. 2004). TorsinA is widely believed to reside in the lumen of the ER (Kustedjo et al. 2000; O'Farrell et al. 2002; Kustedjo et al. 2003; Bragg and Breakefield 2004; Gonzalez-Alegre and Paulson 2004; Goodchild and Dauer 2004; Naismith et al. 2004). In contrast to the ER localization of wild-type torsinA, torsinA ΔE mutant protein was reported to co-localize with nuclear envelope (NE) marker proteins (Bragg et al. 2004; Gerace 2004; Gonzalez-Alegre and Paulson 2004; Goodchild and Dauer 2004; Naismith et al. 2004), and overexpression of torsinA ΔE mutant may lead to the formation of cytoplasmic perinuclear inclusions (Hewett et al. 2000; Kustedjo et al. 2000; O'Farrell et al. 2002; Bragg and Breakefield 2004; Bragg et al. 2004). The effect of the torsinA Δ323-8 mutation on the localization of torsinA protein has not yet been determined.

Sequence analysis reveals that torsinA is a member of the AAA^+ (ATPases associated with a variety of cellular activities) superfamily of ATPases (Beyer 1997; Ozelius et al. 1997; Ozelius and Breakefield 1998). Members of the AAA^+ family often have molecular chaperone activities and facilitate changes in protein conformation (Neuwald et al. 1999; Ogura and Wilkinson 2001). They are involved in a wide variety of cellular processes, such as membrane trafficking and transcriptional regulation. The AAA^+ proteins are known to oligomerize into multimeric complexes (Patel and Latterich 1998; Neuwald et al. 1999; Vale 2000; Dalal and Hanson 2001; Maurizi and Li 2001; Ogura and Wilkinson 2001; Lupas and Martin 2002; Hanson and Whiteheart 2005). Previous results regarding torsinA oligomerization have been controversial, with some showing that torsinA exists in a monomeric form (Kustedjo et al. 2003) and others showing that torsinA oligomerizes (Torres et al. 2004; Pham et al. 2006). Moreover,

whether dystonia-associated torsinA ΔE and torsinA Δ323-8 mutations affect the oligomerization of torsinA protein remains unclear.

An unexplored, key question is how wild-type and dystonia-associated mutant torsinA proteins are degraded in cells. Protein degradation serves as an important mechanism by which cells regulate the expression levels of specific proteins and consequently the cellular processes in which these proteins participate (Ciechanover 2005). In addition, selective degradation of misfolded proteins, which are generated by genetic mutations or oxidative damage, is essential for cell homeostasis (Rubinsztein 2006). The ubiquitin-proteasome and macroautophagy (hereafter referred to as autophagy)-lysosome pathways are the two major intracellular proteolytic systems for degradation of both normal cellular proteins and misfolded proteins (Ciechanover 2005; Rubinsztein 2006). Whether one or both of these pathways are involved in wild-type or mutant torsinA protein degradation is unknown, and the effects of dystonia-associated mutations on torsinA protein stability remain undefined.

In this study, we characterized the localization, oligomerization, and degradation of wild-type torsinA protein and investigated the effects of dystonia-associated torsinA ΔE and torsinA Δ323-8 mutations. Our results reveal that both dystonia-associated mutations cause neuronal cell type-specific mislocalization of torsinA protein to the nuclear envelope without affecting torsinA oligomerization and promote torsinA protein degradation by both the proteasome and autophagy-lysosome pathways. These findings provide new insights into the pathogenic mechanisms of torsinA ΔE and torsinA Δ323-8 mutations and have important implications for understanding and treating dystonia.

EXPERIMENTAL PROCEDURES

Expression constructs and antibodies

Conventional molecular biological techniques (Sambrook et al. 1989) were used to subclone DNA fragments encoding torsinA WT, ΔE, Δ323-8, and NT into mammalian vectors expressing C-terminal HA, Myc, or FLAG tags for transfection into cells. A rabbit polyclonal anti-torsinA antibody was raised against the N-terminal region of torsinA and affinity purified as described previously (Chin et al. 2000; Kirk et al. 2006). Other antibodies used in this study are as follows: anti-KDEL (Stressgen); anti-β-actin (Chemicon); mouse monoclonal anti-HA (12CA5); and anti-Myc (9E10) (Kirk et al. 2006). Horseradish peroxidase-conjugated secondary antibodies were used for immunoblotting (Jackson Immunoresearch Laboratories, Inc.). Flourescein isothiocyanate (FITC)- and Texas Red (TR)-conjugated secondary antibodies were used for immunofluorescence microscopy (Jackson Immunoresearch Laboratories, Inc.).

Cell transfections and co-immunoprecipitation

Transfections of HeLa and SH-SY5Y cells with the indicated plasmids were performed using Lipofectamine 2000 reagent (Invitrogen) according to the manufacturer's instructions. Cell lysates were prepared from transfected cells and immunoprecipitations were carried out as described previously (Olzmann et al. 2004; Kirk et al. 2006) using anti-HA or anti-Myc antibodies. Immunocomplexes were recovered by incubation with protein G-sepharose beads (Upstate). After washing, the immunocomplexes were analyzed by SDS-PAGE and immunoblotted with the appropriate antibodies and

horseradish peroxidase-conjugated secondary antibodies. Results were visualized using enhanced chemiluminescence (ECL).

Primary cell culture

Primary cortical neuronal cultures were prepared from embryonic day 18 mice as described (Rogers et al. 2004; Lee et al. 2008) and maintained in NeuroBasal Media (Gibco) supplemented with AraC (Sigma) for 3-7 days. Mouse embryonic fibroblast cultures were prepared from embryonic day 13 mice by using a well-established method (Bi et al. 2004; Ma et al. 2004; Olzmann et al. 2007), and early passage cells were used for all experiments.

Immunofluorescence confocal microscopy

Cells were fixed in 4% paraformaldehyde, stained with appropriate primary and secondary antibodies and processed for indirect immunofluorescence microscopy as described previously (Olzmann et al. 2004; Olzmann et al. 2007; Lee et al. 2008). Analysis and acquisition was performed using a Zeiss LSM 510 confocal laser-scanning microscope. Images were exported in TIFF format using LSM-510 software (Carl Zeiss MicroImaging, Inc.) and processed using Adobe Photoshop Version 7.0 software (Adobe Systems, Inc.) to adjust the contrast and brightness.

Quantitative analysis of the NE/ER distribution

Quantification of the NE/ER distribution of torsinA or KDEL was performed on unprocessed images of cells double labeled for torsinA and KDEL by using MetaMorph

Imaging System Software (Molecular Devices). Using the region tool in the MetaMorph program, we outlined the whole cell and demarcated the nuclear envelope area, which was clearly apparent in the KDEL staining of almost all images (Volpicelli et al. 2001; Volpicelli et al. 2002). The fluorescence in the cytoplasmic region outside of the nuclear envelope area was defined as the ER staining. The amount of torsinA or KDEL fluorescence in the NE and ER of each cell was quantified with MetaMorph as described previously (Volpicelli et al. 2001; Volpicelli et al. 2002; Kim et al. 2007). The obtained NE/ER ratio of torsinA was compared with that of the ER marker KDEL from the same double-labeled cell. For each torsinA genotype (torsinA WT, ΔE or Δ323-8), 30-45 cells were randomly selected for analysis. Analysis was carried out in a blinded manner by an investigator without any knowledge of torsinA genotype of the cells, and the result was confirmed by a second, independent investigator. Experiments were repeated at least three times, and the data were subjected to statistical analysis by unpaired Student's *t* test.

[^{35}S]Methionine pulse-chase analysis

Pulse-chase experiments were performed as described previously (Chin et al. 2002; Wheeler et al. 2002; Olzmann et al. 2004). Briefly, SH-SY5Y cells expressing C-terminally HA-tagged torsinA WT, ΔE or Δ323-8 were labeled by incubation for 1 hr with Met/Cys-free medium containing 100 μCi of [^{35}S]Met/Cys express protein labeling mix (MP Biologicals). After extensive washes, cells were incubated for the indicated chase time in non-radioactive media containing excess Met/Cys in the absence or presence of the proteasome inhibitor MG132 (20 μM, Sigma), the lysosomal cysteine protease inhibitor E64 (50 μM, Sigma), or vehicle [dimethyl sulfoxide (Me_2SO, DMSO);

final concentration, 0.1%]. At the indicated time points, cells were lysed and equal amount of proteins from each lysate was subjected to immunoprecipitation using an anti-HA antibody. Immunoprecipitated proteins were resolved by SDS-PAGE and analyzed by a PhosphorImager (Amersham Biosciences).

Treatment of cells with proteasome, autophagy, and lysosome inhibitors

SH-SY5Y cells expressing C-terminally HA-tagged wild-type or mutant torsinA were incubated for 24 hr at 37 ˚C with the proteasome inhibitor MG132 (20 μM, Sigma), the lysosome inhibitor chloroquine (100 μM, Sigma), the lysosome inhibitor ammonium chloride (NH_4Cl, 50 mM), the autophagy inhibitor 3-Methyladenine (3-MA, 10 mM) or vehicle [0.1 % Me_2SO (DMSO)]. Cells were then lysed, and an equal amount of proteins from each lysate was analyzed by immunoblotting for HA-tagged torsinA and actin. The relative level of wild-type or mutant torsinA was quantified by measuring the intensity of the torsinA band from the image of immunoblot using the NIH Image program and normalized against the actin level in the corresponding cell lysate from the same gel. To control for the possibility of overexposure, each immunoblot was subjected to multiple exposures. The intensities of the torsinA bands from at least two different exposures of the same immunoblot were quantified and the average of those numbers was used for comparison. Experiments were repeated at least three times, and the data were subjected to statistical analysis by unpaired Student's *t* test.

RESULTS

Analysis of torsinA localization reveals neuronal cell type-specific enrichment in the nuclear envelope

Given the widespread expression of torsinA (Shashidharan et al. 2000), it is unclear why torsinA mutations lead to a neuronal phenotype. To determine whether there is a difference between torsinA localization in neuronal versus non-neuronal cell types, we used human HeLa cells, a well-established non-neuronal cell line (Chin et al. 1994), and human SH-SY5Y cells, a dopaminergic neuronal cell model (Chin et al. 2002). Double-labeling immunofluorescence confocal microscopic analysis was performed to determine the intracellular distribution of C-terminally HA-tagged wild-type (WT) torsinA in HeLa and SH-SY5Y cells. We found that torsinA WT protein exhibited extensive co-localization with the ER marker KDEL in both HeLa and SH-SY5Y cells (Figure II-1A). Both torsinA WT and KDEL immunoreactivity was predominantly localized to the ER, but a subset of the signal was also found at the NE (Figure II-1A).

Because of the direct continuity of the ER and NE membranes (Ellenberg et al. 1997), it is difficult to find markers that are exclusively localized to the ER or NE. In addition, the amount of ER or NE membranes visible under the confocal microscope can vary greatly depending on the plane of focus. To control for these variables, we quantified the relative distribution of torsinA in NE and ER and compared the obtained NE/ER ratio with that of the ER marker KDEL from the same double labeling experiments. The result showed no significant difference between the relative NE/ER distribution of torsinA WT and that of KDEL in HeLa cells (Figure II-1B), indicating that torsinA WT is primarily associated with the ER in these non-neuronal cells. In contrast, the NE/ER ratio of torsinA WT was significantly greater than the NE/ER ratio of KDEL

in SH-SY5Y cells (Figure II-1B), indicating an enhanced preferential localization of torsinA WT to the NE compared to the ER marker KDEL in the neuronal cells. We found that the NE/ER ratio of KDEL in SH-SY5Y cells was significantly higher than the NE/ER ratio of KDEL in HeLa cells (Figure II-1B). To control for the cell-type variation in the relative NE/ER distribution of the ER marker, we determined the NE preference of torsinA by normalizing the NE/ER ratio of torsinA to the corresponding NE/ER ratio of KDEL in the same cells (Figure II-1C). The results showed that the NE preference of torsinA relative to KDEL was increased from 1.03 ± 0.04 in HeLa cells to 1.92 ± 0.8 in SH-SY5Y cells, indicating a neuronal cell type-specific enrichment of torsinA in the NE compared to the ER marker.

Next, we performed double-labeling immunofluorescence confocal microscopic analysis to examine the NE/ER distribution of endogenous torsinA in mouse embryonic fibroblasts and primary cortical neurons. We observed significant co-localization between endogenous torsinA and the ER marker KDEL in both fibroblasts and cortical neurons (Figure II-2A). Quantification analysis of the NE/ER distribution of torsinA and KDEL signal revealed no significant difference between the NE/ER ratio of torsinA and that of KDEL in fibroblasts (Figure II-2B), indicating that endogenous torsinA is primarily associated with the ER in these non-neuronal cells. In primary cortical neurons, however, the NE/ER ratio of endogenous torsinA was significantly greater than the NE/ER ratio of KDEL (Figure II-2B). After normalization to the NE/ER ratio of KDEL in the same cells, the NE preference of endogenous torsinA was increased from 0.97 ± 0.03 in fibroblasts to 1.58 ± 0.14 in cortical neurons. These data are consistent with the result of exogenous

torsinA localization in HeLa and SH-SY5Y cells (Figure II-1) and provide additional support for a neuronal cell-type specific enrichment of torsinA in the NE.

Dystonia-associated mutations cause neuronal cell type-specific translocation of torsinA from the ER to nuclear envelope

To determine the effects of dystonia-associated mutations on the subcellular localization of torsinA protein, we examined and compared the intracellular distribution of C-terminally HA-tagged torsinA WT, torsinA ΔE, and torsinA Δ323-8 mutants in HeLa (Figure II-3A) and SH-SY5Y (Figure II-3B) cells by double-labeling immunofluorescence confocal microscopy. We found that, in HeLa cells, torsinA ΔE and torsinA Δ323-8 mutants had similar NE/ER ratios compared to torsinA WT and KDEL (Figure II-3C), indicating that dystonia-associated mutations do not affect the subcellular localization of torsinA in these non-neuronal cells. However, in SH-SY5Y cells, both torsinA ΔE and torsinA Δ323-8 mutants showed a significantly higher NE/ER ratio compared to KDEL (Figure II-3C). Moreover, the NE/ER ratio of both torsinA mutants was significantly greater than that of torsinA WT in SH-SY5Y cells (Figure II-3C). After normalization to the NE/ER ratio of KDEL in the same SH-SY5Y cells, torsinA ΔE and torsinA Δ323-8 mutants had an NE preference of 2.29 ± 0.13 and 2.22 ± 0.11, respectively (Figure II-3D), both of which represent a significant increase in the percentage of NE-associated mutant torsinA compared to the NE localization of torsinA WT. Together, these results indicate that dystonia-associated mutations induce translocation of torsinA from the ER to NE in neuronal cells but not in non-neuronal cells.

Dystonia-associated mutations do not disrupt torsinA oligomerization

Given our finding that dystonia-associated mutations selectively alter torsinA localization in SH-SY5Y cells but not in HeLa cells (Figure II-3) and our interest in addressing issues that are pertinent to the neuronal phenotype of dystonia, we focused the remainder of our studies of wild-type and mutant torsinA proteins in SH-SY5Y cells. Since torsinA belongs to the AAA^+ family of ATPases and many AAA^+ members oligomerize and are only functional in their oligomerized state (Dalal and Hanson 2001; Lupas and Martin 2002; Hanson and Whiteheart 2005), we performed co-immunoprecipitation experiments to examine the *in vivo* self-association of wild-type and dystonia-associated mutant torsinA in SH-SY5Y cells. As shown in Figure II-4A, Myc-tagged torsinA WT co-immunoprecipitated with HA-tagged torsinA WT, but not with the HA vector alone, indicating the presence of torsinA WT oligomers in SH-SY5Y cells. We found that both dystonia-associated torsinA ΔE and torsinA Δ323-8 mutants were able to co-immunoprecipitate torsinA WT (Figure II-4B), demonstrating that the ability of torsinA to oligomerize is not altered by dystonia-associated mutations.

TorsinA oligomerization does not require its C-terminal region

Given the involvement of the C-terminal region in the oligomerization of several AAA^+ proteins (Ogura and Wilkinson 2001), we next tested whether the C-terminal region of torsinA is required for its oligomerization. We made a torsinA N-terminal (NT) expression construct (Figure II-5A) by deleting its C-terminal region (residues 189-332) and examined the ability of torsinA NT to bind torsinA WT by co-immunoprecipitation.

The result showed that torsinA NT was able bind torsinA WT in SH-SY5Y cells (Figure II-5B), suggesting that the C-terminal region of torsinA is not required for its oligomerization. Moreover, we found that the interaction between torsinA NT with full-length torsinA was not affected by dystonia-associated torsinA ΔE and torsinA Δ323-8 mutations (Figure II-5C), further supporting the results seen in Figure II-4.

Dystonia-associated mutations destabilize torsinA protein

Next, we performed pulse-chase experiments to determine whether dystonia-associated torsinA ΔE and torsinA Δ323-8 mutations alter torsinA protein stability in SH-SY5Y cells. As shown in Figure II-6A, torsinA WT had a half-life of ~80 hr, indicating that torsinA is normally a very stable protein. In contrast, we found that more than 70% of torsinA ΔE and torsinA Δ323-8 mutant proteins had been degraded at the 24-hr chase time point (Figure II-6A), suggesting that both dystonia-associated mutant proteins are considerably less stable compared to wild-type torsinA. To further examine the effects of dystonia-associated mutations on torsinA turnover rate, we took a closer look at the first 24-hr time period by performing additional pulse-chase experiments which measured the changes in wild-type and mutant torsinA protein levels every 6 hours. We found the half-lives of torsinA ΔE and torsinA Δ323-8 mutant proteins were reduced to ~18 hr (Figure II-6B), further confirming that dystonia-associated mutations accelerate the degradation of torsinA.

Dystonia-associated mutations promote the degradation of torsinA by both the proteasome and autophagy-lysosome pathways

The ubiquitin-proteasome pathway is a major intracellular proteolytic system for the degradation of both normal cellular proteins and misfolded proteins (Ciechanover 2005; Rubinsztein 2006). Misfolded ER proteins are usually retrotranslocated to the cytoplasm for degradation by the proteasome through a process known as ER-associated degradation (ERAD) (Meusser et al. 2005; Nishikawa et al. 2005). Whether the proteasome participates in the degradation of misfolded NE proteins or normal ER and NE proteins remains unclear. To determine whether the proteasome is involved in the degradation of wild-type or mutant torsinA proteins, we first examined the effects of proteasome inhibition on the steady-state levels of torsinA WT, torsinA ΔE, and torsinA Δ323-8 in SH-SY5Y cells. We found that, in vehicle (DMSO)-treated control cells, the steady-state levels of both torsinA ΔE and torsinA Δ323-8 mutant proteins were significantly ($p < 0.05$) lower than the steady-state level of torsinA WT (Figure II-7), in agreement with the decreased stability of these torsinA mutants observed in the pulse-chase experiments (Figure II-6). The steady-state levels of torsinA ΔE and torsinA Δ323-8 mutant proteins were significantly ($p < 0.05$) increased by treatment of cells with the proteasome inhibitor MG132 (Figure II-7). In contrast, proteasome inhibition by MG132 had no significant effect on the steady-state level of wild-type torsinA (Figure II-7). Moreover, pulse-chase analysis revealed that proteasome inhibition selectively delayed degradation of torsinA ΔE and torsinA Δ323-8 mutants, but not torsinA WT protein (Figure II-8). Together, these results provide strong evidence supporting a role for the proteasome in the selective degradation of dystonia-associated mutant torsinA proteins.

The autophagy-lysosome pathway is another major intracellular proteolytic system for degradation of both normal cellular proteins and misfolded proteins

(Ciechanover 2005; Rubinsztein 2006). This pathway involves the formation of a double-membrane structure called an autophagosome to engulf a portion of the cytoplasm and the subsequent fusion of the autophagosome with the lysosome to allow the degradation of its contents by lysosomal hydrolases. In contrast to proteasome-mediated degradation, which requires proteins to be first unfolded for entry into the 20S proteasome core particle, the autophagy-lysosome pathway is able to breakdown completely folded proteins, misfolded and aggregated proteins, as well as entire organelles (Xie and Klionsky 2007). To determine whether the autophagy-lysosome pathway is involved in the degradation of wild-type or mutant torsinA proteins, we examined the effects of pharmacological inhibition of this pathway on steady-state levels of torsinA WT, torsinA ΔE, and torsinA Δ323-8 in SH-SY5Y cells (Figure II-7). We assessed the changes in the steady-state levels caused by treatment with the following inhibitors: chloroquine and ammonium chloride (NH_4Cl), which inhibit the lysosomal proteases by raising the pH, and 3-methyladenine (3-MA), a specific inhibitor of autophagosome formation (Seglen and Gordon 1982). We found that treatment with each of these three inhibitors significantly ($p < 0.05$) increased the steady-state levels of torsinA WT, torsinA ΔE, and torsinA Δ323-8 proteins (Figure II-7), suggesting that the autophagy-lysosome pathway is involved in the degradation of wild-type torsinA as well as the dystonia-associated mutant torsinA proteins. In addition, our pulse-chase analysis revealed that the rates of degradation of torsinA WT, torsinA ΔE, and torsinA Δ323-8 proteins in SH-SY5Y cells were significantly ($p < 0.05$) reduced by the lysosomal cysteine protease inhibitor E64 (Figure II-8), providing additional support for a role of the autophagy-lysosome pathway in the degradation of wild-type torsinA and dystonia-associated mutant torsinA proteins.

DISCUSSION

Given the widespread expression of torsinA in multiple tissues and cell types, it is unclear why genetic mutations in human torsinA result in mainly a neuronal phenotype (Shashidharan et al. 2000). In addition, it is not understood why torsinA null and torsinA ΔE knock-in mice have abnormal NE membranes in neurons but not in non-neuronal cells (Goodchild et al. 2005). Previous studies have reported the mislocalization of torsinA ΔE to the NE in both neuronal and non-neuronal cell types f(Gonzalez-Alegre and Paulson 2004; Naismith et al. 2004; Goodchild and Dauer 2005; Kock et al. 2006). However, these studies did not provide a quantitative analysis of the relative NE/ER distribution which is crucial given the direct continuity between the NE and ER. In addition, the torsinA Δ323-8 mutation has not been included in these studies. By using quantitative double-labeling immunofluorescence confocal microscopic analysis of the relative NE/ER distribution, we found that wild-type torsinA shows a preferential localization to the NE in neuronal SH-SY5Y cells compared to torsinA WT in non-neuronal HeLa cells. Similar preferential NE localization was also observed for endogenous torsinA in primary cortical neurons compared to endogenous torsinA in fibroblasts. The preferential NE localization suggests that torsinA may have a neuronal cell-specific role at the NE. In addition, our results indicate that the dystonia-associated torsinA ΔE and torsinA Δ323-8 mutations cause translocation of torsinA from the ER to NE in SH-SY5Y cells but not in HeLa cells. Together, these data suggest that the

neuronal NE may be especially susceptible to torsinA dysfunction, which help explain the neuronal cell-specific phenotype of dystonia-associated torsinA mutations.

Previous studies regarding torsinA oligomerization have been controversial (Kustedjo et al. 2003; Torres et al. 2004; Pham et al. 2006). Our data suggest that torsinA WT is capable of self-associating into an oligomeric complex. Because the C-terminal region of AAA^+ proteins is thought to be necessary for oligomerization (Ogura and Wilkinson 2001), it has been suggested that the dystonia-associated mutations may disrupt oligomerization. A previous study showed that torsinA ΔE mutation disrupted interaction with torsinA WT and torsinA ΔE and prevented formation of a stable oligomeric complex (Pham et al. 2006). In contrast, Torres et al. reported that the ΔE mutation appears to render torsinA more susceptible to oligomerization (Torres et al. 2004), and it has been shown that the presence of torsinA ΔE can increase the amount of torsinA WT in the nuclear envelope (Goodchild and Dauer 2004). Our results indicate that neither of the dystonia-associated mutations disrupts the ability of torsinA to self-associate. To further analyze torsinA self-interaction, we created a deletion mutant that lacked the C-terminal region. The N-terminal portion of torsinA was able to interact with torsinA WT as well as with both dystonia-associated mutant forms of torsinA, suggesting that the N-terminal region of torsinA is sufficient for oligomerization.

The structural and functional consequences of torsinA Δ323-8 mutation remain mostly unknown. Due to its co-occurrence with a mutation in another dystonia-related protein, epsilon-sarcoglycan (Klein et al. 2002), it is unclear whether Δ323-8 is actually a dystonia-causing mutation. In addition, its reported lack of apparent mislocalization phenotype has led to the suggestion that the Δ323-8 and ΔE mutant torsinA proteins may

follow different pathogenic pathways (O'Farrell et al. 2002). Our finding that both Δ323-8 and ΔE mutations in torsinA cause enhanced NE preference and premature degradation suggest that these two mutations share the same pathogenic pathway.

Many neurological diseases, including familial Alzheimer's disease and Parkinson's disease, have been linked to mutations in proteins that render them unstable and result in premature degradation and subsequent loss of function (Bross et al. 1999; Olzmann et al. 2004). Our data suggest that this could also be a pathogenic mechanism for DYT1 dystonia. Previous studies have shown that torsinA ΔE inhibits torsinA function (McLean et al. 2002; Torres et al. 2004; Hewett et al. 2006; Muraro and Moffat 2006) and that torsinA null and torsinA ΔE knock-in mice display similar phenotypes (Goodchild et al. 2005), suggesting that torsinA ΔE is a loss-of-function mutation. We found that, although the wild-type torsinA is a highly stable protein with a half-life of several days, both torsinA ΔE and torsinA Δ323-8 mutant proteins have significantly reduced half-lives, indicating a higher rate of turnover, which suggests that the torsinA mutant proteins are unstable or misfolded. Our data provide, for the first time, evidence that torsinA ΔE and torsinA Δ323-8 mutations cause premature degradation of torsinA and support a loss-of-function pathogenic mechanism for both dystonia-associated mutations.

The ubiquitin-proteasome and autophagy-lysosome pathways are the two main routes of protein degradation in cells (Ciechanover 2005; Rubinsztein 2006). The proteasome pathway usually mediates selective degradation of short-lived regulatory proteins and misfolded proteins, whereas the autophagy-lysosome pathway is a relatively non-selective, bulk clearance system that is primarily responsible for the turnover of

long-lived proteins as well as organelles (Ding and Yin 2008). Our inhibitor studies reveal that wild-type torsinA is degraded through the autophagy-lysosome pathway but not the proteasome pathway, consistent with our finding that torsinA WT is a long-lived, ER/NE protein.

Although proteasome inhibition did not affect degradation of wild-type torsinA, it significantly delayed the degradation of both torsinA ΔE and torsinA Δ323-8 mutant proteins, indicating that dystonia-associated torsinA mutant proteins, but not wild-type torsinA, is selectively targeted to the proteasome for degradation. The mechanism(s) by which torsinA ΔE and torsinA Δ323-8 mutant proteins are specifically recognized and earmarked for proteasome-mediated degradation is unclear. One possibility is that torsinA ΔE and torsinA Δ323-8 mutations induce aberrant folding of torsinA protein, leading to exposure of hydrophobic patches or unmasking of a cryptic degron. The hydrophobic patches or degron serve as a signal for recognition by an ER chaperone or E3 ubiquitin-protein ligase, which cooperates with other ERAD components to facilitate retrotranslocation from the ER to the cytosol and delivery of torsinA mutant proteins to the proteasome for degradation (Meusser et al. 2005; Nishikawa et al. 2005; Kostova et al. 2007). Our data indicate that, in addition to proteasome–mediated degradation, the autophagy-lysosome pathway is also involved in the clearance of dystonia-associated torsinA ΔE and torsinA Δ323-8 mutant proteins. These results support the emerging view that the autophagy-lysosome pathway provides an alternative ER quality control mechanism for the clearance of misfolded proteins in the ER lumen (Yorimitsu and Klionsky 2007). In conclusion, our findings obtained from this study provide new insights into the pathogenic mechanisms of torsinA ΔE and torsinA Δ323-8 mutations

and have important implications for developing novel therapeutic strategies to treat dystonia.

ACKNOWLEDGEMENTS

This work was supported by grants from National Institutes of Health (NS054334, AG021489, NS050650, and ES015813).

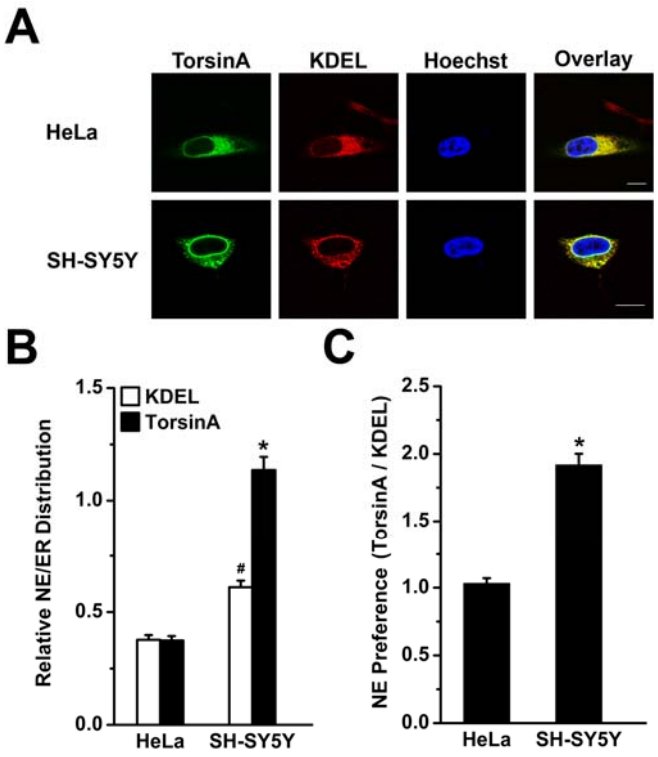

FIGURE II-1. TorsinA is enriched in the nuclear envelope in SH-SY5Y cells but not in HeLa cells. (A) HeLa or SH-SY5Y cells expressing C-terminally HA-tagged torsinA WT were stained with primary antibodies against HA and ER marker KDEL, followed by detection with secondary antibodies conjugated to TR (KDEL, red) or FITC (torsinA, green). Hoechst stain was used to visualize the nucleus. **(B)** Quantification shows the relative distribution of torsinA and KDEL in the NE versus the ER. Data represent mean ± S.E. from at least three independent experiments. *Significantly different from the NE/ER ratio of KDEL in SH-SY5Y cells ($p < 0.05$). #Significantly different from the NE/ER ratio of KDEL in HeLa cells ($p < 0.05$). **(C)** NE preference of torsinA was determined by normalizing the NE/ER ratio of torsinA in HeLa or SH-SY5Y cells to the corresponding NE/ER ratio of KDEL in the same cells. Data represent mean ± S.E. from

at least three independent experiments. *Significantly different from HeLa cells ($p < 0.05$). Scale bars, 10 μm.

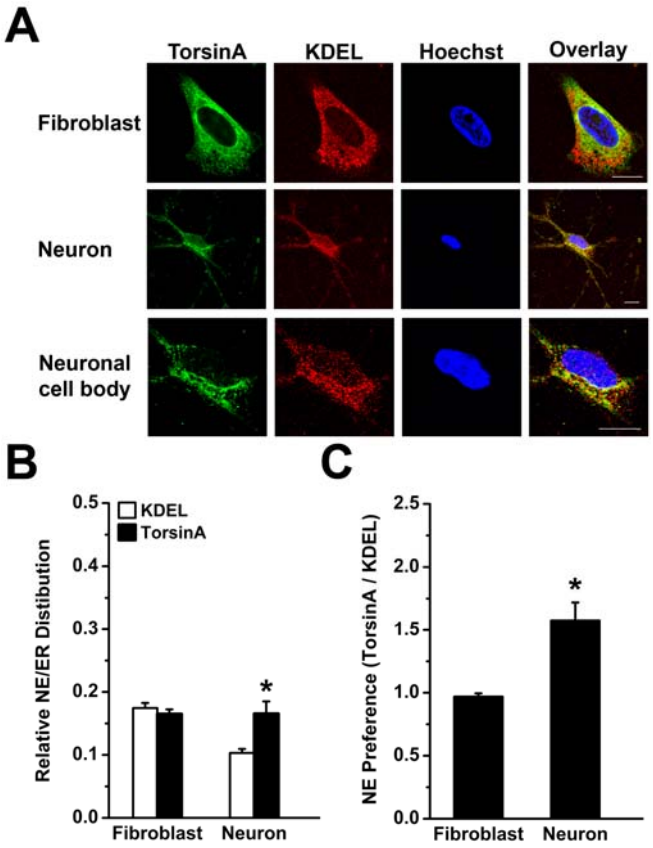

FIGURE II-2. Endogenous torsinA shows preferential NE localization in primary cortical neurons compared to fibroblasts. (A) Mouse embryonic fibroblasts or primary cortical neurons were stained with primary antibodies against torsinA and ER marker KDEL, followed by detection with secondary antibodies conjugated to TR (KDEL, red) or FITC (torsinA, green). Hoechst stain was used to visualize the nucleus. Neuronal cell body shows an enlarged view of the cell body area from the same neuron. **(B)** Quantification shows the relative distribution of torsinA and KDEL in the NE versus the ER. Data represent mean ± S.E. from at least three independent experiments. *Significantly different from the NE/ER ratio of KDEL in cortical neurons ($p < 0.05$). **(C)** NE preference of torsinA was determined by normalizing the NE/ER ratio of torsinA in fibroblasts or neurons to the corresponding NE/ER ratio of KDEL in the same cells.

Data represent mean ± S.E. from at least three independent experiments. *Significantly different from fibroblasts ($p < 0.05$). Scale bars, 10 μm**.**

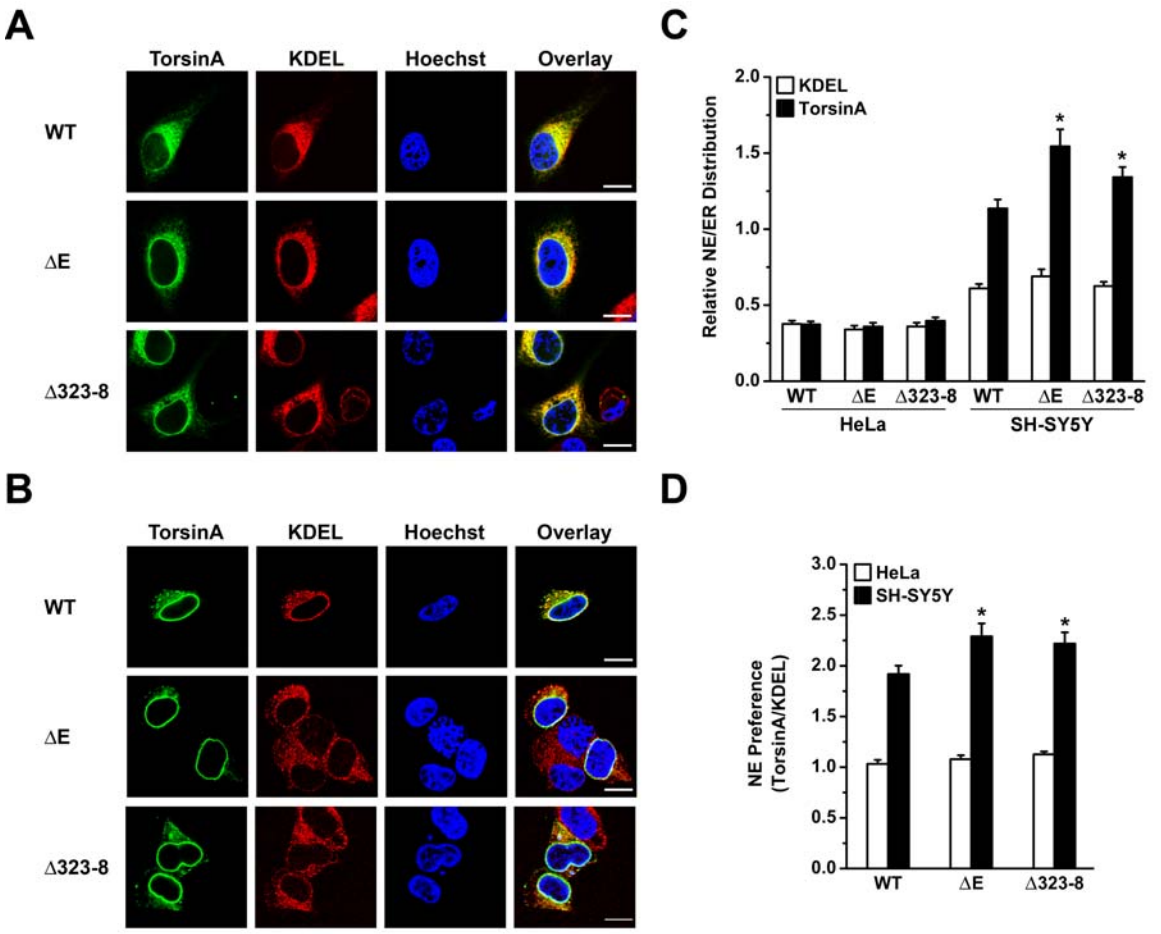

FIGURE II-3. Dystonia-associated mutations cause torsinA translocation to the nuclear envelope in SH-SY5Y cells but not in HeLa cells. (A) HeLa or **(B)** SH-SY5Y cells expressing C-terminally HA-tagged torsinA WT, ΔE, or Δ323-8 were stained with primary antibodies against HA and ER marker KDEL, followed by detection with secondary antibodies conjugated to TR (KDEL, red) or FITC (torsinA, green). Hoechst stain was used to visualize the nucleus. **(C)** Quantification shows the relative distribution of torsinA and KDEL in the NE versus the ER. Data represent mean ± S.E. from at least three independent experiments. *Significantly different from the NE/ER ratio of torsinA WT in SH-SY5Y cells ($p < 0.05$). **(D)** NE preference of torsinA was determined by normalizing the NE/ER ratio of torsinA in HeLa or SH-SY5Y cells to the corresponding

NE/ER ratio of KDEL in the same cells. Data represent mean ± S.E. from at least three independent experiments. *Significantly different from the NE preference of torsinA WT in SH-SY5Y cells ($p < 0.05$). Scale bars, 10 μm.

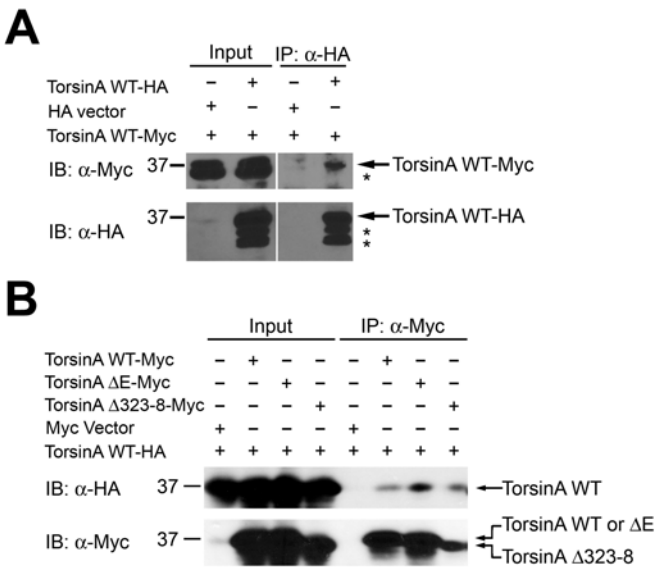

FIGURE II-4. Dystonia-associated mutations have no effect on torsinA oligomerization. (A) Interaction of torsinA WT with itself. SH-SY5Y cells expressing C-terminally Myc-tagged torsinA WT and C-terminally HA-tagged torsinA WT or HA vector were lysed and subjected to immunoprecipitation with anti-HA antibody followed by immunoblotting with anti-HA and anti-Myc antibodies. *Asterisks* indicate torsinA degradation products. **(B)** Interaction of torsinA WT with dystonia-associated mutant torsinA. SH-SY5Y expressing C-terminally HA-tagged torsinA WT and either C-terminally Myc-tagged torsinA WT, ΔE, Δ323-8 or Myc vector were lysed and subjected to immunoprecipitation with anti-Myc antibody followed by immunoblotting with anti-HA and anti-Myc antibodies.

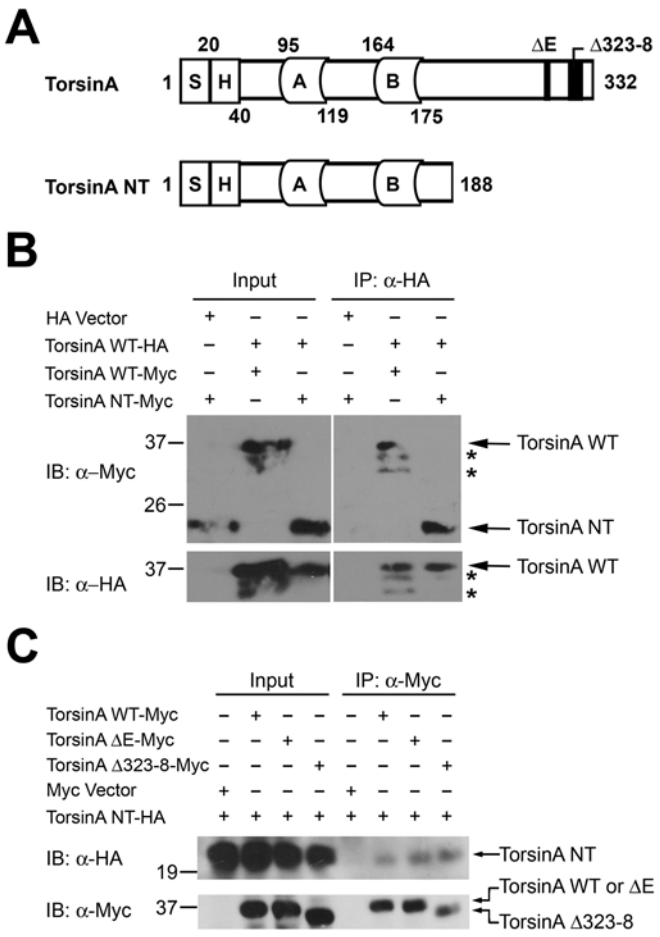

FIGURE II-5. The N-terminal region of torsinA is sufficient for torsinA oligomerization. (A) Domain structure of torsinA and its deletion construct. *S*, signal sequence; *H*, hydrophobic domain; *A*, Walker A motif; *B*, Walker B motif. **(B)** Interaction of torsinA WT with torsinA N-terminal region (NT). SH-SY5Y cells expressing C-terminally Myc-tagged torsinA WT or NT and C-terminally HA-tagged torsinA WT or HA vector were lysed and subjected to immunoprecipitation with anti-HA antibody followed by immunoblotting with anti-HA and anti-Myc antibodies. *Asterisks* indicate torsinA degradation products. **(C)** Interaction of dystonia-associated mutants with torsinA N-terminal region. SH-SY5Y cells expressing C-terminally HA-tagged torsinA NT and C-terminally Myc-tagged torsinA WT, ΔE, Δ323-8 or Myc vector were

lysed and subjected to immunoprecipitation with anti-Myc antibody followed by immunoblotting with anti-HA and anti-Myc antibodies.

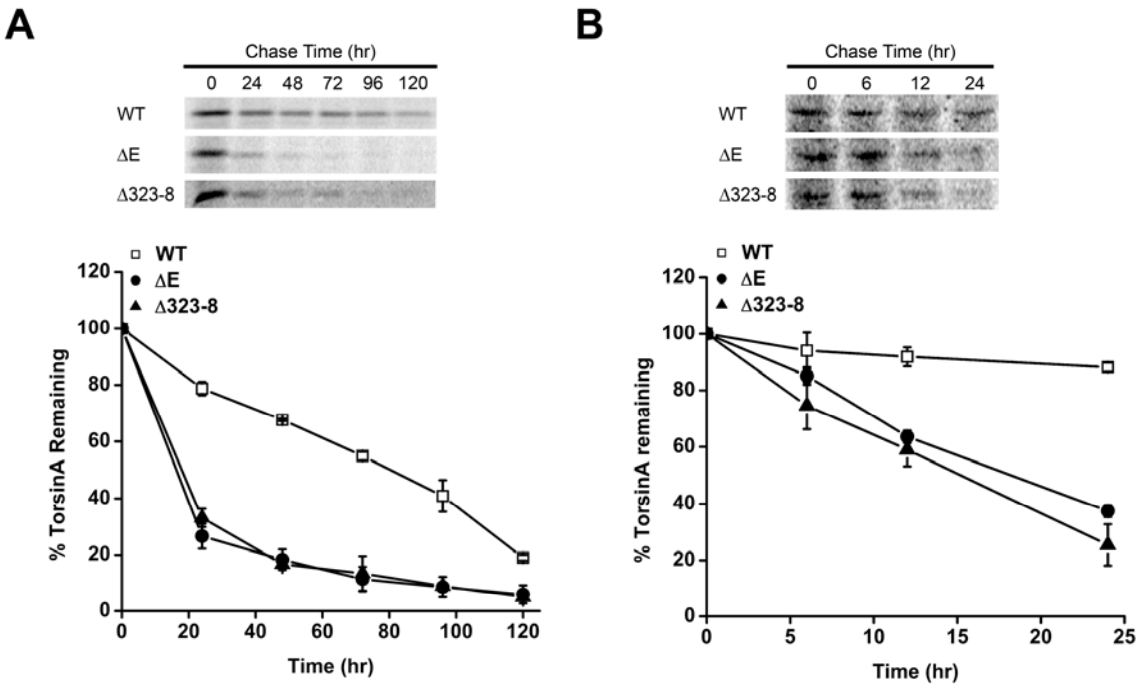

FIGURE II-6. Dystonia-associated mutations cause premature degradation of torsinA protein. SH-SY5Y cells expressing HA-tagged torsinA WT (open square), ΔE (closed circle) or Δ323-8 (closed triangle) were pulse-labeled for 1 hr in [^{35}S]Met/Cys-containing medium and chased with non-radioactive Met/Cys for the indicated time. Time points were taken every 24 hr over 5 days **(A)** and every 6 hr over the first 24 hr **(B)**. ^{35}S-labeled WT or mutant torsinA proteins were immunoprecipitated from lysates with anti-HA antibodies and detected by SDS-PAGE and autoradiography. The levels of wild-type or mutant torsinA proteins were quantified and plotted relative to the corresponding torsinA levels at 0 h. Data represent mean ± S.E. of the results from at least three independent experiments.

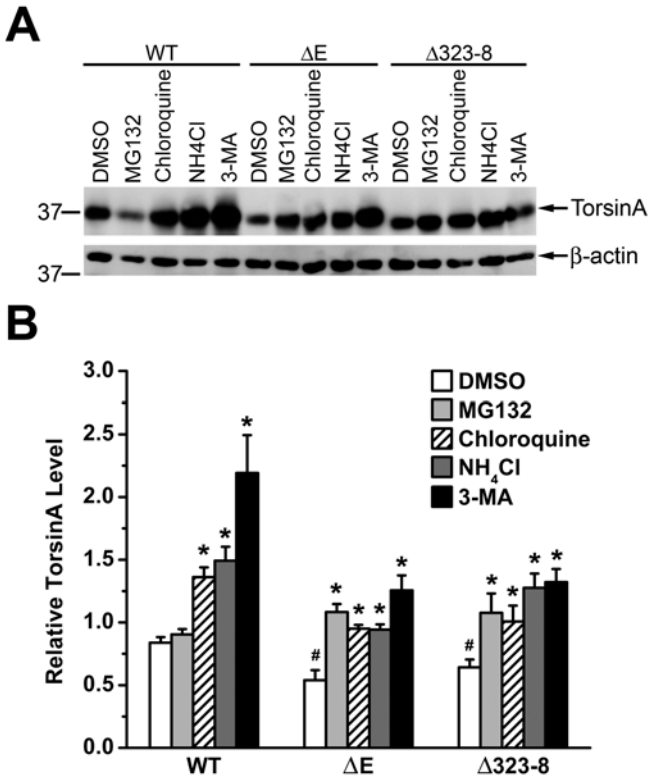

FIGURE II-7. Effects of proteasome, autophagy, and lysosome inhibition on wild-type and mutant torsinA levels. (A) SH-SY5Y cells expressing HA-tagged torsinA WT, ΔE or Δ323-8 were treated with the indicated proteolysis inhibitors or DMSO control. Lysates were analyzed by SDS-PAGE and immunoblotting with anti-HA and anti-actin antibodies. **(B)** The relative level of wild-type or mutant torsinA was measured by quantification of the intensity of the wild-type or mutant torsinA band and normalized to the actin level in the corresponding cell lysate. Results are shown as mean ± S.E. from at least three independent experiments. *Significantly different from the corresponding vehicle (DMSO)-treated control cells expressing the same type of torsinA ($p < 0.05$). #Significantly different from the vehicle-treated, torsinA WT-expressing cells ($p < 0.05$).

.

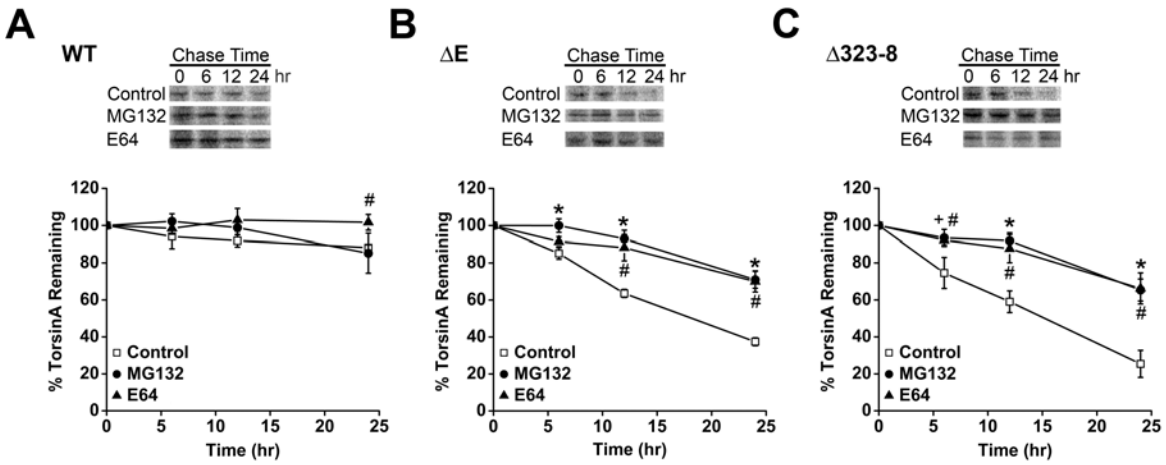

FIGURE II-8. Degradation of torsinA mutants by both the proteasome and lysosome pathways. SH-SY5Y cells expressing HA-tagged torsinA WT **(A)**, ΔE **(B)**, or Δ323-8 **(C)** were pulse labeled for 1 h with medium containing [^{35}S]Met/Cyc and chased with non-radioactive Met/Cys containing MG132 (closed circle), E64 (closed triangle), or vehicle control (open square) for the indicated time. Lysates were immunoprecipitated with anti-HA antibodies and detected by SDS-PAGE and autoradiography. Proteins levels were quantified using a PhosphorImager and plotted relative to the corresponding torsinA levels at 0 h. Data are shown as mean ± S.E. of the results from at least three independent experiments. The *asterisks* indicate a statistically significant ($p < 0.05$) increase in the level of torsinA in MG132-treated cells versus vehicle-treated controls. The *plus sign* indicates an increase approaching significance ($p < 0.065$) in the level of torsinA in MG132-treated cells versus vehicle-treated controls. The *pound signs* indicate a statistically significant ($p < 0.05$) increase in the level of torsinA in E64-treated cells versus vehicle-treated controls.

CHAPTER III

PRINTOR, A NOVEL TORSINA-INTERACTING PROTEIN IMPLICATED IN DYSTONIA PATHOGENESIS

Part of the work described in this chapter is in preparation for submission to *Human Molecular Genetics*

Giles, L.M., Li, L., and Chin, L.-S. (2008) Printor, a novel torsinA-interacting protein implicated in dystonia pathogenesis. In preparation.

ABSTRACT

Early-onset torsion dystonia (DYT1) has been linked to two mutations in the C-terminus of the protein torsinA. Although several torsinA-interacting proteins have been reported, none has been demonstrated to have altered interaction properties with either dystonia-associated mutant compared to torsinA WT. Here we report the identification and characterization of a novel torsinA-interacting protein, printor. Printor co-distributes with torsinA in brain and other tissues, and exists in both cytosolic and membrane-associated pools. Printor is localized to the ER, where it co-localizes with torsinA. Unlike torsinA, which shows an NE preference in neuronal cell-types, printor localizes predominantly to the ER. Printor shows reduced levels of co-localization with ΔE torsinA and ATP-bound torsinA. Furthermore, printor does not interact with ΔE torsinA or ATP-bound torsinA. Printor is therefore unlikely to be a torsinA substrate, but may play a regulatory role. These findings suggest that printor is a novel component of the DYT1 pathogenic pathway.

INTRODUCTION

Early onset generalized dystonia (DYT1) is the most common and severe form of hereditary dystonia, a movement disorder characterized by involuntary movements and prolonged muscle contraction, resulting in twisting body motions, tremor, and abnormal posture (Bressman et al. 2001). DYT1, which is autosomal dominant with a 30-40% penetrance and usually presents between ages 1 and 28 has been linked to two independent mutations (Ozelius et al. 1997; Leung et al. 2001) of the *dyt1* gene on chromosome 9q34, which encodes the protein torsinA (Ozelius et al. 1997). A 3 base pair (GAG) deletion that results in the loss of one of a pair of glutamine residues at position 302/303 (torsinA ΔE) is responsible for most inherited cases of DYT1 (Ozelius et al. 1997). In addition, a second mutation, an 18 base pair in frame deletion that results in the loss of amino acids F323-Y328 (torsinA Δ323-8), has been identified in a single family (Leung et al. 2001).

TorsinA is expressed in multiple tissues (Shashidharan et al. 2000), and displays a widespread expression pattern in the brain. TorsinA has been seen in the cytoplasm, neuronal processes and synaptic terminals in rat and human brains (Shashidharan et al. 2000; Konakova and Pulst 2001; Walker et al. 2001; Walker et al. 2002; Augood et al. 2003; Rostasy et al. 2003; Xiao et al. 2004), and has been shown to co-localize with markers of the endoplasmic reticulum (ER) and the nuclear envelope (NE) in cultured cells (Hewett et al. 2000; Gonzalez-Alegre and Paulson 2004; Goodchild and Dauer 2004; Kamm et al. 2004; Naismith et al. 2004; Giles et al. 2008). In neuronal cell-types, torsinA displays an increased presence in the NE, compared to non-neuronal cells, a

phenotype which is further enhanced by both dystonia-associated mutations (Giles et al. 2008). However, a number of identified torsinA-interacting proteins are cytosolic proteins (Kamm et al. 2004; Hewett et al. 2006; Granata et al. 2008), suggesting that a population of torsinA faces the cytosol, or that a cytosolic pool of torsinA protein exists.

Although the specific function of torsinA is currently unknown, sequence analysis reveals torsinA to be a member of the AAA^+ (ATPases associated with a variety of cellular activities) superfamily of Walker type ATPases (Beyer 1997; Ozelius et al. 1997; Ozelius and Breakefield 1998). Because members of the AAA^+ family are known to facilitate changes in protein conformation (Neuwald et al. 1999; Ogura and Wilkinson 2001), it has been hypothesized that torsinA may function as a chaperone protein (Shashidharan et al. 2000; Sharma et al. 2001; McLean et al. 2002; Caldwell et al. 2003; Walker et al. 2003; Caldwell and Caldwell 2004). TorsinA shares homology with the Hsp100/ClpB family of molecular chaperones (Ozelius and Breakefield 1998), and several studies display a chaperone-like activity in torsinA that is disrupted by the ΔE mutation (McLean et al. 2002; Caldwell et al. 2003; Caldwell and Caldwell 2004). However, it is still not clear how torsinA chaperone activity is utilized in the cell, nor have any endogenous substrates been identified.

TorsinA null mice die within 48 hours of birth and display a neuron-specific abnormal NE ultrastructure (Goodchild et al. 2005). Mice homogeneously expressing the ΔE torsinA mutation display a similar phenotype to torsinA null mice, which has led to the suggestion that the ΔE torsinA mutation is a loss of function mutation (Goodchild et al. 2005). Transgenic knock-in mice develop gait abnormalities, impaired motor learning (Dang et al. 2005; Sharma et al. 2005; Shashidharan et al. 2005; Grundmann et al. 2007;

Zhao et al. 2008), as well as alterations in dopamine levels, release or turnover (Shashidharan et al. 2005; Balcioglu et al. 2007; Grundmann et al. 2007; Zhao et al. 2008). Similar alterations in dopamine uptake and turnover have also been reported in DYT1 patients (Otsuka et al. 1992; Augood et al. 2002). In an inducible torsinA knock-down model, mice displayed a similar phenotype to knock-in models, further supporting the idea that ΔE torsinA is a loss of function mutation (Dang et al. 2006).

It is unclear why mutations to torsinA result in a neurological disease (Shashidharan et al. 2000). Because both dystonia related mutations occur in the C-terminus, which is thought to be involved in protein-protein interactions (Neuwald et al. 1999; Ogura and Wilkinson 2001), dystonia-related mutations may disrupt normal torsinA function by altering the properties of necessary interactions. However, torsinA mutation does not appear to affect its ability to interact with any of its known interacting proteins (Kamm et al. 2004; Torres et al. 2004; Hewett et al. 2006; Esapa et al. 2007; Granata et al. 2008). To identify additional players in the torsinA pathogenic pathway, we performed yeast two-hybrid screens to search for torsinA-interacting proteins in the brain. In this study, we report the identification of a novel torsinA-interacting protein named printor (protein interactor of torsinA). We characterized the expression of the printor protein in tissues and brain regions, and examined the subcellular localization of printor in neuroblastoma cells. Moreover, we investigated the effects of dystonia-associated torsinA mutations and torsinA ATP bound state on the interaction. Our results reveal that printor is a ubiquitously expressed protein that localizes and interacts with torsinA at the ER. Moreover, printor is the first identified torsinA-interacting protein that interacts with

torsinA WT but not torsinA ΔE, which suggests that printor may play a role in the pathogenic development of DYT1.

EXPERIMENTAL PROCEDURES

Expression constructs and antibodies

Full-length human printor cDNA was received from KIAA (accession number AB037805). Conventional molecular biological techniques (Sambrook et al. 1989) were used to subclone DNA fragments encoding full-length and truncated forms of torsinA, and full-length printor into the pPC97 and pPC86 vectors for yeast two-hybrid interaction studies. Full-length printor was also subcloned into mammalian vectors expressing N-terminal HA, Myc or FLAG tags for transfection into cells. DNA fragments encoding torsinA WT, WTΔ40, ΔE, Δ323-8, K108A, and E171Q were also subcloned into mammalian vectors expressing C-terminal HA, Myc, or FLAG tags for transfection into cells. A rabbit polyclonal anti-printor antibody was raised against the N-terminal region of printor and affinity purified as described previously (Chin et al. 2000; Kwong et al. 2000; Kirk et al. 2006). Other antibodies used in this study are as follows: anti-torsinA (Giles et al. 2008); anti-EEA1 and anti-Tim23 (BD transduction); anti-LAMP-2 (H4B4; DSHB-U of Iowa); anti-FLAG (M2; Sigma); anti-calnexin; anti-KDEL (Stressgen); anti-β-actin (Chemicon); mouse monoclonal anti-HA (12CA5); and anti-Myc (9E10) (Kirk et al. 2006). Horseradish peroxidase-conjugated secondary antibodies were used for immunoblotting (Jackson Immunoresearch Laboratories, Inc.). Flourescein isothiocyanate (FITC)-, Texas Red (TR)-, and Cy-5-conjugated secondary antibodies

were used for immunofluorescence microscopy (Jackson Immunoresearch Laboratories, Inc.).

Yeast two-hybrid screen

The bait plasmids were constructed by inserting the entire open reading frame of wild type (WT) or N-terminally truncated WT (WTΔ40) human torsinA into the vector pPC97 (Kwong et al. 2000; Chin et al. 2001; Kirk et al. 2006). The yeast strain CG-1945 (Clontech) was sequentially transformed with bait plasmid and a rat hippocampal/cortical two-hybrid cDNA library (Chin et al. 2000; Li et al. 2002; Kirk et al. 2006). Positive clones were selected on 3-aminotriazole-containing medium lacking leucine, tryptophan, and histidine, and confirmed by filter assay for β-galactosidase activity. Prey plasmids from positive clones were rescued and re-transformed into fresh yeast cells with the torsinA bait(s) to confirm the interaction.

Western blot analysis

Rat tissues were homogenized in 1% SDS and subjected to SDS-PAGE. The proteins were transferred onto nitrocellulose membranes and probed with anti-printor, anti-torsinA and anti-actin antibodies. Antibody binding was detected by using enhanced chemiluminescence (ECL).

Immunofluorescence microscopy

Cells were fixed in 4% paraformaldehyde, stained with appropriate primary and secondary antibodies and processed for indirect immunofluorescence microscopy as

described previously (Olzmann et al. 2004; Kirk et al. 2006; Olzmann et al. 2007; Giles et al. 2008; Lee et al. 2008). Analysis and acquisition were performed using a Zeiss LSM 510 confocal laser-scanning microscope. Images were imported in TIFF format using LSM-510 software (Carl Zeiss MicroImaging, Inc.) and processed using Adobe Photoshop CS Version 8.0 (Adobe Systems, Inc.) to adjust the contrast and brightness.

Immunohistochemistry

Mice were euthanized under deep flurothane anesthesia and brains were removed and immersed in 4% paraformaldehyde fixative over night. Brains were sliced coronally in 1- to 2-mm slices, dehydrated in a graded series of alcohols and xylenes, and infiltrated with paraffin using an automated tissue processor (Shandon Hypercenter XP), and then embedded in paraffin blocks. Eight-micrometer sections were cut using a Shandon AS325 microtome. Eight-micrometer-thick paraffin-embedded sections were immunohistochemically labeled as described (Gearing et al. 1993). Briefly, sections were deparaffinized in a series of xylenes and graded alcohols and were blocked with normal serum and then incubated with purified anti-printor antibody, followed by biotinylated secondary antibody and avidin–biotin–peroxidase complex (ABC Elite Kit; Vector Laboratories, Burlingame, CA). The chromagen used for color development was 3,3′-diaminobenzidine (DAB), and sections were counterstained with hematoxylin. Negative control consisted of omission of the primary antibody.

Co-immunoprecipitation

Transfections of SH-SY5Y cells were performed using Lipofectamine 2000 reagent (Life Technologies, Inc.) according to the manufacturer's instructions with the indicated plasmids. Immunoprecipitations were prepared from transfected cell lysates as described previously (Olzmann et al. 2004; Kirk et al. 2006; Olzmann et al. 2007; Giles et al. 2008; Lee et al. 2008) using anti-HA (12CA5), anti-FLAG (FLAGM2) or anti-Myc (9E10) antibodies. Immunocomplexes were recovered by incubation with protein G-sepharose beads (Upstate). Co-immunoprecipitations of endogenous proteins were performed using Seize Primary Mammalian Immunoprecipitation Kit (Pierce) according to manufacturer's instructions. Anti-printor antibody and pre-immune serum were conjugated to Amino-Link beads (Pierce) for use in columns. Mouse cerebellum extracts were prepared as described (Li et al. 2001). Mouse cerebellum was homogenized in homogenization buffer (20mM HEPES pH7.4, 300mM sucrose, 100mM NaCl). Triton X-100 was added to the homogenates to a final concentration of 1% and incubated at 4 C for 30 minutes. Insoluble material was removed by centrifugation at 100,000 x g for 1 h at 4 C, and the supernatant was used as the mouse cerebellum extract and applied to anti-printor or pre-immune serum conjugated columns. After elution from column or beads, samples were analyzed by SDS-PAGE, and immunoblotting with appropriate antibodies and horseradish peroxidase conjugated secondary antibodies. Results were visualized using ECL.

Subcellular fractionation

Subcellular fractionation was performed as previously described (Chin et al. 2000; Li et al. 2001; Chin et al. 2002). SH-SY5Y cells were collected by centrifugation and the pellet

was homogenized in 1ml homogenization buffer (250mM Sucrose, 10mM HEPES/KOH pH 7.4, 10mM KCl, 0.1mM EGTA, 0.1mM EDTA) containing protease inhibitors and DTT and disrupted with 25 strokes using Dounce B homogenizer. Nuclear and unbroken material was pelleted out in a 10-minute centrifugation at 1,000 x g. Post-nuclear material was subjected to a 30-minute centrifugation at 100,000 x g to retrieve the cytosolic (supernatant) and membrane (pellet) fractions. Bands were quantified using NIH Scion Image Software.

Opti-prep gradient fractionation

Opti-prep gradient fractionation was performed as previously described (Liang et al. 2006). SH-SY5Y cells were collected by centrifugation and the pellet was homogenized in 1ml of fractionation buffer (250mM sucrose, 10mM HEPES/KOH, pH 7.4, 1mM EDTA) and disrupted with 25 strokes using Dounce B homogenizer. Nuclear and unbroken material was pelleted out in a 10-minute centrifugation at 1,000 X g. Supernatant was then layered on a 10-30% Opti-Prep (Nycomed) gradient formed in fractionation buffer containing 42mM sucrose, and centrifuged at 4°C for 5 h at 100,000 X g. Following centrifugation, the gradient was harvested into 250-µl fractions using an Auto Densi-Flow gradient harvester (Labconco). Equal volumes of each fraction were analyzed by SDS-PAGE and by sequential immunoblotting for torsinA, printor and organelle markers. Bands were quantified using NIH Scion Image Software.

Quantitative analysis of the NE/ER distribution

Quantification of the NE/ER distribution of printor, torsinA or KDEL was performed on unprocessed images of cells double labeled for printor and KDEL, or torsinA and KDEL, by using MetaMorph Imaging System Software (Molecular Devices) as previously described (Giles et al. 2008). Using the region tool in the MetaMorph program, we outlined the ER as defined by the presence of KDEL immunoreactivity, and demarcated the nuclear envelope area, which was clearly apparent in the KDEL staining of almost all images. The fluorescence in the KDEL positive region outside of the nuclear envelope area was defined as the ER staining. The amount of printor, torsinA or KDEL fluorescence in the NE or ER of each cell was quantified with MetaMorph as described previously. The obtained NE/ER ratio of printor or torsinA was compared with that of the ER marker KDEL from the same double-labeled cell. 30-45 cells were randomly selected for each analysis. Analysis was carried out in a blinded manner and the result was confirmed by a second, independent investigator. Experiments were repeated at least three times, and the data were subjected to statistical analysis by unpaired Student's *t* test.

Quantitative analysis of co-localization

Quantification of torsinA-printor co-localization was performed on unprocessed images of cells double labeled for printor and torsinA by using MetaMorph Imaging System Software as previously described (Webber et al. 2008). For each torsinA genotype (torsinA WT, ΔE, Δ323-8, K108A, or E171Q), 30-45 cells were randomly selected for analysis. Analysis was carried out in a blinded manner by an investigator without any knowledge of torsinA genotype of the cells and the result was confirmed by a second,

independent investigator. Experiments were repeated at least three times, and the data were subjected to statistical analysis by unpaired Student's *t* test.

RESULTS

Identification of printor, a torsinA-interacting protein

To identify novel proteins that interact with torsinA in neuronal cells, we screened a rat brain hippocampal/cortical cDNA library using a yeast two-hybrid selection using the full length torsinA WT as bait. This screen did not result in the isolation of any positive clones. Because yeast-two hybrid requires translocation into the nucleus it was possible that the purported signal sequence and hydrophobic domain of torsinA were interfering with the bait reaching the nucleus, so we constructed a bait construct encoding an N-terminally truncated torsinA (torsinA WTΔ40) lacking these regions (Fig III-1A). In a yeast two-hybrid screen using torsinA WTΔ40 as bait, we identified several positive clones. Three positive clones encoded the C-terminal region (residues 125-628) of a novel protein that we named printor (Fig III-1B) because it is a protein interactor of torsinA. Database searches revealed that the printor is the rat homologue of KIAA1384, also known as KLHL14, an uncharacterized protein discovered by the KIAA project (Nagase et al. 2000).

Printor is 628 amino acids in length, has a calculated molecular mass of 70.7 kDa and a theoretical isoelectric point (pI) of 6.68. Sequence analysis reveals neither a known signal sequence nor a potential transmembrane domain. Printor contains an N-terminal region with homology to BTB/POZ (broad complex, tramtrack, bric-a-brac / Pox virus

and Zinc Finger) domain (Fig III-1B), BTB/POZ is a protein-protein interaction region that has been shown to mediate dimerization (Chen et al. 1995) and is known to interact with cullin3, a component of a multi-subunit E3 ubiquitin ligase (Geyer et al. 2003; Krek 2003; Gingerich et al. 2005). However it is unclear whether this region is functional due to a unique proline/glutamine rich (P/Q) interruption (Fig III-1B), which is not found in any other BTB/POZ containing protein. The BTB/POZ homology region is followed by a central BACK (BTB and C-terminal Kelch) domain, of unknown function (Stogios and Prive 2004). At the C-terminus, printor contains six kelch repeats (Fig III-1B). The 50-amino acid kelch repeat motif, was first identified in the Drosophila ovarian ring canal protein Kelch (Robinson and Cooley 1997). Kelch repeats form a B-propeller structure that contains multiple protein-protein contact sites (Adams et al. 2000). Kelch repeats are best characterized as being an actin-interacting domain (Way et al. 1995; Robinson and Cooley 1997), however, a number of kelch containing proteins have no association with actin (Adams et al. 2000).

Data base searches revealed the presence of printor orthologues as uncharacterized or predicted proteins from genome projects in a number of organisms including rat (accession number XP_344653.3), chicken (NP_001012884.1), and zebrafish (XP_001334729.1), but not in C. elegans or Drosophila. The amino acid sequence of printor is highly conserved, with the human printor sequence sharing 99% overall amino acid identity with rat printor, 95% overall amino acid identity with chicken printor, and 88% overall amino acid identity with zebrafish printor (Fig III-1C). The highly conserved sequence and domain structure among printor homologues indicate that printor is an evolutionarily conserved protein among vertebrates.

Printor co-distributes with torsinA in brain as well as other tissues

In order to further characterize printor we generated a rabbit anti-printor antibody against an 18-amino acid N-terminal region (aa 1-18) of printor that has 100% amino acid identity across species. To investigate the specificity of the printor antibody, immunoblot analysis was performed using cell lysates from untransfected SH-SY5Y cells, as well as transfected SH-SY5Y cells expressing myc-tagged printor (Fig III-2A). The anti-printor antibody specifically recognized recombinant printor protein in transfected cells (Fig III-2A). Anti-Myc antibody was used to confirm the size of the myc-tagged recombinant printor protein (Fig III-2A). In addition, the anti-printor antibody also recognized the 70kD endogenous printor protein in both transfected and untransfected cells (Fig III-2A). In contrast, the pre-immune serum did not show any immunoreactivity to either endogenous or recombinant printor protein, confirming the specificity of our anti-printor antibody (Fig III-2A).

Immunoblotting cell lysates from human non-neuronal HeLa, human neuroblastoma derived SH-SY5Y and rat pheochromocytoma derived PC12 cells with anti-printor antibody demonstrated that the antibody detects printor in different cell types and across species (Fig III-2B). To further characterize the tissue distribution of printor, western blot analysis of multiple rat tissue samples was performed using the printor antibody. This demonstrated that printor is expressed in many tissues, including heart, lung, liver, spleen, kidney and pancreas (Fig III-2C), which agrees with the mRNA expression profile found in the HUGE database (Human Unidentified Gene Encoded; http://www.kazusa.or.jp/huge/gfpage/KIAA1384/). In addition, printor has a similar

tissue distribution pattern to torsinA. To further examine printor neuronal expression, various brain regions were dissected from adult rat brain and subjected to western blot analysis using the anti-printor and anti-torsinA antibodies. The result shows that printor is widely expressed throughout the brain and exhibits relatively higher protein expression levels in hippocampus, medulla oblongata, and cerebellum, similar to the pattern of expression of torsinA (Fig III-2D).

To determine whether our anti-printor antibody could be used for immunocytochemistry, double label immunofluorescence confocal microscopy was used to determine the intracellular distribution of endogenous and overexpressed printor protein in SH-SY5Y cells. Anti-printor antibody shows can be seen throughout the cell body (Fig III-2E). In addition, in SH-SY5Y cells overexpressing Myc-tagged printor, both anti-Myc and anti-printor antibody display a similar pattern of distribution (Fig III-2E). No immunoreactivity was observed when pre-immune serum was used, confirming the specificity of the anti-printor antibody (data not shown). To further confirm that printor is expressed in neurons, we examined primary cortical neurons using anti-printor antibody and compared the distribution of printor to MAP2, a brain specific microtubule associated protein (Fig III-2E). Printor is present in the cell body and in the MAP2-containing neurites (Fig III-2E).

We then used our anti-printor antibody to determine the cellular distribution of printor protein in mouse brain by immunohistochemistry. Printor immunoreactivity was widely distributed in many neurons through the brain. In the cerebral cortex, printor staining appeared limited to layer II (Fig III-3G), where staining of neuron perikarya and processes was observed (Fig III-3H). Other cortical layers did not show printor

immunoreactivity. Printor was also observed in select neurons of the striatum (Fig III-3I and J). Consistent with the results of Western blot analysis (Fig III-2D), intense printor immunostaining was observed in the hippocampus (Fig III-3K-N) and the cerebellum (Fig III-3O-Q). Pyramidal cell neurons of the CA1 (Fig III-3K and L) and CA3 (Fig III-3M and N) contained printor immunoreactivity in their perikarya, although staining appeared stronger in the CA3 region compared to the CA1 region. Purkinje cells of the cerebellum displayed strong immunoreactivity in their perikarya and processes (Fig III-3P and Q). Granular cells of the cerebellum also displayed printor immunoreactivity, but to a lesser degree than Purkinje cells (Fig III-3P and Q). Printor immunoreactivity was also observed in the medial septum, ventral pallidum, thalamus, hypothalamus, amygdala, inferior colliculi, Locus Coeruleus, peripyramidal nucleus, raphe nucleus, reticular formation, spinal trigeminal nucleus, and vestibular nuclei (data not shown). In addition, no immunoreactivity was observed in the corpus callosum, suggesting printor is primarily localized to neurons, not glia (data not shown). The specificity of printor immunoreactivity was confirmed in controls where anti-printor primary antibody was omitted (Fig III-3B, D, and F).

Printor interacts and co-localizes with torsinA in cells

To verify the interaction detected between torsinA and printor in the yeast-two hybrid screens, occurs *in vivo*, co-immunoprecipitation assays were performed. Because the interaction was first detected using torsinAWTΔ40 bait, HeLa cells transfected with Myc-tagged printor and either HA-tagged torsinAWTΔ40 or HA vector were subjected to immunoprecipitation using anti-HA antibody (Chen et al. 1993) as previously described

(Li et al. 2002). Printor co-immunoprecipitated with HA-tagged torsinAWTΔ40, but not with HA alone (Fig III-4A), indicating a specific interaction. We then examined interaction between full length torsinA WT and printor. TorsinA WT, but not the vector control, was able to co-immunoprecipitate printor protein (Fig III-4B). These results confirmed a specific interaction between torsinA and printor in transfected cells. Double-label immunofluorescence confocal microscopic analysis demonstrated that printor and torsinA WT co-localized in transfected SH-SY5Y cells (Fig III-4C).

To verify printor and torsinA interaction endogenously, co-immunoprecipitation of mouse cerebellum lysate was performed using columns containing immobilized pre-immune serum or affinity purified anti-printor antibody. TorsinA was precipitated using affinity-purified anti-printor antibody, but not with pre-immune serum (Fig III-4D). This demonstrates the existence of an endogenous torsinA-printor complex. Double-label immunofluorescence confocal microscopic analysis on untransfected SH-SY5Y cells using anti-printor and anti-torsinA antibodies reveals that endogenous printor and torsinA co-localize, further supporting the existence of an endogenous torsinA-printor complex (Fig III-4E).

Printor exists in both cytosolic and membrane-associated pools and is localized to ER

To investigate the intracellular distribution of printor protein, we first performed subcellular fractionation experiments to separate the postnuclear supernatant from untransfected SH-SY5Y cells into cytosol and membrane fractions. Western blot analysis of these fractions revealed that printor was present in both the cytosol and membrane

fractions, although the relative amount of printor in the membrane fraction was greater than that in the cytosol fraction (Fig III-5A). Quantification analysis revealed that 16.17 ± 1.44 percent of printor is in the cytosolic fraction versus 83.82 ± 1.44 percent in the membrane-associated pool (Fig III-5B). This is in contrast to torsinA, which is present only in the membrane fraction (Fig III-5A). Calnexin, a known integral membrane protein was used as a control (Fig III-5A).

In order to determine what membrane structures printor is associated with, double-label immunofluorescence confocal microscopy was performed on SH-SY5Y cells transfected with Myc tagged printor and simultaneously stained for Myc and either ER marker KDEL early endosomal marker EEA1, lysosomal marker LAMP2, or mitochondrial marker TIM23 (Fig III-5C). Significant co-localization between printor and KDEL was observed suggesting that printor, like torsinA, is localized to the ER (Fig III-5C). However, we detected no significant co-localization between printor and EEA1, LAMP2, or TIM23 suggesting that printor is not localized to early endosomes, lysosomes or mitochondria (FIG III-5C).

Printor co-localizes with torsinA in the ER but not the NE

Next we used triple-label immunofluorescence confocal microscopy to determine if printor and torsinA co-localized in the ER. SH-SY5Y cells overexpressing C-terminally HA-tagged torsinA and Myc-tagged printor were simultaneously stained for HA, Myc and KDEL. Co-localization between all three proteins was seen, suggesting that torsinA and printor co-localize in the ER (Fig III-6A). A similar pattern was observed with endogenous proteins (Fig III-6A). As a complementary approach, we used a density

gradient fractionation to determine if torsinA and printor associate with the same population of membranes. Since both printor and torsinA were contained in the membrane fraction, membrane fractions were pelleted out of SH-SY5Y post-nuclear supernatant, resuspended in fractionation buffer and fractionated using a 10-30% linear Opti-prep gradient. Fractions were collected and analyzed by SDS-PAGE and western blot analysis (Fig III-6B). There is clear co-fractionation between printor and torsinA in fractions 4-11, suggesting that the membrane-bound pools of these two proteins associate with the same population of membranes (Fig III-6B). We next determined the organellar origin of the membrane compartment to which printor and torsinA are co-localized. Immunofluorescence analysis demonstrated that printor and torsinA localize to the ER. Based on this, the population of membranes on which torsinA and printor co-localize is likely to represent the ER. Western blot analysis for the ER integral membrane protein calnexin was used to confirm this (Fig III-6B). Comparison of the distribution of printor and torsinA with calnexin suggests that printor and torsinA primarily associate on the ER membrane. Quantification analysis demonstrates that the majority of printor, torsinA and calnexin are all found in fraction 7, further confirming their association (Fig III-6C).

Because the ER and NE are subdomains of a contiguous membrane (Ellenberg et al. 1997), it can be difficult to find markers that are exclusive to either the ER or NE. Therefore, we used a previously published method (Giles et al. 2008) to determine the relative distribution of printor between ER and NE. Double-label immunofluorescence confocal microscopic analysis was performed to determine the intracellular distribution of Myc-tagged printor in HeLa and SH-SY5Y cells. We found that printor co-localized with ER marker KDEL in both HeLa and SH-SY5Y cells (Fig III-7A). We then

quantified the relative distribution of printor in NE and ER of both HeLa and SH-SY5Y cells, and compared the obtained NE/ER ration with that of the ER marker KDEL from the same double labeling experiments. The result showed that in both cell types, the NE/ER ratio of printor is significantly lower than the NE/ER ratio of KDEL, indicating that printor has an enhanced preferential localization to the ER compared to the ER marker KDEL (Fig III-7B). To control for cell-type variation in the relative NE/ER distribution of the ER marker, we determined the NE preference of printor by normalizing the NE/ER ratio of printor to the corresponding NE/ER ratio of KDEL in the same cells (Fig III-2C). The results showed that the NE preference of printor in both cell types was less than 1, which is consistent with an enhanced ER preference. This is in direct contrast to the previously established neuronal-cell type specific NE preference of torsinA (Giles et al. 2008).

Printor shows reduced co-localization with ATP-bound form of torsinA

Since torsinA contains a AAA^+ ATPase domain and is predicted to be a chaperone protein that binds a substrate(s) in an ATPase cycle-dependent manner (Patel and Latterich 1998; Neuwald et al. 1999; Hanson and Whiteheart 2005) , we also analyzed the subcellular localization of the ATP-binding-deficient mutant torsinA K108A, which would be unable to bind the substrate(s), and the ATP-hydrolysis-deficient mutant torsinA E171Q, which would bind tightly to the substrate(s). Double label immunofluorescent confocal microscopic analysis was used to examine the co-localization between C-terminally HA-tagged torsinA WT, torsinA K108A or torsinA E171Q and Myc-tagged printor in transfected SH-SY5Y cells. TorsinA K108A, like

torsinA WT, visibly co-localized with printor, but torsinA E171Q appeared to have decreased levels of co-localization (Fig III-8A). Quantification analysis of co-localization using MetaMorph revealed that 51.54 ± 1.31 percent of printor co-localizes with torsinA K108A, which is similar to percent of printor that co-localizes with torsinA WT (Fig III-8B). However, only 36.13 ± 2.07 percent of printor co-localized with torsinA E171Q, which represents a significant reduction (Fig III-8B).

In order to examine whether the loss of co-localization observed was attributable to a change in torsinA localization, we examined and compared the intracellular distribution of C-terminally HA-tagged torsinA WT, torsinA K108A and torsinA E171Q in SH-SY5Y cells by double label immunofluorescence microscopic analysis (Fig III-9A). As previously described, we quantified the relative distribution of torsinA in NE and ER and compared the obtained NE/ER ratio with that of the ER marker KDEL from the same double labeling experiments (Giles et al. 2008). We found that the NE/ER ratio of torsinA K108A was similar to that of torsinA WT, but that torsinA E171Q showed a significantly higher NE/ER ratio compared to torsinA WT (Fig III-9B). To control for variation in the relative NE/ER distribution of the ER marker, we determined the NE preference of torsinA by normalizing the NE/ER ratio of torsinA to the corresponding NE/ER ratio of KDEL in the same cells (Fig III-9C). The results showed that the NE preference of torsinA E171Q was increased to 2.27 ± 0.07 compared to 1.92 ± 0.08 for torsinA WT and 1.91 ± 0.07 for torsinA K108A. Together these results indicate that ATP-binding induces translocation of torsinA from the ER to the NE, and results in reduced co-localization with printor.

Printor co-localization with torsinA is reduced by dystonia-associated mutation

To examine whether dystonia-associated mutations altered torsinA co-localization with printor, we used double-label immunofluorescence confocal microscopy to examine the co-localization of C-terminally HA-tagged torsinA WT, torsinA ΔE or torsinA Δ323-8 with Myc-tagged printor in transfected SH-SY5Y cells. TorsinA WT visibly co-localized with printor, but torsinA ΔE and Δ323-8 appeared to have decreased levels of co-localization with printor (Fig III-9A). Quantification analysis of co-localization using MetaMorph revealed that, while 53.68 ± 2.11 percent of printor co-localizes with torsinA WT, significant reductions to 41.98 ± 1.60 and 43.67 ± 1.51 percent of printor co-localizing with torsinA were seen with the ΔE and Δ323-8 mutants, respectively (Fig III-9B). These data suggest that the enhanced NE preference seen in dystonia-associated mutant torsinA reduces co-localization with printor

Printor does not interact with torsinA ΔE or torsinA E171Q

ATPases in their ATP-bound state tend to show a higher affinity for substrate proteins (Vale 2000). We next sought to determine whether the ATP-bound state of torsinA had any effect on its ability to bind printor. SH-SY5Y cells transfected with HA-tagged printor and either Myc vector, C-terminally Myc-tagged torsinA WT, torsinA K108A, or torsinA E171Q were subjected to immunoprecipitation with anti-Myc antibody. TorsinA WT and torsinA K108A were able to co-immunoprecipitate printor, however printor did not co-immunoprecipitate torsinA E171Q (Fig III-8C).

Next we examined the effect of dystonia-associated ΔE and Δ323-8 mutations on torsinA interaction with printor. SH-SY5Y cells transfected with HA-tagged printor and

either Myc vector, C-terminally Myc-tagged torsinA WT, torsinA ΔE or torsinA Δ323-8 were subjected to immunoprecipitation with anti-Myc antibody. TorsinA WT and torsinA Δ323-8 were able to co-immunoprecipitate printor, however printor did not co-immunoprecipitate with torsinA ΔE (Fig III-8C). These data indicate that printor does not interact with activated torsinA, and suggest that torsinA ΔE may exist primarily in an activated state.

DISCUSSION

Two mutations in the C-terminal region of the protein torsinA have been linked to the development of DYT1 dystonia. To understand the physiological function of torsinA, and the pathological mechanism by which mutant torsinA results in dystonia, a major research effort in the field has been directed towards the search for binding partners of torsinA. Thus far, this effort has resulted in the isolation of several binding partners (Kamm et al. 2004; Goodchild and Dauer 2005; Hewett et al. 2005; Granata et al. 2008). To date none of the known interactions are disrupted by the dystonia-associated torsinA mutations, therefore their involvement in the pathogenesis of torsinA is unclear. In contrast, our study identifies, for the first time, a protein that interacts preferentially with torsinA WT but not with torsinA ΔE, the mutation associated with a majority of DYT1 cases.

We have identified and characterized printor, a novel protein that interacts with torsinA. Printor is a 70kD protein that contains an N-terminal region with homology to the BTB/POZ domain, a BACK domain and six kelch repeats. Although both the

BTB/POZ domain and kelch repeats can exist alone or in combination with other domains, there are as many as 51 BTB-BACK-Kelch (BBK) superfamily proteins in the human genome, and the BBK family comprises 72% of identified kelch proteins in humans (Prag and Adams 2003). Interestingly, there are no known BBK proteins in yeast, suggesting that the BBK domain architecture developed during the evolution of multicellular organisms (Prag and Adams 2003). BBK proteins have been implicated in neuronal development (Hernandez et al. 1997; Kim et al. 1998; Soltysik-Espanola et al. 1999), and mutations of at least one known BBK protein, gigaxonin, leads to neuronal dysfunction (Bomont et al. 2000; Yang et al. 2007).

BTB/POZ domain containing proteins have been associated with transcriptional regulation, ion channel oligomerization, cytoskeletal stabilization and ubiquitination (Albagli et al. 1995; Stogios et al. 2005; Perez-Torrado et al. 2006). The BTB/POZ domain has been shown to be necessary for both homo- and heterodimerization, and in a number of BTB/POZ containing proteins, dimerization is necessary for proper folding and function (Chen et al. 1995; Collins et al. 2001; Stogios et al. 2005; Perez-Torrado et al. 2006). In addition, the BTB/POZ domain has been shown to recruit transcriptional co-factors or bind directly to DNA through a protein-protein interaction surface formed at the dimer interface (Albagli et al. 1995; Ahmad et al. 1998; Stogios et al. 2005; Perez-Torrado et al. 2006). The BTB/POZ domain has also been shown to interact with the cullin family of E3 ubiquitin ligases, where it recruits substrates for ubiquitination (Geyer et al. 2003; Krek 2003; Stogios et al. 2005; Perez-Torrado et al. 2006). It is currently unclear whether the N-terminus comprises a functional BTB/POZ domain due to the presence of a P/Q rich interruption.

Kelch repeats form a beta-propeller that provides multiple protein-protein interaction surfaces on both sides of the propeller and in the grooves between the blades (Adams et al. 2000; Gettemans et al. 2003). Kelch repeats are often considered actin-interacting motifs, due to the number of kelch repeat-containing proteins that interact with actin (Way et al. 1995; Hernandez et al. 1997; Robinson and Cooley 1997; Soltysik-Espanola et al. 1999), however a number of kelch repeat-containing proteins have other functions (von Bulow et al. 1995; Way et al. 1995; Soltysik-Espanola et al. 1999; Adams et al. 2000; Bomont et al. 2000). For instance, in spermatazoa, α-scruin is known to stabilize actin bundles while β-scruin is localized in a region which does not contain actin, despite a 67% homology between the two proteins (Way et al. 1995; Adams et al. 2000). The kelch repeat beta propeller has also been shown to contain the catalytic site for the fungal enzyme galactose oxidase (Adams et al. 2000). Due to the multiple binding sites provided by the beta propeller, kelch repeats can act as an organizing center for multimeric complexes, such as clathrin which binds β-arrestin and the AP-2 complex in different regions of the propeller (Adams et al. 2000). Because both the BTB/POZ and kelch domains contain multiple protein-protein interaction sites, printor could potentially interact with multiple proteins or be involved in the formation of multi-protein complexes.

The interaction of printor with torsinA was demonstrated in the yeast two-hybrid system and confirmed by co-immunoprecipitation. Printor and torsin are distributed in a similar pattern, and can be found in multiple tissues as well as throughout the brain. Immunocytochemical analysis revealed that torsinA and printor co-localize with the ER

marker KDEL, and torsinA and printor co-fractionate with ER resident protein calnexin, providing further support that the interaction is physiologically significant.

Examination of printor co-localization with ATP-bound and –unbound torsinA demonstrated a reduction in co-localization with ATP-bound torsinA compared to both torsinA WT and ATP-unbound torsinA. Although previous studies have reported the translocation of ATP-bound torsinA from the ER to the NE, these studies have never provided a quantitative analysis of the relative NE/ER distribution (Gonzalez-Alegre and Paulson 2004; Goodchild and Dauer 2004; Naismith et al. 2004). Our results indicate that ATP-bound torsinA has an enhanced NE preference in neuroblastoma SH-SY5Y cells but not in non-neuronal HeLa cells that results in the reduced co-localization with printor protein in SH-SY5Y cells. This is consistent with our previous study, which demonstrated a neuronal cell-type specific NE preference for torsinA (Giles et al. 2008). The function of the interaction between torsinA and printor is not yet known, however, our data demonstrates that printor preferentially interacts with ATP-unbound torsinA over ATP-bound torsinA. Because most AAA+ proteins display a higher affinity for their target proteins when in their ATP-bound state (Vale 2000), printor is not likely to be a substrate for torsinA. However, printor could perform a regulatory role, or possibly recruit torsinA to a multi-subunit complex through its multiple protein-protein interaction domains.

Examination of printor co-localization dystonia-associated mutant torsinA demonstrated a reduction in co-localization with both torsinA ΔE and torsinA Δ323-8 compared to torsinA WT. Co-immunoprecipitation analysis revealed that torsinA WT and torsinA Δ323-8 were able to co-immunoprecipitate printor, but not torsinA ΔE. The

mechanism through which the ΔE mutation disrupts the torsinA-printor interaction is unclear. Although our co-localization analysis revealed that torsinA ΔE displayed a reduced level of co-localization with printor, the same effect was also seen with torsinA Δ323-8, which does interact with printor. One possible explanation is that the ΔE mutation causes a structural change that disrupts the printor binding site. The ΔE torsinA mutation, unlike the Δ323-8 torsinA mutation, falls within the AAA+ domain of torsinA. This raises the question of whether the ΔE torsinA mutation but not the Δ323-8 torsinA mutation disrupts the ATPase activity of torsinA. The effect of dystonia-associated mutations on torsinA ATPase activity has been examined by two groups, however, one group reported no effect (Kustedjo et al. 2003), while the other group reported a disruption in ATPase activity in both mutant proteins, with torsinA ΔE reported as having a more severe effect than torsinA Δ323-8 (Konakova and Pulst 2005). Our results suggest that torsinA ATP-binding disrupts printor interaction, thus, torsinA ΔE having a reduced level of ATP hydrolysis compared to torsinA WT and torsinA Δ323-8 could also explain our results. Further study into the function of both printor and torsinA, as well as the functional consequence of the interaction could have important implications for understanding the pathogenesis of dystonia.

ACKNOWLEDGEMENTS

We are grateful to Dr. Paul Worley (Johns Hopkins University) for providing the rat hippocampal/cortical cDNA library and Dr. William T. Dauer (Columbia University) for

providing pcDNA3.1/V5-His-TOPO torsinA E171Q and torsinA K108A. This work was supported by grants from National Institutes of Health (NS054334, NS050650, ES015813, and GM082828).

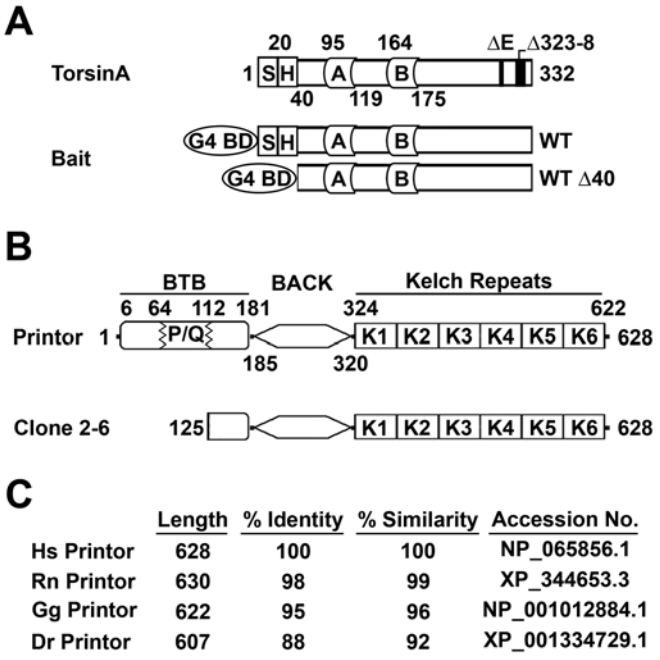

FIGURE III-1. . Isolation of rat printor as a torsinA-interacting protein from yeast-two hybrid screen. (**A)** Domain structure of torsinA. The following domains are indicated: *SS*, signal sequence; *HD*, hydrophobic domain; *A*, Walker A motif; *B*, Walker B motif. Dystonia related mutations are indicated. Baits used for yeast-two hybrid screen are indicated below the domain structure. (**B)** Domain structure of printor. The following domains are indicated: *BTB*, broad complex, tramtrack, bric-a-brac / Pox virus and Zing Finger**;** *P/Q***,** proline/glutamine rich domain; *BACK*, BTB and C-terminal Kelch domain; *Kelch*, kelch repeat domain. The location of the torsinA-interacting printor clone isolated from the yeast-two hybrid screen is indicated below the domain structure. (**C)** The amino acid identity and similarity of printor and its homologues. Accession numbers for the sequences are as follows: *Hs* printor, NP_065856.1; *Rn* printor, XP_344653.3; *Gg* printor, NP_001012884.1; *Dr* printor, XP_001334729.1. *Hs*, Homo sapiens; *Rn*, Rattus norvegicus; *Gg*, Gallus gallus; *Dr,* Danio rerio.

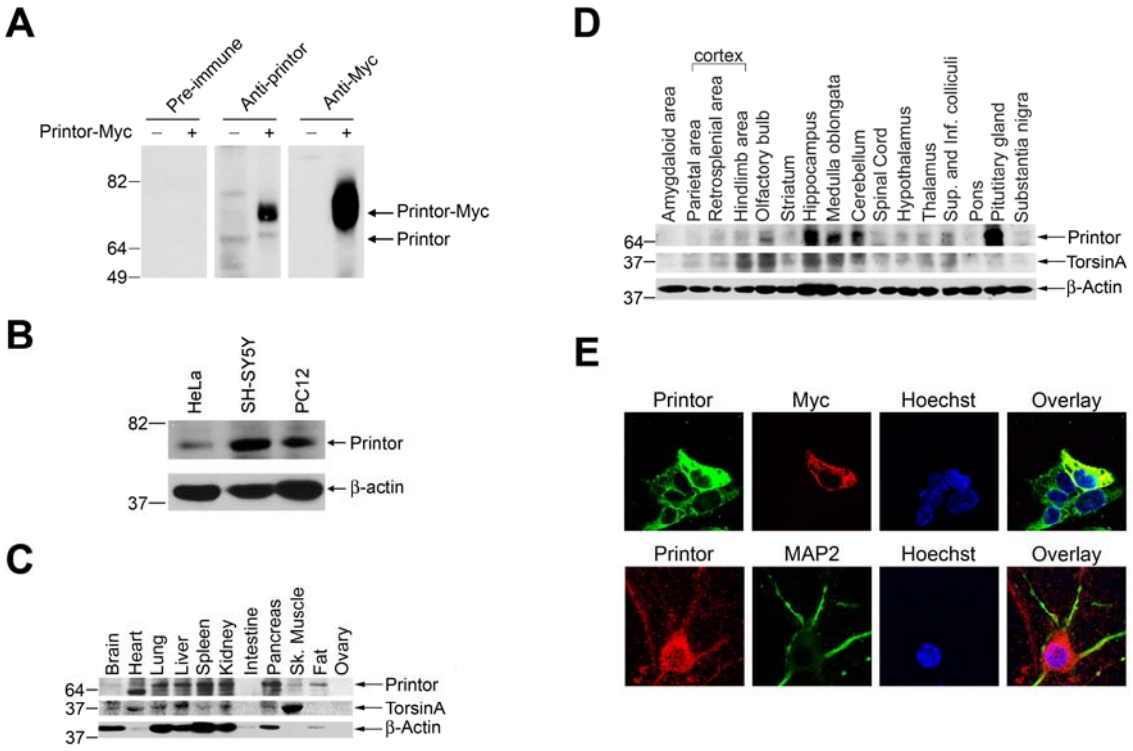

FIGURE III-2. Printor co-distributes with torsinA in multiple tissues and brain regions. (**A)** Lysates from untransfected SH-SY5Y cells, or cells overexpressing Myc-tagged printor were immunoblotted with either pre-immune serum, affinity purified anti-printor antibody, or anti-Myc antibody. (**B)** Equal amounts of homogenates (50µg) from the indicated cultured cell lines were analyzed by immunoblotting using anti-printor and anti-actin antibodies. **(C)** Equal amounts of homogenates (100µg) from the indicated rat tissues were analyzed by immunoblotting using anti-printor, anti-torsinA and anti-actin antibodies. *Sk.*, skeletal. (**D)** Equal amounts of homogenates (100µg) from the indicated rat brain regions were analyzed by immunoblotting using anti-printor, anti-torsinA and anti-actin antibodies. *Sup.,* superior; *Inf.,* inferior. All data are representative of at least three independent experiments. **(E))** SH-SY5Y cells overexpressing Myc-tagged printor

(top) were immunostained with primary antibodies against printor and Myc, followed by detection with secondary antibodies conjugated to TR (Myc, red) or FITC (printor, green). Hoechst stain was used to visualize the nucleus. Primary cortical neurons (bottom) were immunostained with primary antibodies against printor and MAP2, followed by detection with secondary antibodies conjugated to TR (printor, red) or FITC (MAP2, green). Hoechst stain was used to visualize the nucleus.

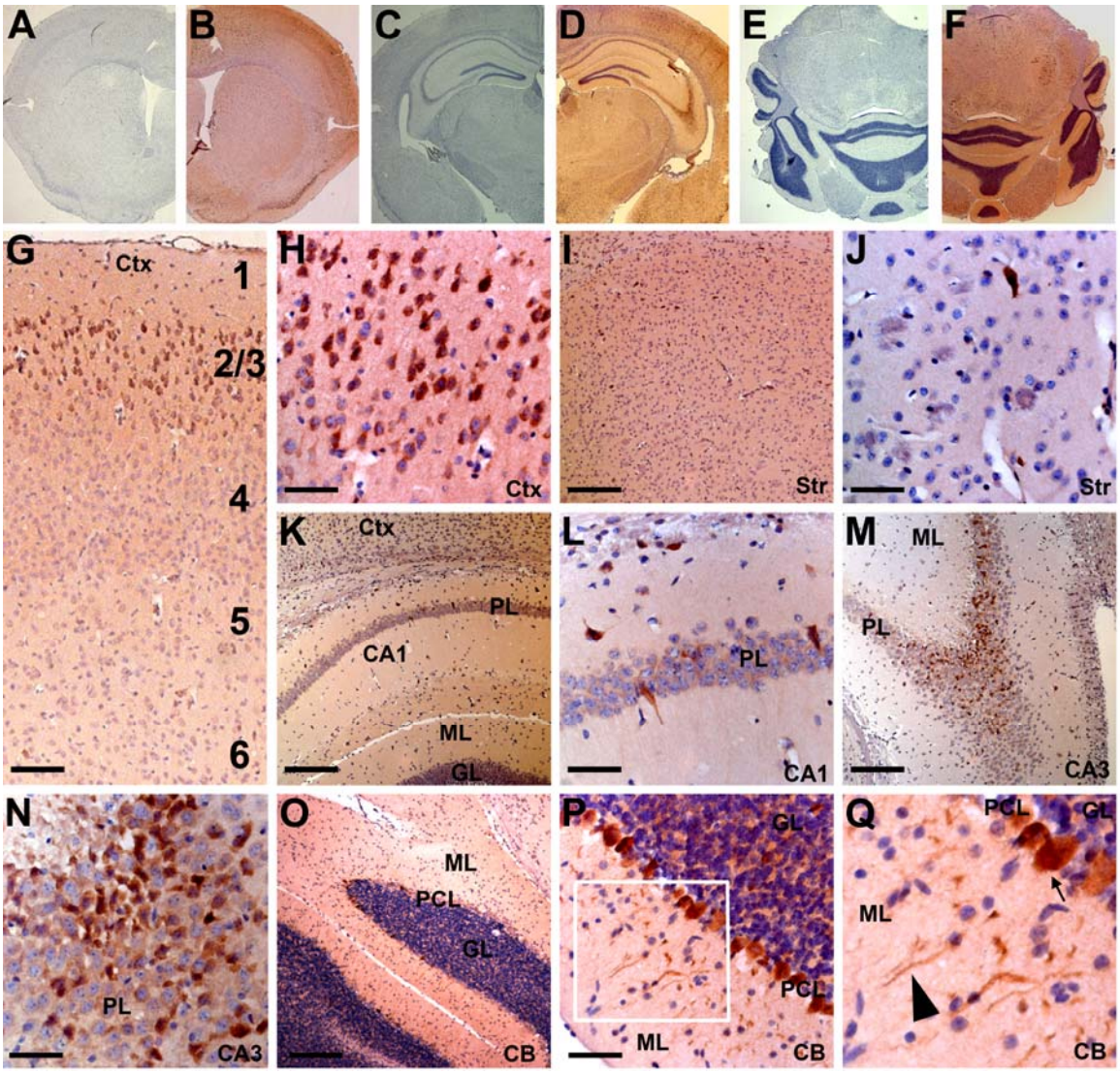

FIGURE III-3. Immunohistochemical analysis of printor protein distribution in mouse brain. Coronal sections through striatum (**A** and **B**), hippocampus (**C** and **D**) and cerebellum (**E** and **F**) immunostained with either no primary antibody (**A**, **C**, and **F**) or anti-printor antibody (**B**, **D**, and **F**). (**A)** Striatum, no primary added control. (**B)** Striatum, anti-printor (**C)** Hippocampus, no primary added control (**D)** Hippocampus, anti-printor. (**E)** Cerebellum, no primary antibody control. (**F)** Cerebellum, anti-printor (**G)** Immunoreactive neurons are present in layer 2 of the cortex (*Ctx*), Numbers identify cortical layers. (**H)** Cortex. (**I)** Striatum (**J)** Striatum (**K)** Immunoreactivity is seen in the

pyramidal layer (*PL*) of the hippocampal CA1 region, and not in the molecular layer (*ML*) or granular layer (*GL*). (**L)** Hippocampal CA1 region pyramidal layer (*PL*). (**M)** Immunoreactivity is seen in the pyramidal layer (*PL*) of the hippocampal CA3 region, and not in the molecular layer (*ML*). (**N)** Hippocampal CA3 region pyramidal layer (*PL*). (**O)** Immunoreactivity is stronger in the purkinje cell layer (*PCL*) and granular layer (*GL*) of the cerebellum (*CB*), but not in the molecular layer (*ML*). (**P)** Purkinje cell layer (*PCL*) neurons display stronger immunostaining compared to the granular layer (*GL*). Purkinje cell projections in the molecular layer (*ML*) display immunoreactivity. (**Q)** Box enlargement. Arrows indicate cell bodies, arrowheads indicate neurites. Scale bar = 250μM in *G*; 125μm in *I, K, O,* and Q; 30μM in *H, J, L, N,* and *P*.

.

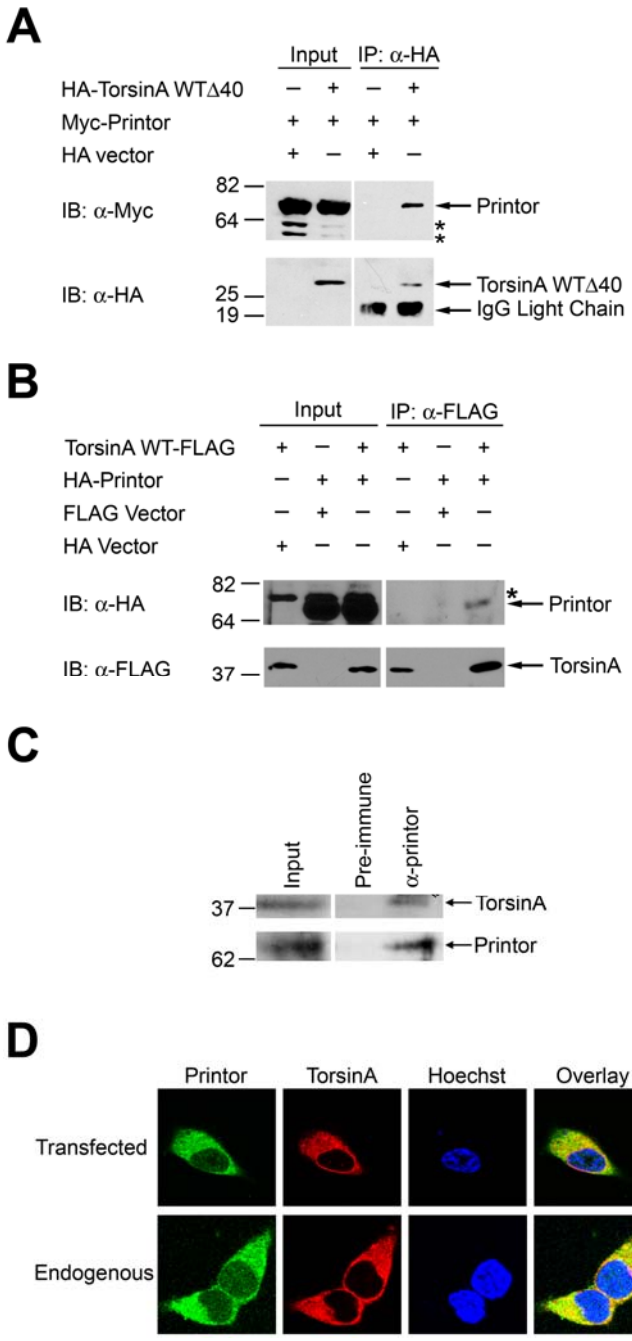

FIGURE III-4. Printor and torsinA interact *in vivo*. (A) Co-immunoprecipitation of printor with torsinAWTΔ40 from HeLa cells. Extracts from HeLa cells expressing either HA-tagged torsinA WTΔ40 or HA vector and Myc-tagged printor were subjected to immunoprecipitation with anti-HA antibody (12CA5). Immunoprecipitates were analyzed

by immunoblotting (IB) with anti-HA and anti-Myc antibodies. (**B**) Co-immunoprecipitation of printor with torsinA. Extracts from HeLa cells expressing HA-tagged printor or HA vector and C-terminally FLAG-tagged torsinA or FLAG vector were subjected to immunoprecipitation with anti-FLAG antibody. The immunoprecipitates were analyzed by immunoblotting with anti-FLAG and anti-HA antibodies. (**C)** Co-immunoprecipitation of endogenous torsinA with printor from mouse cerebellum. Mouse cerebellum lysate was subjected to immunoprecipitation using immobilized anti-printor pre-immune serum or affinity purified anti-printor antibody bound to Amino-Link (Pierce) beads. Eluted proteins were analyzed by immunoblotting with anti-printor and anti-torsinA antibodies. (**D)** Co-localization of printor and torsinA in SH-SY5Y cells. SH-SY5Y cells expressing Myc-tagged printor and C-terminally HA-tagged torsinA (top) were immunostained with primary antibodies against Myc and HA, followed by detection with secondary antibodies conjugated to TR (torsinA, red) or FITC (printor, green). Hoechst stain was used to visualize the nucleus. Untransfected SH-SY5Y cells (bottom) were immunostained with primary antibodies against printor and torsinA, followed by detection with secondary antibodies conjugated to TR (torsinA, red) or FITC (printor, green). Hoechst stain was used to visualize the nucleus. Scale bars, 10μm.

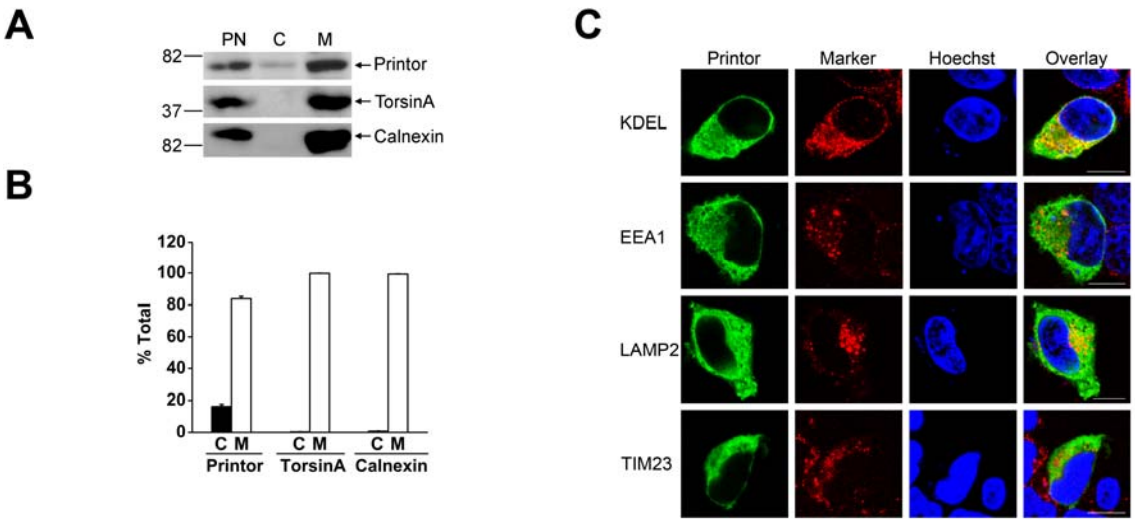

FIGURE III-5. Printor is found in both cytosolic and membrane-associated fractions. (A) Post-nuclear supernatant (*PN*) from SH-SY5Y cells was separated into cytosol (*S*) and total membrane (*P*) fractions. Post-nuclear supernatant was also separated into heavy membrane (*HM*), microsomal (*MS*) and cytosolic (*C*) fractions. Aliquots representing an equal percentage of each fraction were analyzed by immunoblotting with anti-printor, anti-torsinA and anti-calnexin antibodies. **(B)** Fractions were quantified using NIH Scion Image and shown as percent total. Data represent mean ± S.E. from at least three independent experiments. **(C)** SH-SY5Y cells expressing Myc-tagged printor were immunostained primary antibodies against -Myc and either anti-KDEL, anti-EEA1, anti-LAMP2, or anti-TIM23 followed by detection with secondary antibodies conjugated to TR (marker proteins, red), or FITC (printor, green). Hoechst stain was used to visualize the nucleus. Scale bars, 10μm.

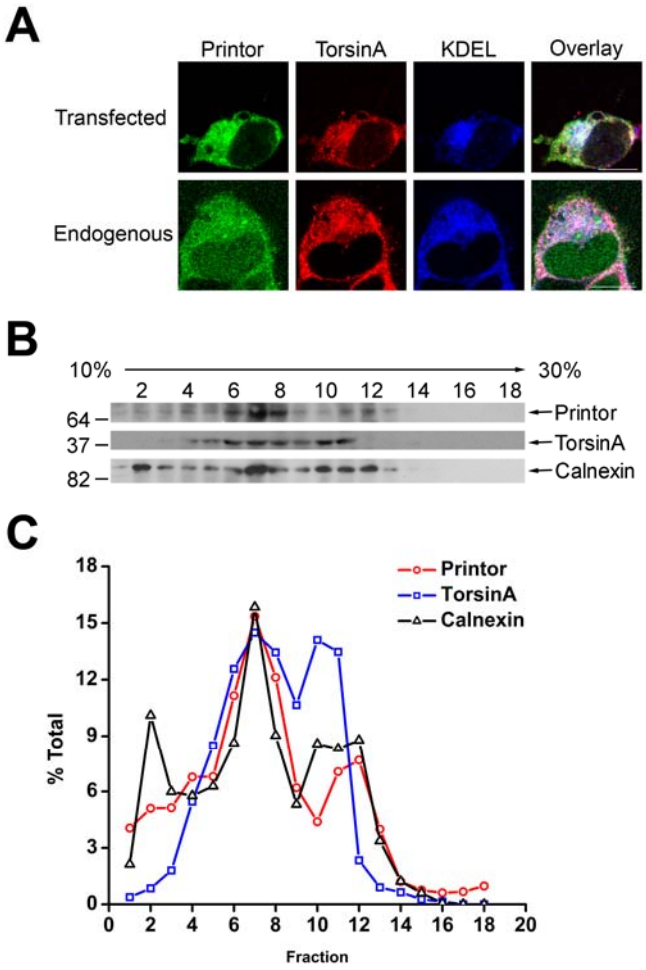

FIGURE III-6. Co-localization of printor and torsinA in the ER but not NE. (A) SH-SY5Y cells expressing Myc-tagged printor and C-terminally HA-tagged torsinA (top) were immunostained with primary antibodies against Myc, HA, and ER marker KDEL, followed by detection with secondary antibodies conjugated to TR (torsinA, red), FITC (printor, green), or Cy-5 (KDEL, blue). Untransfected SH-SY5Y cells (bottom) were immunostained with primary antibodies against printor, torsinA, and ER marker KDEL, followed by detection with secondary antibodies conjugated to TR (torsinA, red), FITC (printor, green), or Cy-5 (KDEL, blue). (**B**) Post-nuclear supernatant was prepared from SH-SY5Y cells and fractionated on a 10-30% Opti-prep gradient as described in

"Materials and Methods". The gradient was divided into 18 fractions, with fraction 1 corresponding to the top of the gradient. Equal volumes of each fraction were analyzed by SDS-PAGE followed by immunoblotting using anti-printor, anti-torsinA and anti-calnexin antibodies. **(C)** Fractions were quantified using NIH Scion Image and shown as percent total. Data are representative of at least three independent experiments. Scale bars, 10μm.

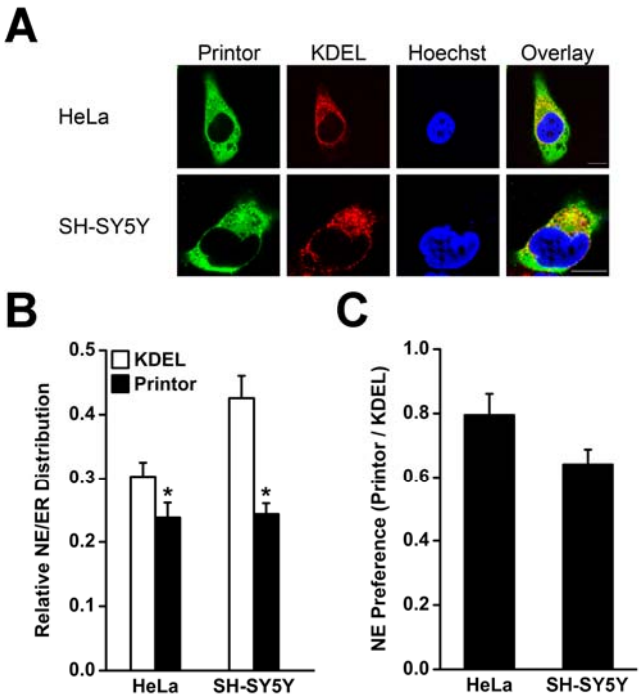

FIGURE III-7. Printor displays ER preference in both HeLa and SH-SY5Y cells. **(A)** HeLa or SH-SY5Y cells expressing Myc-tagged Printor were stained with primary antibodies against Myc and ER marker KDEL, followed by detection with secondary antibodies conjugated to TR (KDEL, red) or FITC (printor, green). Hoechst stain was used to visualize the nucleus. **(B)** Quantification shows the relative distribution of printor and KDEL in the NE versus the ER. Data represent mean ± S.E. from at least three independent experiments. *Significantly different from the NE/ER ratio of KDEL. ($p < 0.05$). **(C)** NE preference of printor was determined by normalizing the NE/ER ratio of printor in HeLa or SH-SY5Y cells to the corresponding NE/ER ratio of KDEL in the same cells. Data represent mean ± S.E. from at least three independent experiments. Scale bars, 10μm.

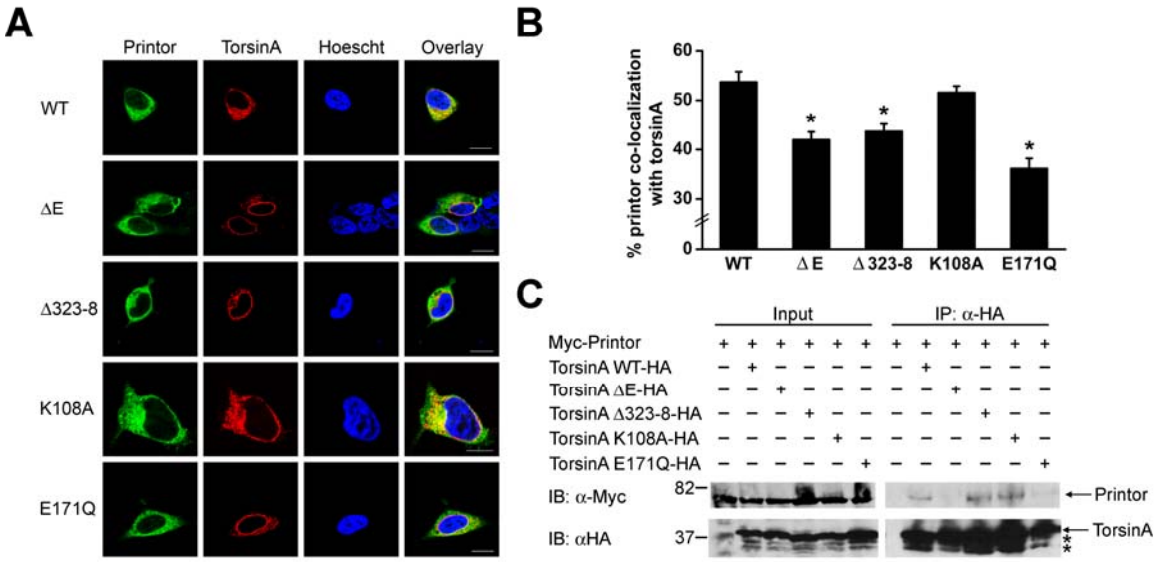

FIGURE III-8. Printor interaction and co-localization is disrupted by ΔE and E171Q torsinA mutation. (A) Co-localization between printor and torsinA proteins. SH-SY5Y cells expressing Myc-tagged printor and C-terminally HA-tagged torsinA WT, torsinA ΔE, torsinA Δ323-8, torsinA K108A or torsinA E171Q were stained with primary antibodies against HA and Myc, followed by detection with secondary antibodies conjugated to TR (torsinA, red) or FITC (printor, green). Hoechst stain was used to visualize the nucleus. **(B)** Quantification shows the percent of printor protein that co-localizes with torsinA. Data represent mean ± S.E. from at least three independent experiments. *Significantly different from the percent printor co-localization with torsinA WT ($p < 0.05$). **(C)** Extracts fromSH-SY5Y cells expressing Myc-tagged printor and C-terminally HA-tagged torsinA WT, ΔE, Δ323-8, K108A or E171Q were subjected to immunoprecipitation with ant-HA antibody followed by immunoblotting with anti-HA and anti-Myc antibodies. Scale bars, 10μm.

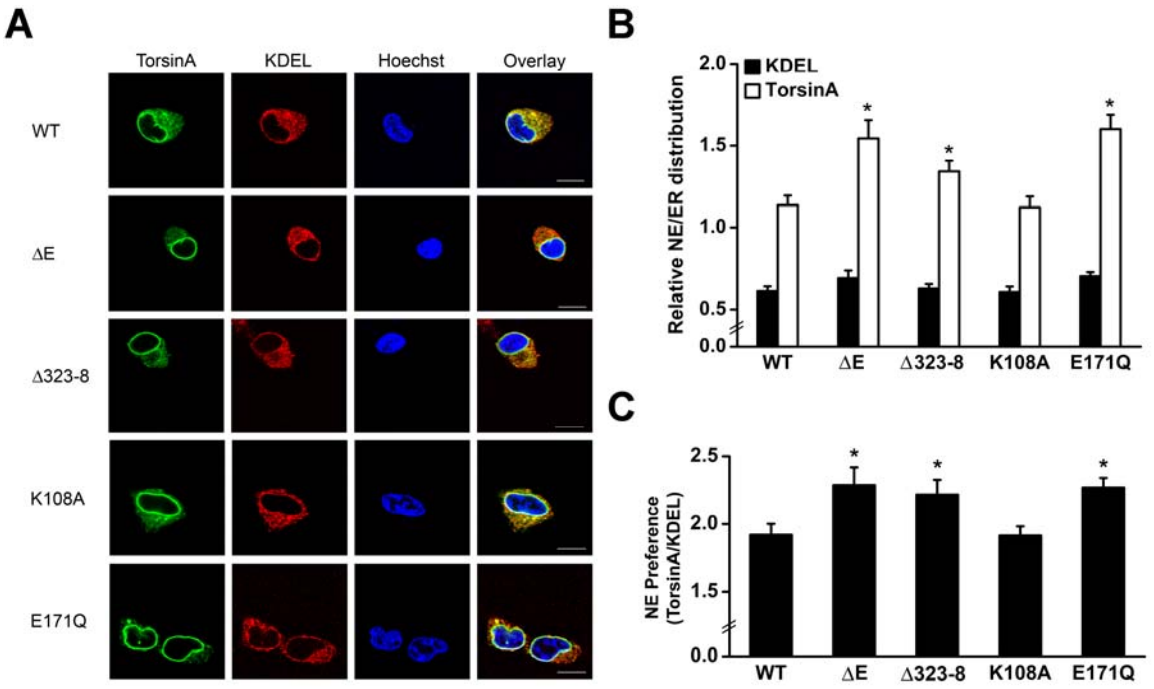

FIGURE III-9. ATP-bound torsinA displays enhanced NE preference. (A) SH-SY5Y cells expressing C-terminally HA-tagged torsinA WT, torsinA ΔE, torsinA Δ323-8, torsinA K108A, or torsinA E171Q were stained with primary antibodies against HA and ER marker KDEL, followed by detection with secondary antibodies conjugated to TR (KDEL, red) or FITC (torsinA, green). Hoechst stain was used to visualize the nucleus. **(B)** Quantification shows the relative distribution of torsinA and KDEL in the NE versus the ER. Data represent mean ± S.E. from at least three independent experiments. *Significantly different from the NE/ER ratio of torsinA WT ($p < 0.05$). **(C)** NE preference of torsinA was determined by normalizing the NE/ER ratio of torsinA to the corresponding NE/ER ratio of KDEL in the same cells. Data represent mean ± S.E. from at least three independent experiments. *Significantly different from torsinA WT ($p < 0.05$). Scale bars, 10μm.

CHAPTER IV

DISCUSSION AND CONCLUSIONS

Summary of findings

The discovery that mutations in the gene encoding torsinA contributed to the development of DYT1 dystonia was an important milestone in understanding the underlying pathogenesis of the disease (Ozelius et al. 1997). However, the effects of the dystonia-associated mutations on torsinA remain poorly understood. In this dissertation I investigated and characterized the distribution, oligomerization and degradation pathways for torsinA WT and dystonia-associated mutant proteins. I also identified a novel torsinA-interacting protein, printor, which regulates torsinA turnover. The findings presented in Chapters II and III demonstrate:

1) TorsinA has a neuronal cell-type specific NE preference, that is enhanced by dystonia associated mutations and ATP-bound state.
2) TorsinA WT is a long-lived protein degraded through the autophagy-lysosome pathway, while dystonia-associated mutations promote premature degradation by both the proteasome and autophagy-lysosome pathways.
3) The identification of a novel-torsinA binding protein printor which may represent a novel member of the BTB-BACK-Kelch (BBK) superfamily
4) Printor co-distributes with torsinA in brain and other tissues, co-localizes with torsinA at the ER, and preferentially interacts with torsinA WT and ATP-unbound torsinA, but not with torsinA ΔE or ATP-bound torsinA.

A discussion of these findings and their implications for understanding the molecular mechanisms of DYT1 pathogenesis and potential future directions are provided in this chapter.

Neuronal Cell-Type Specific NE Localization of TorsinA

It is unclear why genetic mutations in human torsinA result in a neuronal phenotype, despite widespread expression of the protein in multiple tissues (Shashidharan et al. 2000). It is also a mystery why torsinA null and torsinA ΔE knock-in mice have neuron-specific NE membrane abnormalities (Goodchild et al. 2005). TorsinA is commonly reported to be localized to the ER and has also been observed in the NE (Gonzalez-Alegre and Paulson 2004; Goodchild and Dauer 2004; Naismith et al. 2004), however, the relative distribution of torsinA has never been quantified, which is significant due to the contiguous nature of the ER and NE (Ellenberg et al. 1997). In addition, previous studies have reported the mislocalization of torsinA ΔE and ATP-bound torsinA E171Q to the NE (Gonzalez-Alegre and Paulson 2004; Naismith et al. 2004; Goodchild and Dauer 2005; Kock et al. 2006), however these studies have never included a quantitative analysis. TorsinA Δ323-8 localization has only been examined once, where it was reported to have a localization similar to torsinA WT, however, this study was never repeated (O'Farrell et al. 2002).

To address these issues, we examined torsinA localization in both non-neuronal HeLa cells as well as neuroblastoma derived SH-SY5Y cells. Using quantitative double-label immunofluorescence confocal analysis, we were able to show that torsinA WT

displays NE preference in neuronal SH-SY5Y cells compared to non-neuronal HeLa cells (Giles et al. 2008). When we examined endogenous torsinA, we found that torsinA in primary cortical neurons showed a NE preference compared to torsinA in fibroblasts (Giles et al. 2008). Our quantitative analysis of the localization of both dystonia-associated mutant forms of torsinA revealed that both torsinA ΔE and torsinA Δ323-8 displayed an enhanced NE preference compared to torsinA WT in neuronal SH-SY5Y cells, but not in non-neuronal HeLa cells. Further, our quantitative analysis of the localization of ATP-unbound and ATP-bound torsinA showed that ATP-bound torsinA displayed a greater NE preference than either torsinA WT, torsinA ΔE or torsinA Δ323-8 in SH-SY5Y cells but had no effect on torsinA localization in HeLa cells.

The presence or absence of ATP or GTP can regulate the spatial distribution of nucleotide binding proteins (Babst et al. 1998; Meng et al. 2006). Our studies suggest that, in neuronal cells, ATP-bound torsinA has an enhanced NE preference compared to both torsinA WT and ATP-unbound torsinA. This suggests the existence of a neuronal-specific torsinA substrate on the NE. To date, only one of the known torsinA interactors, LAP1 (Goodchild and Dauer 2005), is localized to the NE, however database searches reveal that LAP1, like torsinA, is widely expressed, suggesting that the interaction between torsinA and LAP1 is unlikely to be neuron-specific. In addition, the effect of torsinA dystonia-associated mutations on LAP1 interaction has not been examined.

Together, these data suggest that torsinA plays a neuron-specific role at the NE, which makes the neuronal NE especially vulnerable to torsinA dysfunction and could explain the neuronal-cell specific phenotype of dystonia-associated torsinA mutations. Identification of NE localized torsinA-interacting proteins is therefore likely to lead to a

better understanding of the role of torsinA in neurons. Further, our findings stress the need for careful interpretation of experiments conducted in non-neuronal cell lines and highlight the importance of choosing appropriate cellular models for studying diseases with neuron-specific phenotypes.

TorsinA Protein Degradation Pathways

An unexplored area of torsinA research has been the effect of mutation on torsinA stability and degradation. The two main routes of protein degradation in cells are the ubiquitin-proteasome pathway, which usually mediates selective degradation of short-lived regulatory proteins and misfolded proteins, and the autophagy-lysosome pathway, hereafter referred to as autophagy, which is thought to be a relatively non-selective bulk-clearance system responsible for the turnover of long-lived proteins and organelles (Ciechanover 2005; Rubinsztein 2006; Ding and Yin 2008). Our pulse-chase studies demonstrated that torsinA wild-type (WT) is an extremely stable protein, with a half-life of several days (Giles et al. 2008). In addition, our inhibitor studies reveal that wild-type torsinA is degraded through the autophagy pathway, but not the proteasome pathway, consistent with our finding that torsinA WT is a long-lived protein (Fig. IV-1) (Giles et al. 2008). ER resident proteins typically have a long half-life, on the order of 2-6 days, but the mechanism of their turnover is not clear (Bonifacino and Kalusner 1994). One possibility is that proteins destined for degradation gather in a subdomain of the ER compartment that is then removed and targeted for the lysosome, however, the necessary signals for creating and maintaining such a subdomain are not known.

Unlike the long-lived torsinA WT, our studies revealed that both dystonia-associated mutations destabilized torsinA considerably, reducing the half-life to ~18 hr (Giles et al. 2008). In direct contrast to torsinA WT, we found that proteasomal inhibition significantly delayed the degradation of both torsinA ΔE and torsinA Δ323-8 mutant proteins, indicating that dystonia-associated torsinA mutant proteins are selectively targeted to the proteasome for degradation (Fig. IV-1) (Giles et al. 2008). Unfolded or misfolded proteins are translocated from the ER to the cytoplasm where they can be tagged by ubiquitin and targeted to the proteasome for degradation through a process known as ER assisted degradation (ERAD) (Kleizen and Braakman 2004; Meusser et al. 2005; Kincaid and Cooper 2007). Our data indicates that torsinA ΔE and Δ323-8 mutant proteins are likely substrates for ERAD, suggesting that both dystonia-associated mutations perturb the folding process and may be unable to reach the correct native conformation (Giles et al. 2008). Previous studies have shown that torsinA ΔE inhibits torsinA function and that torsinA null and torsinA ΔE knock-in mice display similar phenotypes, suggesting that torsinA ΔE is a loss-of-function mutation (McLean et al. 2002; Torres et al. 2004; Goodchild et al. 2005). However, the mechanism through which functional loss occurred was not clear. Our data suggests that mutation associated misfolding and subsequent targeting for premature degradation may be the underlying cause of functional loss, which would add dystonia to a growing body of diseases that are associated with protein misfolding (Bross et al. 1999; Olzmann et al. 2004).

Our inhibitor studies also revealed that both dystonia-associated mutant proteins are also processed through the autophagy pathway (Giles et al. 2008). Autophagy has recently been recognized as a secondary pathway that can be turned on in the event of

ERAD overflow or disruption (Yorimitsu and Klionsky 2007; Yorimitsu and Klionsky 2007). Because torsinA WT is also regulated through the autophagy pathway, it is not clear whether dystonia-associated mutant clearance by autophagy is part of an ERAD overflow response, or part of the normal torsinA clearance, especially since we showed that torsinA WT and torsinA mutants are capable of complexing (Giles et al. 2008). Autophagy can also be used to clear insoluble ER aggregates that are unable to be processed by ERAD (Fujita et al. 2007). TorsinA ΔE has been previously reported to form perinuclear inclusion, which are thought to be associated with high levels of exogenous expression (Hewett et al. 2000; Goodchild et al. 2005). Although we did not observe such inclusions in our model, we cannot exclude the possibility that small undetectable aggregates may have formed that would require clearance through the autophagy pathway.

TorsinA is believed to reside in the endoplasmic reticulum (ER) lumen, and has also been observed in the nuclear envelope (NE) (Gonzalez-Alegre and Paulson 2004; Goodchild and Dauer 2004; Naismith et al. 2004). Our studies revealed that torsinA shows a neuronal cell-type specific NE preference, which is further enhanced by both mutations (Giles et al. 2008). In addition, previous studies have reported NE abnormalities in cells lacking torsinA, as well as in cells overexpressing both WT and mutant torsinA (Goodchild et al. 2005; Grundmann et al. 2007). This raises the question of how NE-localized torsinA is degraded. Although there is some evidence that NE proteins can be processed through ERAD, it is unclear whether this process requires NE proteins to relocate to the ER or whether translocation can occur on the cytoplasmic face of the NE (McBratney and Winey 2002; Muchir et al. 2006). As with ERAD, the role of

autophagy in NE protein clearance is not yet known. In yeast, a process known as piecemeal microautophagy (PMN) is used to target portions of the nuclear envelope and associated nuclear envelopes in conditions of nutrient starvation, however it is not clear whether there is a similar mechanism for mammalian systems.(Roberts et al. 2003; Kvam and Goldfarb 2006) It is also unclear whether the NE utilizes the same signals and systems as the ER or whether NE-specific signaling systems exist to identify and target proteins for degradation. Further investigation into these issues could have important implications in understanding the mechanisms of torsinA clearance in both the NE and the ER.

Printor, a Novel TorsinA-interacting Protein, May Belong to the BBK Superfamily

The identification of torsinA-interacting proteins is hoped to lead to a better functional understanding of torsinA protein as well as provide insight into how the DYT1-associated mutations result in disease. To identify torsinA-interacting proteins, we performed yeast-two hybrid screens of a rat brain hippocampal/cortical cDNA library using torsinA WT and torsinA WTΔ40 as bait. We discovered a novel torsinA-interacting protein, which we named printor for protein interactor of torsinA (Chapter III). Printor is a 70 kDa protein with an N-terminal region that displays homology to the BTB/POZ domain, followed by a BACK domain and six C-terminal kelch repeats (Chapter III). This domain structure places printor into the BBK (BTB/POZ-BACK-Kelch) superfamily of proteins (Prag and Adams 2003; Stogios and Prive 2004; Stogios et al. 2005). However, it is unclear at this

time whether the BTB/POZ domain of printor is functional due to the presence of a P/Q rich interruption (Chapter III).

BTB/POZ domain

The BTB/POZ domain was identified in the *Drosophila* transcription factors Bric-a-brac, Tramtrak and Broad Complex (BTB) (Perez-Torrado et al. 2006). Concurrently, it was noticed that certain Poxvirus proteins contained regions of homology to known Zinc finger proteins, and this domain was named Poxvirus and Zinc finger (POZ), and the domain became known as the BTB/POZ domain (Perez-Torrado et al. 2006). The BTB/POZ domain, hereafter referred to as BTB domain, is evolutionarily conserved in eukaryotes, but is not found in bacteria (Stogios et al. 2005; Perez-Torrado et al. 2006). BTB domain containing proteins can be divided into different sub-families based on the other domains present, and the size of the BTB domain can vary between sub-families (Stogios et al. 2005; Perez-Torrado et al. 2006). The core BTB domain consists of 95 residues, of which little more than a dozen residues are highly conserved between proteins (Stogios et al. 2005; Perez-Torrado et al. 2006). These highly conserved residues are hydrophobic in nature and are thought to be pivotal in determining the structural folds of the BTB domain (Stogios et al. 2005; Perez-Torrado et al. 2006). In contrast, the exposed residues are highly variable between sub-families, which allows the BTB domain to be used for a variety of different functions including transcription repression, cytoskeleton regulation, tetramerization and gating of ion channels, and protein ubiquitination (Stogios et al. 2005; Perez-Torrado et al. 2006).

Although proteins can consist of only the BTB domain, such as Skp1 and ElonginC, which are both involved in ubiquitination, the BTB domain is more frequently found in combination with other domains (Stogios et al. 2005; Perez-Torrado et al. 2006). The most frequent domains found with BTB domains are the MATH (meprin and tumor necrosis factor receptor associated factor homology), kelch, zinc-finger (ZF), and ion transport channel (Stogios et al. 2005; Perez-Torrado et al. 2006). Interestingly, the BTB domain found in combination with other domains tends to be slightly elongated at the amino-terminal, and this elongation is thought to be critical to dimer and oligomer formation (Stogios et al. 2005; Perez-Torrado et al. 2006). While BTB-only proteins Skp1 and ElonginC are known to act as monomers, proteins containing the elongated BTB domain are thought to require dimerization (Stogios et al. 2005; Perez-Torrado et al. 2006). BTB-zinc finger proteins PLZF and BCL6 become unfolded and non-functional when dimerization is disrupted (Collins et al. 2001; Stogios et al. 2005; Perez-Torrado et al. 2006).

The two best characterized functions of the BTB domain containing proteins are transcriptional regulation and ubiquitination (Collins et al. 2001; Xu et al. 2003; Stogios et al. 2005; Perez-Torrado et al. 2006). The BTB domain of transcriptional regulators PLZF and BCL6 is thought to mediate homo- and heterodimerization, and recruit co-repressors to inhibit transcription (Collins et al. 2001; Perez-Torrado et al. 2006). The BTB domain of *Drosophila* transcriptional regulator GAGA is responsible for oligomerization and DNA binding (Collins et al. 2001). BTB domains have been shown to interact with the cullin family of E3 ubiquitin ligases (Geyer et al. 2003; Xu et al. 2003; Stogios et al. 2005; Perez-Torrado et al. 2006). There are six known members of

the cullin family, which form multi-subunit E3 ubiquitin ligase complex with the Ring-H2 protein Rbx1 (also known as Roc1), which binds the E2 (Geyer et al. 2003; Xu et al. 2003). Cullin E3 ubiquitin ligases derive substrate specificity by binding a BTB containing protein (Xu et al. 2003). Skp1 and ElonginC, which are both BTB-only domains, recruit F-box or SOCS-box proteins, respectively, which in turn recruit the substrate to be ubiquitinated (Xu et al. 2003; Stogios et al. 2005; Perez-Torrado et al. 2006). However, BTB proteins that contain other domains can recruit their substrates direction through interaction with the other domains (Geyer et al. 2003; Krek 2003; Xu et al. 2003; Perez-Torrado et al. 2006). Although many BTB containing proteins have been shown to interact with cullin family members, it is not clear whether all BTB containing proteins are involved in ubiquitination.

BACK domain

The BTB and C-terminal Kelch (BACK) domain was identified in a majority of proteins that contain both the BTB domain and kelch repeats (Stogios and Prive 2004; Stogios et al. 2005). The BACK domain has also been identified in proteins containing only the BTB domain or only the kelch domain, as well as in some proteins with neither domain (Stogios and Prive 2004; Stogios et al. 2005). The BACK domain is highly conserved across species and proteins, suggesting an unknown structural or functional role (Stogios and Prive 2004).

Kelch domain

The kelch repeat was originally identified in the *Drosophila* kelch protein (Robinson et al. 1994; Robinson and Cooley 1997). The kelch repeat is 44-56 amino acids in length, and is generally found as 4-7 sequential repeats (Adams et al. 2000). Kelch repeats have a low degree of homology, even within the same protein, however, there are 8 highly conserved residues that are necessary for kelch repeat function (Adams et al. 2000). Kelch repeats form a beta propeller in which each kelch repeat domain forms one blade made up of beta sheets (Adams et al. 2000). This provides multiple regions for protein-protein interactions, on both sides of the propeller blade and in the grooves between the blades (Adams et al. 2000). The *Drosophila* kelch protein binds to and stabilizes actin in oocyte ring canals (Robinson et al. 1994; Robinson and Cooley 1997), and a number of other kelch proteins have also been found to interact with actin, however, there are a number of kelch containing proteins that show no sign of interacting with actin (von Bulow et al. 1995; Way et al. 1995; Soltysik-Espanola et al. 1999; Adams et al. 2000). For instance, in spermatazoa, α-scruin is known to stabilize actin bundles while β-scruin is localized in a region which does not contain actin, despite a 67% homology between the two proteins (Way et al. 1995; Adams et al. 2000). The catalytic site for the fungal enzyme galactose oxidase is contained in the kelch repeat beta propeller, therefore it is possible that other kelch-containing proteins may display some kind of enzymatic activity (Adams et al. 2000). In addition, due to the multiple binding sites provided by the beta propeller, kelch repeats can act as an organizing center for multimeric complexes, such as clathrin which binds β-arrestin and the AP-2 complex in different regions of the propeller (Adams et al. 2000).

BBK protein superfamily

There are as many as 51 BTB-BACK-Kelch (BBK) superfamily proteins in the human genome, and the BBK family comprises 72% of identified kelch proteins in humans (Prag and Adams 2003). Of the 19 known kelch proteins in *Drosophila* and the 16 known kelch proteins in *C. elegans*, 11 and 7 are BBK proteins, respectively (Prag and Adams 2003). There are no known BBK proteins in yeast, suggesting that the BBK domain architecture developed during the evolution of multicellular organisms (Prag and Adams 2003). The BTB domain is thought to mediate dimerization, and in the *Drosophila* kelch protein, while the kelch domain is sufficient for localization to ring canals, the BTB domain is necessary for actin organization (Robinson and Cooley 1997; Adams et al. 2000).

BBK proteins Mayven, ENC-1, NRP/B and gigaxonin have all been implicated in neuronal development (Hernandez et al. 1997; Kim et al. 1998; Soltysik-Espanola et al. 1999; Bomont et al. 2000; Yang et al. 2007). Mayven is a brain-enriched actin-interacting protein that may be involved in the organization of the actin cytoskeleton in neurons and oligodendrocytes (Soltysik-Espanola et al. 1999; Williams et al. 2005). Expression of ENC-1 (Ectodermal-Neural Cortex-1), an actin-interacting protein, is highly specific for neural tissue and is expressed during embryogenesis and development of the nervous system (Hernandez et al. 1997). NRP/B (Nuclear Restricted Protein/Brain), a nuclear matrix protein, is highly expressed in fetal brain in a neuron-specific manner and appears to play a role in neuron differentiation (Kim et al. 1998). Gigaxonin is a ubiquitously expressed protein that regulates cytoskeletal binding partners such as the light chain of microtubule-associated protein 1B through ubiquitin-dependent degradation, and

mutations in gigaxonin result in giant axonal neuropathy (Bomont et al. 2000; Yang et al. 2007).

Printor Does Not Interact with ΔE TorsinA or ATP-Bound TorsinA

Because printor is a novel and uncharacterized protein, we developed an anti-printor antibody to characterize its distribution in brain and other tissues, as well as at the subcellular level (Chapter III). Our findings demonstrated that printor and torsinA co-distribute throughout the brain as well as in other tissues (Chapter III). Further examination of printor in the brain slices and primary neurons demonstrated that printor localized primarily to neuronal cell bodies, but could also be seen in neurites (Chapter III). At the subcellular level, we demonstrated that printor is present in both cytosolic and membrane-associated pools (Chapter III). Double label immunofluorescent confocal analysis demonstrated that printor is most likely associated with the ER and not early endosomes, lysosomes or mitochondria (Chapter III). A combination of triple label immunofluorescence confocal microscopy and opti-prep gradient fractionation analysis demonstrated that printor and torsinA co-localize with ER markers (Chapter III). Further, our quantification analysis showed that printor has an ER preference in both non-neuronal HeLa and neuroblastoma derived SH-SY5Y cells, unlike torsinA, which displays a neuronal-cell type specific NE preference. These data suggest that printor and torsinA may interact in multiple tissues, including brain. Moreover, these data suggest that printor and torsinA are localized to the same subcellular compartment. Together, our

findings suggest that printor appropriately localized to be a physiologically relevant torsinA-interacting protein.

To better understand the pathological mechanisms through which mutant torsinA results in dystonia, a major effort has been made to identify torsinA-interacting proteins. Although a number of torsinA-interacting proteins have been identified (Kamm et al. 2004; Torres et al. 2004; Goodchild and Dauer 2005; Hewett et al. 2006; Esapa et al. 2007; Granata et al. 2008), none of these interactions are affected by the presence of dystonia-associated mutations. Furthermore, although torsinA is a known ATPase, only one study examined the effect of ATP on torsinA interaction (Goodchild and Dauer 2005).

We first established that printor was able to interact with torsinA WT in transfected cells and further demonstrated the existence of an endogenous printor-torsinA complex in mouse cerebellum (Chapter III). We also demonstrated that printor and torsinA co-localized in transfected and untransfected SH-SY5Y cells (Chapter III). To examine the effect of the ATP-bound state on torsinA co-localization with printor, we used quantitative double label immunofluorescence microscopy. Our results demonstrated that printor co-localized with ATP-unbound torsinA to a similar degree as torsinA WT, but had a reduced level of co-localization with ATP-bound torsinA (Chapter III). The reduction in co-localization is likely due to the enhanced NE preference of ATP-bound torsinA compared to torsinA WT (Chapter III). We then examined the ability of printor to interact with ATP-bound and –unbound torsinA. Our studies showed that printor preferentially interacts with ATP-unbound torsinA, but not with ATP-bound torsinA. Because AAA+ proteins tend to display an increased affinity for their target

proteins in their ATP-bound state, printor is not likely to be a substrate for torsinA. Instead, printor may regulate torsinA ATPase activity.

We then examined the effect of dystonia-associated mutations on printor-torsinA interaction using quantitative double label immunofluorescence microscopy. Our results demonstrated that printor displayed reduced co-localization with both forms of dystonia-associated torsinA, which is consistent with our previous observation that dystonia-associated mutant torsinA shows an enhanced NE preference (Giles et al. 2008). When we examined the effect of dystonia-associated mutation on printor-torsinA interaction, we found that printor interacted with Δ323-8 torsinA but not with ΔE torsinA. This is the first report of a torsinA binding partner that interacts preferentially with torsinA WT but not with ΔE torsinA, the mutation linked to the majority of DYT cases.

Although the mechanism through with ΔE torsinA disrupts printor-torsinA interaction is not clear, it is possible that the ΔE mutation results in a greater affinity for ATP or reduced levels of ATP-hydrolysis and therefore exists primarily in the ATP-bound state. The ΔE mutation, unlike the Δ323-8 mutation, is located within the AAA+ domain, which is considered essential for coordinating both ATP-binding and ATP-hydrolysis (Neuwald et al. 1999). In addition, one study reported that both dystonia-associated mutations displayed reduced levels of ATP-hydrolysis, with the ΔE mutation reported as having a more severe loss of function (Konakova and Pulst 2005). However, a separate study reported no change between torsinA WT and torsinA ΔE ATPase activity (Kustedjo et al. 2003), therefore the effect of the dystonia-associated mutations on torsinA ATPase activity is still unclear. Another possible explanation for the observed

loss of printor-torsinA interaction is that the ΔE mutation may be located in the printor binding region of torsinA.

Another possibility is that printor interacts with only the monomer or only the oligomeric form of torsinA, which our method is unable to distinguish between. Although our previous results demonstrated that torsinA ΔE and torsinA Δ323-8 were still able to interact with torsinA WT, we did not examine whether either form was more or less likely to exist in a multimeric state. Previous studies have suggested that torsinA ΔE is more likely to oligomerize than torsinA WT (Torres et al. 2004), and some AAA+ proteins only oligomerize when ATP-bound (Akoev et al. 2004). If printor interacts preferentially with a monomeric form of torsinA, and torsinA ΔE and torsinA E171Q are more likely to exist in the multimeric form, this could also explain the loss of interaction.

Printor is the first reported torsinA-interacting protein that does not bind to ΔE torsinA. It is also the first reported torsinA-interacting protein that preferentially interacts with ATP-unbound torsinA. Together, these data suggest that printor plays a role in the pathogenic pathway of dystonia.

Future Directions

Discerning the functional role of torsinA

Although a number of hypotheses exist, the function of torsinA still remains a mystery. TorsinA has been suggested to be a molecular chaperone based on sequence homology to known chaperone proteins (Ozelius et al. 1998). Overexpression of torsinA has been shown to reduce aggregates in both cell and animal models (McLean et al. 2002;

Caldwell et al. 2003; Cao et al. 2005), which is comparable to the overexpression of known chaperone proteins. However, to date torsinA has not been demonstrated to have specific chaperone activity, and more importantly, no protein has been identified as a substrate for torsinA activity. The identification of torsinA-binding partners is essential to determining what role the putative chaperone activity plays in normal cell functions.

Although torsinA has been characterized as an ER lumenal protein, a number of studies have reported a cytosolic population (Hewett et al. 2000; Shashidharan et al. 2000; Shashidharan et al. 2000; Konakova and Pulst 2001; Walker et al. 2001; Walker et al. 2002; Augood et al. 2003; Hewett et al. 2003; Rostasy et al. 2003). In addition, aside from LAP1/LULL1, none of the identified torsinA-interacting proteins are ER-localized proteins (Kamm et al. 2004; Torres et al. 2004; Goodchild and Dauer 2005; Hewett et al. 2006; Granata et al. 2008). TorsinA has been suggested to play a role in neurite extension (Ferrari-Toninelli et al. 2004; Hewett et al. 2006) and has been observed in neuritis and growth cones (Kamm et al. 2004). TorsinA has also been observed in secretory granules, and appears to play a role in the exo-endocytic pathway (Granata et al. 2008). TorsinA also affects the plasma membrane levels of polytopic receptors and the secretion of luciferase (Hewett et al. 2007). Although some of these observations may be due to alterations in the secretory pathway originated through torsinA activity in the ER, it seems likely that a cytosolic pool of torsinA exists. The size of this pool relative to ER-localized torsinA appears to be quite small in cultured cells, which makes it difficult to study using conventional methods. However, differentiating these two pools of torsinA, determining the signals that sort torsinA between the ER and the cytosol, and identifying

the function of both pools will be important in determining how torsinA is utilized in cells.

Although our method (Giles et al. 2008) was able to quantify a change in torsinA localization, we are unable to distinguish between the membrane and lumen of the organelles. It is therefore unclear whether the populations of torsinA that we observed faced the lumen or the cytosol, whether the population consisted entirely of membrane associated torsinA or whether torsinA was free within the ER lumen, and in the case of the NE, whether torsinA is associated with the inner or outer NE membrane. Determining how torsinA is oriented within both the ER and the NE will be important to understanding how torsinA is sorted between the two subdomains as well as what factors influence sorting.

TorsinA knock-out animals and torsinA ΔE double knock-in animals display neuron-specific NE perturbations (Goodchild et al. 2005). Combined with our data showing a neuron-specific NE preference for torsinA (Giles et al. 2008), this suggests a neuron-specific torsinA function in the NE. TorsinA knock-out mice displayed abnormal vesicle formation in the lumen of the nuclear envelope that appeared to be derived from the inner nuclear membrane (Goodchild et al. 2005), suggesting that torsinA may play a role in organizing the NE of neurons. The exact mechanism involved is unknown, as the only known NE torsinA-interacting protein LAP1 is ubiquitously expressed (Goodchild and Dauer 2005). Further identification of neuronal NE torsinA-interacting proteins will shed more light on the function of torsinA at the neuronal NE.

In addition, because our studies were performed in cultured cells, it will be important to examine the localization of torsinA in intact systems. Although cultured

cells can be an important tool in understanding cellular systems, it is possible that the presence of intact networks of neurons can affect how proteins act. It is also likely, given that torsinA mutations result in a specific motor defect, that there exist sub-populations that are more susceptible to changes in torsinA activity, which we were unable to examine in our system. Determining the behavior of both torsinA WT and torsinA mutants in the intact nervous system will likely shed further light on what neurologic pathways require intact torsinA activity for proper function.

How do the dystonia-associated mutations disrupt torsinA function?

Determining how dystonia-associated mutations disrupt torsinA function is essential to developing appropriate therapies for patients with DYT1 dystonia. TorsinA ΔE is thought to be a loss of function mutation, which is supported by the similarity between torsinA knock-outs and ΔE torsinA double knock-ins (Goodchild et al. 2005). TorsinA ΔE is also incapable of clearing protein aggregates (McLean et al. 2002; Caldwell et al. 2003) and disrupts luciferase secretion (Hewett et al. 2007). The Δ323-8 mutation is less well characterized, and therefore its effect on torsinA function is not known. Protein mutations can disrupt protein function in a number of ways: disruptions in protein-protein interaction, loss of enzymatic activity, mislocalization, or disruptions in folding that lead to premature degradation or aggregation.

The C-terminus of AAA+ family members is thought to be important for substrate recognition and oligomerization (Ogura and Wilkinson 2001). Because both dystonia-associated mutations are located in the C-terminus, it was thought that they may disrupt oligomerization. Our data shows that the C-terminus of torsinA is not necessary

for self-interaction, and that the dystonia-associated mutations do not disrupt torsinA-torsinA interaction (Giles et al. 2008). However, our study did not address whether dystonia-associated mutations alter torsinA binding affinity for itself. One theory is that dystonia-associated mutation may act as a dominant-negative, and it has been shown that overexpression of torsinA ΔE can alter the localization of torsinA WT (Goodchild and Dauer 2004; Torres et al. 2004). Torres et al. even reported that ΔE torsinA appears to oligomerize more readily than torsinA WT (Torres et al. 2004). However, all of these studies on torsinA interaction, including our own, have been performed *in vivo* and therefore do not preclude the possibility of oligomerization occurring indirectly through a third-party protein. Further investigation into the dynamics of torsinA oligomerization is needed to determine the effect of dystonia-associated mutation.

Although the C-terminus of AAA+ proteins is also thought to be important in substrate binding (Ogura and Wilkinson 2001), to date printor (Chapter III) is the only identified torsinA-interacting protein that interacts with torsinA WT, but not torsinA ΔE. Kinesin light chain, vimentin, snapin, and e-sarcoglycan all bind to torsinA ΔE, while mutant torsinA interaction with DAT, LAP1 and LULL1 was never tested. The effect of torsinA Δ323-8 on interaction has never been tested, except by us (Chapter II, III). It is still possible, however, that torsinA-interaction proteins that have not yet been identified are incapable of binding mutant torsinA. Therefore, continued identification of torsinA-binding partners is necessary.

TorsinA is an ATPase with demonstrated ability to bind and hydrolyze ATP (Shashidharan et al. 2000; Kustedjo et al. 2003; Konakova and Pulst 2005). Early reports suggested that torsinA E171Q, a constitutively ATP-bound form of torsinA, and torsinA

ΔE showed a similar pattern of localization (Gonzalez-Alegre and Paulson 2004; Goodchild and Dauer 2004; Naismith et al. 2004), leading to the hypothesis that the ΔE mutation disrupts ATP hydrolysis. In addition, we showed that both torsinA ΔE and torsinA E171Q disrupted torsinA-printor interaction (Chapter III), providing further evidence of a similarity between these two mutations. Interestingly, the ΔE but not Δ323-8 mutation is located within the AAA+ domain of torsinA (Neuwald et al. 1999). Kustedjo et al. examined ATPase activity of torsinA WT and torsinA ΔE and reported no difference (Kustedjo et al. 2003). However, when Konakova and Pulst examined ATPase activity, they reported a decrease in ATPase activity for both torsinA ΔE and torsinA Δ323-8, with the ΔE mutation having a more severe phenotype (Konakova and Pulst 2005). It is therefore not clear whether the dystonia-associated mutations affect torsinA enzymatic activity, and further investigation is needed.

Our data suggests that dystonia-associated mutations destabilize torsinA, which results in premature degradation (Giles et al. 2008). In addition, torsinA ΔE can form perinuclear NE derived aggregates at high levels of expression (Hewett et al. 2000; Goodchild et al. 2005), which could be a result of protein misfolding. A number of diseases, including cystic fibrosis, have been linked to point mutations in proteins that disrupt protein folding (Bross et al. 1999; Welch 2004; Meusser et al. 2005). However, if these mutant proteins are given increased access to chaperones, they are able to reach a native conformation in which the protein is completely functional (Bross et al. 1999; Welch 2004; Meusser et al. 2005). Current research suggests that the application of chemical chaperones may help rescue some of the loss of function that results from

premature degradation in these misfolded-protein related diseases (Bross et al. 1999; Welch 2004; Meusser et al. 2005). Although current research for DYT1 treatment focuses on allele silencing, (Gonzalez-Alegre et al. 2003; Kock et al. 2005; Hewett et al. 2008), if dystonia-mutations disrupt folding but not function, chemical chaperones could become a secondary treatment option.

Discerning the functional role of printor

Printor is a novel torsinA-interacting protein of unknown function (Chapter III). As a potential member of the BBK protein superfamily, printor contains a putative BTB domain, a BACK domain, and a series of kelch repeats (Chapter III). Based on this domain structure, we can begin to hypothesize possible functions.

BTB domain containing proteins have been shown to bind DNA (Collins et al. 2001; Perez-Torrado et al. 2006), recruit transcriptional co-factors (Collins et al. 2001; Perez-Torrado et al. 2006), mediate dimerization (Stogios et al. 2005; Perez-Torrado et al. 2006), and interact with the cullin family of E3 ligases (Xu et al. 2003; Stogios et al. 2005; Perez-Torrado et al. 2006). Printor contains an interruption in the putative BTB domain, which makes it unclear whether the BTB domain is functional (Chapter III). The RhoBTB family of proteins contains two BTB domains, including one with a large 115 amino-acid insertion that has been shown to be necessary for cullin-3 interaction (Ramos et al. 2002; Wilkins et al. 2004). Sequence alignment demonstrates that the P/Q region of printor falls into the same region as the insertion seen in RhoBTB2 (Figure IV-2), suggesting that the BTB domain of printor may be functional. Further, our preliminary analysis (Fig IV-3) suggests that printor is capable of dimerization, a function of BTB

domains. It must be noted that kelch repeats may also be able to mediate dimerization (Way et al. 1995; Adams et al. 2000), therefore it cannot be concluded at this time that dimerization is mediated through the BTB domain. Further study is needed to determine the effect of the P/Q interruption on BTB domain function.

BBK proteins that have been identified have typically fallen into two categories: actin-interacting proteins and ubiquitinating proteins. Of the identified BBK proteins known to be involved in neuronal development, ENC-1 (Hernandez et al. 1997), NRP/B (Kim et al. 1998), and Mayven (Williams et al. 2005) are all actin-interacting proteins, while gigaxonin regulates cytoskeletal-interacting proteins through ubiquitination (Yang et al. 2007). It is therefore tempting to speculate that printor may also play a role in regulating the cytoskeleton. However, there is currently no evidence to support such an assumption, and further investigation is needed.

BBK proteins have also been shown to mediate ubiquitination. The BTB domain has been shown to interact with the cullin family of E3 ubiquitin ligases (Geyer et al. 2003; Krek 2003; Xu et al. 2003). BTB proteins containing other protein interaction domains, like the BBK family, have been demonstrated to interact with cullin-3 (Geyer et al. 2003; Krek 2003; Xu et al. 2003). Our preliminary data suggests that printor is able to interact with cullin-3 (Figure IV-4). Therefore, printor could potentially mediate the ubiquitination of torsinA. Our preliminary data suggests that torsinA can be ubiquitinated (Figure IV-5). Further, our preliminary data suggests that printor enhances the rate of degradation for torsinA WT but not torsinA ΔE or torsinA Δ323-8 (Figure IV-6). It is possible, however, that printor does not regulate torsinA directly, but rather regulates a yet to be identified third party that regulates torsinA turnover, therefore further study is

needed. In addition, it is not clear what function printor-mediated ubiquitination of torsinA serves. Our data suggests that torsinA WT is not degraded through the proteasome (Giles et al. 2008), the conventional ubiquitination-associated degradation pathway (Pickart 1997; Wilkinson 2000). However, only K48 and K29 ubiquitin linkage has been shown to target proteins for the proteasome, therefore it is possible that printor-mediated ubiquitination of torsinA results in a different linkage that targets torsinA for a different fate (Wilkinson 1999; Pickart and Fushman 2004). One possibility is that printor-mediated ubiquitination of torsinA targets torsinA to a subdomain of the ER that is then degraded through autophagy. Although our studies demonstrated that printor is localized to the ER, it is unclear whether printor is able to enter the ER lumen, or whether it is merely associated with the outer ER membrane. Because the orientation of torsinA is also unclear, it is still unknown exactly where torsinA and printor interact. Further study is necessary to determine whether printor ubiquitinates torsinA and how that affects torsinA.

Final Words

In the experiments described above, we have demonstrated that torsinA has a neuronal-cell type specific NE preference, which suggests a neuronal-cell type specific role for torsinA at the NE. In addition, we have demonstrated that dystonia-associated mutant forms of torsinA as well as ATP-bound torsinA display a further enhanced NE preference, suggesting the existence of a NE localized torsinA substrate. Our research shows that torsinA WT is a long-lived protein that is degraded through autophagy while

mutant torsinA is likely misfolded and targeted for premature degradation through the UPS. Further, we have identified the novel torsinA-interacting protein printor that co-distributes with torsinA and co-localizes with torsinA at the ER. We have demonstrated that printor preferentially binds ATP-unbound torsinA over ATP-bound torsinA, and that printor bind torsinA WT and torsinA Δ323-8 but not torsinA ΔE. This suggests that printor may play a regulatory role for torsinA that is disrupted by the presence of the ΔE mutation. We have identified a novel player in the dystonia pathogenic pathway, and our results have significant implications regarding the pathogenic mechanisms of dystonia-associated mutations.

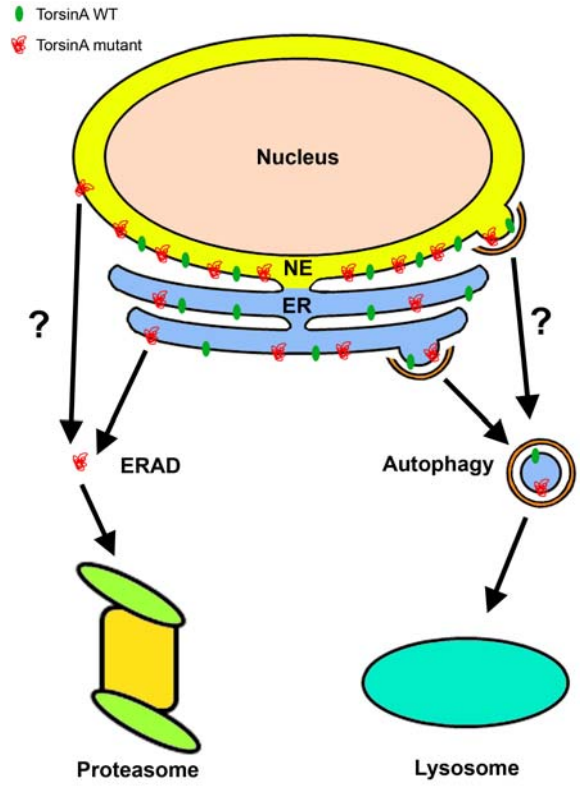

FIGURE IV-1. A model of torsinA degradation. TorsinA WT (green) is recruited to a subdomain of the ER that is sequestered into an autophagosome through an unknown process and transported to the lysosome. TorsinA mutant (red) is retrotranslocated to the cytosol by ERAD and degraded by the proteasome. A population of torsinA mutant is also degraded through the autophagy pathway, though the exact mechanism is unclear. It is uncertain whether these processes can occur directly from the NE membrane.

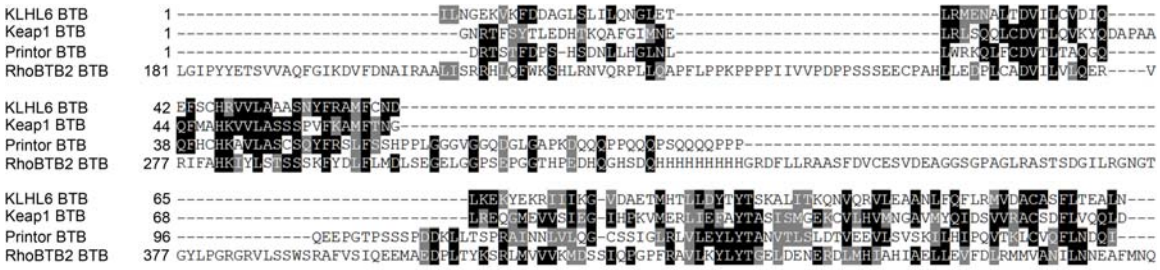

FIGURE IV-2. BTB domain alignment demonstrates printor P/Q insertion coincides with RhoBTB2 insertion. Alignment of the BTB domains of KLHL16, Keap1, Printor and RhoBTB2. Accession numbers for the sequences are as follows: *Hs* KLHL6, NP_569713; *Hs* Keap1, NP_036421; *Hs* Printor, NP_065856.1; *Hs* RhoBTB2, NP_055993.

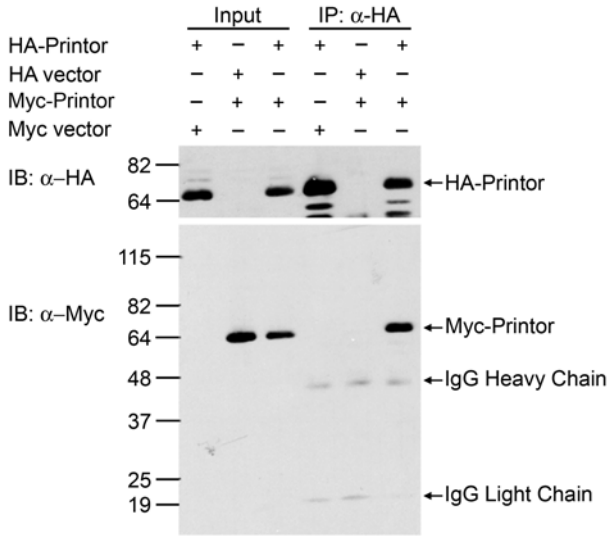

FIGURE IV-3. Printor is capable of self-interaction. HeLa cells expressing HA tagged printor or HA vector and either Myc-tagged printor or Myc vector were lysed and subjected to immunoprecipitation with anti-HA antibody followed by immunoblotting with anti-HA and anti-Myc antibodies. Asterisks indicate printor degradation products.

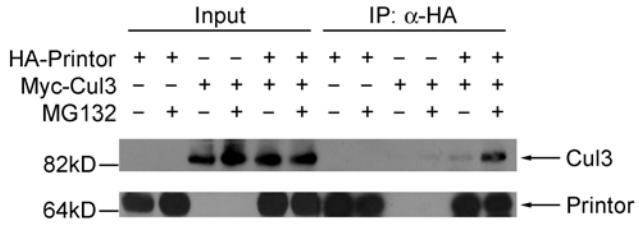

FIGURE IV-4. Printor interacts with cullin-3. SH-SY5Y cells expressing HA-tagged printor or HA vector and Myc-tagged Cul3 were lysed and subjected to immunoprecipitation with anti-HA antibody followed by immunoblotting with anti-HA and anti-Myc antibodies.

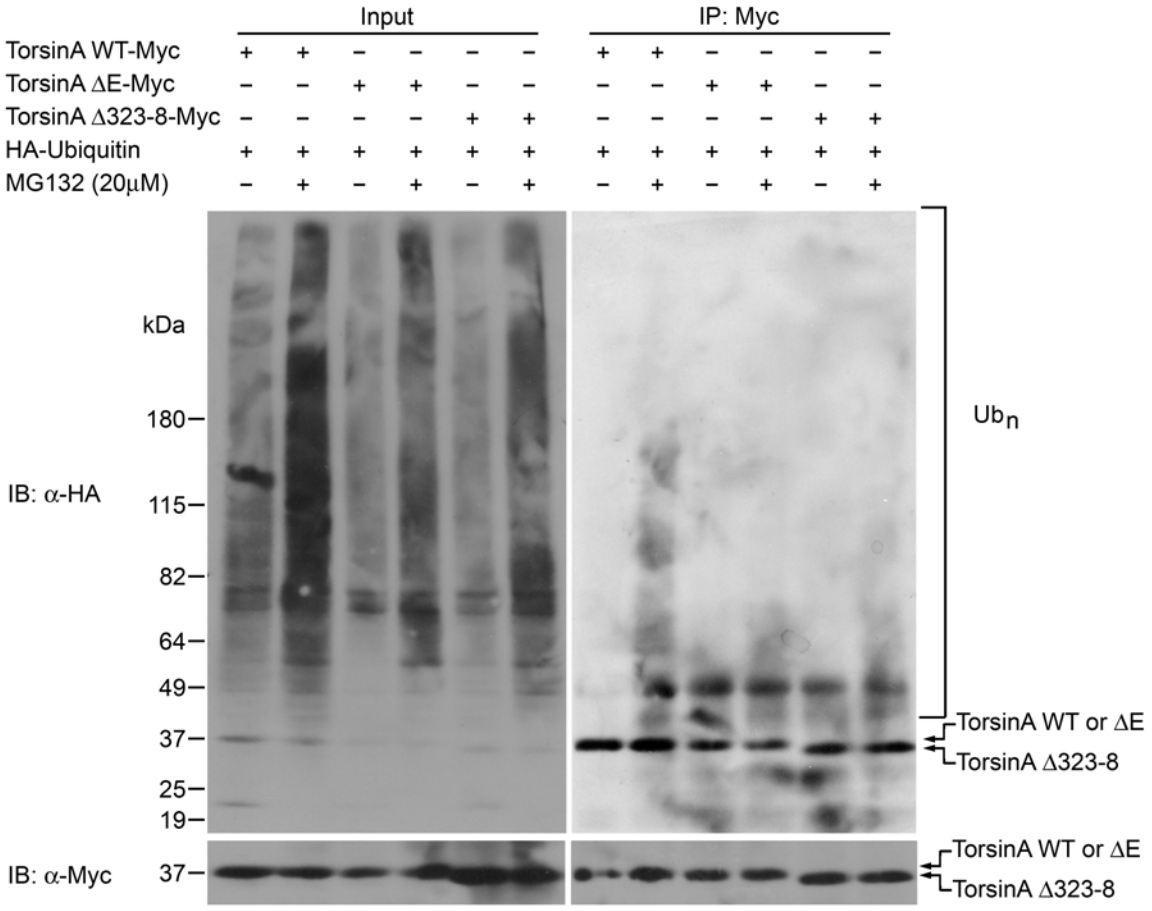

FIGURE IV-5. WT and dystonia-associated mutant torsinA can be ubiquitinated. SH-SY5Y cells expressing C-terminal Myc-tagged WT, ΔE or Δ323-8 torsinA and HA-tagged ubiquitin were treated with either 20μM MG132 or DMSO control for 8 h. Lysates were subjected to immunoprecipitation under denaturing conditions using anti-Myc antibody and immunoblotted with anti-Myc and anti-HA antibodies.

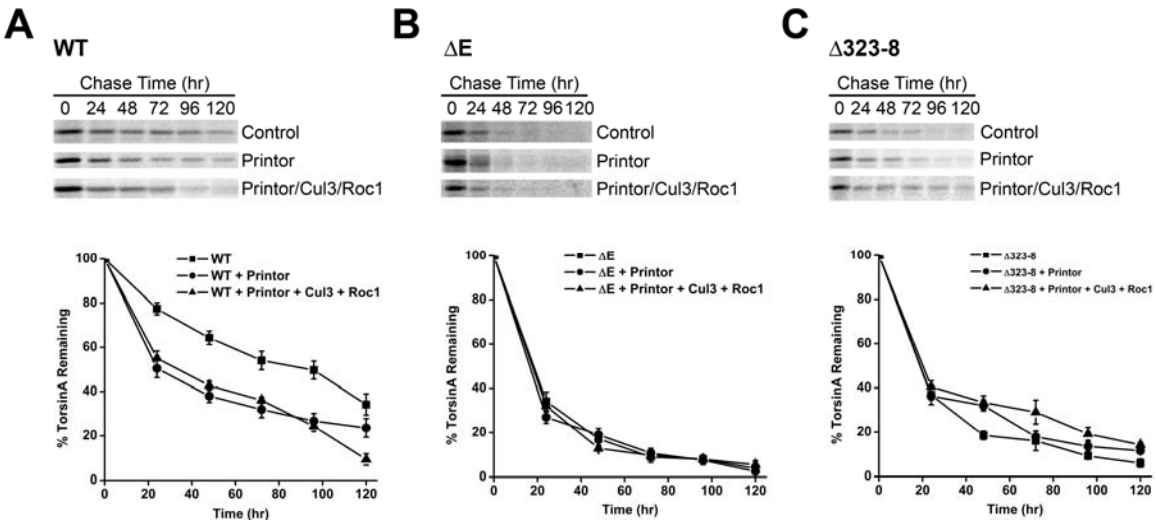

FIGURE IV-6. Printor increases the turnover of torsinA WT but not dystonia-associated mutant torsinA. SH-SY5Y cells expressing Myc-tagged WT **(A)**, ΔE **(B),** or Δ323-8**(C)** torsinA alone (closed square), with HA-tagged printor (closed circle), or with HA-tagged printor, FLAG-tagged cullin-3 and HA-tagged Roc1 (closed triangle) were pulse-labeled for 1 h in [^{35}S]Met/Cys containing medium and chased with non-radioactive Met/Cys for the indicated time. Time points were taken ever 24 h over 5 days. ^{35}S-labeled WT or mutant torsinA proteins were immunoprecipitated from lysates with anti-Myc antibodies and detected by SDS-PAGE and autoradiography. The levels of WT or mutant torsinA proteins were quantified and plotted relative to the corresponding torsinA levels at 0 h. Data represents mean ± S.E. of the results from at least three independent experiments.

REFERENCES

Adams, J., R. Kelso and L. Cooley (2000). "The kelch repeat superfamily of proteins: propellers of cell function." Trends Cell Biol **10**(1): 17-24.

Ahmad, K. F., C. K. Engel and G. G. Prive (1998). "Crystal structure of the BTB domain from PLZF." Proc Natl Acad Sci U S A **95**(21): 12123-12128.

Akoev, V., E. P. Gogol, M. E. Barnett and M. Zolkiewski (2004). "Nucleotide-induced switch in oligomerization of the AAA+ ATPase ClpB." Protein Sci **13**(3): 567-574.

Albagli, O., P. Dhordain, C. Deweindt, G. Lecocq and D. Leprince (1995). "The BTB/POZ domain: a new protein-protein interaction motif common to DNA- and actin-binding proteins." Cell Growth Differ **6**(9): 1193-1198.

Albanese, A. (2003). "The clinical expression of primary dystonia." J Neurol **250**(10): 1145-51.

Albanese, A., M. P. Barnes, K. P. Bhatia, E. Fernandez-Alvarez, G. Filippini, T. Gasser, J. K. Krauss, A. Newton, I. Rektor, M. Savoiardo and J. Valls-Sole (2006). "A systematic review on the diagnosis and treatment of primary (idiopathic) dystonia and dystonia plus syndromes: report of an EFNS/MDS-ES Task Force." Eur J Neurol **13**(5): 433-44.

Almasy, L., S. B. Bressman, D. Raymond, P. L. Kramer, P. E. Greene, G. A. Heiman, B. Ford, J. Yount, D. de Leon, S. Chouinard, R. Saunders-Pullman, M. F. Brin, R. P. Kapoor, A. C. Jones, H. Shen, S. Fahn, N. J. Risch and T. G. Nygaard (1997).

"Idiopathic torsion dystonia linked to chromosome 8 in two Mennonite families." Ann Neurol **42**(4): 670-3.

Auburger, G., T. Ratzlaff, A. Lunkes, H. W. Nelles, B. Leube, F. Binkofski, H. Kugel, W. Heindel, R. Seitz, R. Benecke, O. W. Witte and T. Voit (1996). "A gene for autosomal dominant paroxysmal choreoathetosis/spasticity (CSE) maps to the vicinity of a potassium channel gene cluster on chromosome 1p, probably within 2 cM between D1S443 and D1S197." Genomics **31**(1): 90-4.

Augood, S. J., Z. Hollingsworth, D. S. Albers, L. Yang, J. C. Leung, B. Muller, C. Klein, X. O. Breakefield and D. G. Standaert (2002). "Dopamine transmission in DYT1 dystonia: a biochemical and autoradiographical study." Neurology **59**(3): 445-8.

Augood, S. J., C. E. Keller-McGandy, A. Siriani, J. Hewett, V. Ramesh, E. Sapp, M. DiFiglia, X. O. Breakefield and D. G. Standaert (2003). "Distribution and ultrastructural localization of torsinA immunoreactivity in the human brain." Brain Res **986**(1-2): 12-21.

Augood, S. J., D. M. Martin, L. J. Ozelius, X. O. Breakefield, J. B. Penney, Jr. and D. G. Standaert (1999). "Distribution of the mRNAs encoding torsinA and torsinB in the normal adult human brain." Ann Neurol **46**(5): 761-769.

Auluck, P. K., H. Y. Chan, J. Q. Trojanowski, V. M. Lee and N. M. Bonini (2002). "Chaperone suppression of alpha-synuclein toxicity in a Drosophila model for Parkinson's disease." Science **295**(5556): 865-868.

Babst, M., B. Wendland, E. J. Estepa and S. D. Emr (1998). "The Vps4p AAA ATPase regulates membrane association of a Vps protein complex required for normal endosome function." EMBO J **17**(11): 2982-93.

Bahn, E., S. Siegert, T. Pfander, M. L. Kramer, W. J. Schulz-Schaeffer, J. W. Hewett, X. O. Breakefield, J. C. Hedreen and K. M. Rostasy (2006). "TorsinB expression in the developing human brain." Brain Res **1116**(1): 112-9.

Balcioglu, A., M. O. Kim, N. Sharma, J. H. Cha, X. O. Breakefield and D. G. Standaert (2007). "Dopamine release is impaired in a mouse model of DYT1 dystonia." J Neurochem **102**(3): 783-8.

Baptista, M. J., C. A. O'Farrell and M. R. Cookson (2004). "Dominant torsinA mutations in cellular systems." Adv Neurol **94**: 73-8.

Basham, S. E. and L. S. Rose (2001). "The Caenorhabditis elegans polarity gene ooc-5 encodes a Torsin-related protein of the AAA ATPase superfamily." Development **128**(22): 4645-4656.

Beyer, A. (1997). "Sequence analysis of the AAA protein family." Protein Sci **6**(10): 2043-2058.

Bi, Y., R. D. Palmiter, K. M. Wood and Q. Ma (2004). "Induction of metallothionein I by phenolic antioxidants requires metal-activated transcription factor 1 (MTF-1) and zinc." Biochem J **380**(Pt 3): 695-703.

Bomont, P., L. Cavalier, F. Blondeau, C. Ben Hamida, S. Belal, M. Tazir, E. Demir, H. Topaloglu, R. Korinthenberg, B. Tuysuz, P. Landrieu, F. Hentati and M. Koenig (2000). "The gene encoding gigaxonin, a new member of the cytoskeletal BTB/kelch repeat family, is mutated in giant axonal neuropathy." Nat Genet **26**(3): 370-4.

Bonifacino, J. S. and R. D. Kalusner (1994). Degradation of Proteins Retained in the Endoplasmic Reticulum. Cellular Proteolytic Systems. A. J. C. a. A. L. Schwarz. New York, Wiley-Liss, Inc.**:** 137-160.

Bragg, D. C., S. M. Camp, C. A. Kaufman, J. D. Wilbur, H. Boston, D. E. Schuback, P. I. Hanson, M. Sena-Esteves and X. O. Breakefield (2004). "Perinuclear biogenesis of mutant torsin-A inclusions in cultured cells infected with tetracycline-regulated herpes simplex virus type 1 amplicon vectors." Neuroscience **125**(3): 651-661.

Bragg, D. C., C. A. Kaufman, N. Kock and X. O. Breakefield (2004). "Inhibition of N-linked glycosylation prevents inclusion formation by the dystonia-related mutant form of torsinA." Mol Cell Neurosci **27**(4): 417-26.

Bragg, D. C., Kaufman, C. A., Kock, N. and X. O. Breakefield (2004). "Inhibition of N-linked glycosylation prevents inclusion formation by the dystonia-related mutant form of torsinA." Mol Cell Neurosci **27**(4): 417-426.

Bressman, S. B., S. Fahn, L. J. Ozelius, P. L. Kramer and N. J. Risch (2001). "The DYT1 mutation and nonfamilial primary torsion dystonia." Arch Neurol **58**(4): 681-682.

Bross, P., T. J. Corydon, B. S. Andresen, M. M. Jorgensen, L. Bolund and N. Gregersen (1999). "Protein misfolding and degradation in genetic diseases." Hum Mutat **14**(3): 186-198.

Caldwell, G. A., S. Cao, C. C. Gelwix, E. G. Sexton and K. A. Caldwell (2004). "An animal model to discern torsin function: suppression of protein aggregation in C. elegans." Adv Neurol **94**: 79-85.

Caldwell, G. A., S. Cao, E. G. Sexton, C. C. Gelwix, J. P. Bevel and K. A. Caldwell (2003). "Suppression of polyglutamine-induced protein aggregation in Caenorhabditis elegans by torsin proteins." Hum Mol Genet **12**(3): 307-319.

Caldwell, G. A., Cao, S., Gelwix, C. C., Sexton, E. G. and K. A. Caldwell (2004). "An animal model to discern torsin function: suppression of protein aggregation in C. elegans." Adv Neurol **94**: 79-85.

Camargos, S., S. Scholz, J. Simon-Sanchez, C. Paisan-Ruiz, P. Lewis, D. Hernandez, J. Ding, J. R. Gibbs, M. R. Cookson, J. Bras, R. Guerreiro, C. R. Oliveira, A. Lees, J. Hardy, F. Cardoso and A. B. Singleton (2008). "DYT16, a novel young-onset dystonia-parkinsonism disorder: identification of a segregating mutation in the stress-response protein PRKRA." Lancet Neurol **7**(3): 207-15.

Cao, S., C. C. Gelwix, K. A. Caldwell and G. A. Caldwell (2005). "Torsin-mediated protection from cellular stress in the dopaminergic neurons of Caenorhabditis elegans." J Neurosci **25**(15): 3801-3812.

Chen, W., S. Zollman, J. L. Couderc and F. A. Laski (1995). "The BTB domain of bric a brac mediates dimerization in vitro." Mol Cell Biol **15**(6): 3424-3429.

Chen, Y. T., C. Holcomb and H. P. Moore (1993). "Expression and localization of two low molecular weight GTP-binding proteins, Rab8 and Rab10, by epitope tag." Proc Natl Acad Sci U S A **90**(14): 6508-6512.

Chin, L. S., L. Li and P. Greengard (1994). "Neuron-specific expression of the synapsin II gene is directed by a specific core promoter and upstream regulatory elements." J Biol Chem **269**(28): 18507-13.

Chin, L. S., R. D. Nugent, M. C. Raynor, J. P. Vavalle and L. Li (2000). "SNIP, a novel SNAP-25-interacting protein implicated in regulated exocytosis." J Biol Chem **275**(2): 1191-1200.

Chin, L. S., M. C. Raynor, X. Wei, H. Q. Chen and L. Li (2001). "Hrs interacts with sorting nexin 1 and regulates degradation of epidermal growth factor receptor." J Biol Chem **276**(10): 7069-78.

Chin, L. S., J. P. Vavalle and L. Li (2002). "Staring, a novel E3 ubiquitin-protein ligase that targets syntaxin 1 for degradation." J Biol Chem **277**(38): 35071-9.

Chin, L. S., J. P. Vavalle and L. Li (2002). "Staring, a novel E3 ubiquitin-protein ligase that targets syntaxin 1 for degradation." J Biol Chem **277**(38): 35071-35079.

Chouery, E., J. Kfoury, V. Delague, N. Jalkh, P. Bejjani, J. L. Serre and A. Megarbane (2008). "A novel locus for autosomal recessive primary torsion dystonia (DYT17) maps to 20p11.22-q13.12." Neurogenetics.

Ciechanover, A. (2005). "Intracellular protein degradation: from a vague idea thru the lysosome and the ubiquitin-proteasome system and onto human diseases and drug targeting." Cell Death Differ **12**(9): 1178-90.

Collins, T., J. R. Stone and A. J. Williams (2001). "All in the family: the BTB/POZ, KRAB, and SCAN domains." Mol Cell Biol **21**(11): 3609-15.

Cuervo, A. M. (2004). "Autophagy: many paths to the same end." Mol Cell Biochem **263**(1-2): 55-72.

Cummings, C. J., M. A. Mancini, B. Antalffy, D. B. DeFranco, H. T. Orr and H. Y. Zoghbi (1998). "Chaperone suppression of aggregation and altered subcellular

proteasome localization imply protein misfolding in SCA1." Nat Genet **19**(2): 148-154.

Dalal, S. and P. I. Hanson (2001). "Membrane traffic: what drives the AAA motor?" Cell **104**(1): 5-8.

Dang, M. T., F. Yokoi, K. S. McNaught, T. A. Jengelley, T. Jackson, J. Li and Y. Li (2005). "Generation and characterization of Dyt1 DeltaGAG knock-in mouse as a model for early-onset dystonia." Exp Neurol **196**(2): 452-463.

Dang, M. T., F. Yokoi, M. A. Pence and Y. Li (2006). "Motor deficits and hyperactivity in Dyt1 knockdown mice." Neurosci Res **56**(4): 470-4.

de Carvalho Aguiar, P., K. J. Sweadner, J. T. Penniston, J. Zaremba, L. Liu, M. Caton, G. Linazasoro, M. Borg, M. A. Tijssen, S. B. Bressman, W. B. Dobyns, A. Brashear and L. J. Ozelius (2004). "Mutations in the Na+/K+ -ATPase alpha3 gene ATP1A3 are associated with rapid-onset dystonia parkinsonism." Neuron **43**(2): 169-75.

de Carvalho Aguiar, P. M. and L. J. Ozelius (2002). "Classification and genetics of dystonia." Lancet Neurol **1**(5): 316-25.

Ding, W. X. and X. M. Yin (2008). "Sorting, recognition and activation of the misfolded protein degradation pathways through macroautophagy and the proteasome." Autophagy **4**(2): 141-50.

Ellenberg, J., E. D. Siggia, J. E. Moreira, C. L. Smith, J. F. Presley, H. J. Worman and J. Lippincott-Schwartz (1997). "Nuclear membrane dynamics and reassembly in living cells: targeting of an inner nuclear membrane protein in interphase and mitosis." J Cell Biol **138**(6): 1193-1206.

Esapa, C. T., A. Waite, M. Locke, M. A. Benson, M. Kraus, R. A. McIlhinney, R. V. Sillitoe, P. W. Beesley and D. J. Blake (2007). "SGCE missense mutations that cause myoclonus-dystonia syndrome impair epsilon-sarcoglycan trafficking to the plasma membrane: modulation by ubiquitination and torsinA." Hum Mol Genet **16**(3): 327-42.

Ferrari-Toninelli, G., S. Paccioretti, S. Francisconi, D. Uberti and M. Memo (2004). "TorsinA negatively controls neurite outgrowth of SH-SY5Y human neuronal cell line." Brain Res **1012**(1-2): 75-81.

Fujita, E., Y. Kouroku, A. Isoai, H. Kumagai, A. Misutani, C. Matsuda, Y. K. Hayashi and T. Momoi (2007). "Two endoplasmic reticulum-associated degradation (ERAD) systems for the novel variant of the mutant dysferlin: ubiquitin/proteasome ERAD(I) and autophagy/lysosome ERAD(II)." Hum Mol Genet **16**(6): 618-29.

Gearing, M., R. W. Wilson, E. R. Unger, E. R. Shelton, H. W. Chan, C. L. Masters, K. Beyreuther and S. S. Mirra (1993). "Amyloid precursor protein (APP) in the striatum in Alzheimer's disease: an immunohistochemical study." J Neuropathol Exp Neurol **52**(1): 22-30.

Gerace, L. (2004). "TorsinA and torsion dystonia: Unraveling the architecture of the nuclear envelope." Proc Natl Acad Sci U S A **101**(24): 8839-8840.

Gettemans, J., K. Meerschaert, J. Vandekerckhove and V. De Corte (2003). "A kelch beta propeller featuring as a G beta structural mimic: reinventing the wheel?" Sci STKE **2003**(191): PE27.

Geyer, R., S. Wee, S. Anderson, J. Yates and D. A. Wolf (2003). "BTB/POZ domain proteins are putative substrate adaptors for cullin 3 ubiquitin ligases." Mol Cell **12**(3): 783-790.

Giles, L. M., J. Chen, L. Li and L. S. Chin (2008). "Dystonia-associated mutations cause premature degradation of torsinA protein and cell-type-specific mislocalization to the nuclear envelope." Hum Mol Genet **17**(17): 2712-22.

Gimenez-Roldan, S., G. Delgado, M. Marin, J. A. Villanueva and D. Mateo (1988). "Hereditary torsion dystonia in gypsies." Adv Neurol **50**: 73-81.

Gingerich, D. J., J. M. Gagne, D. W. Salter, H. Hellmann, M. Estelle, L. Ma and R. D. Vierstra (2005). "Cullins 3a and 3b assemble with members of the broad complex/tramtrack/bric-a-brac (BTB) protein family to form essential ubiquitin-protein ligases (E3s) in Arabidopsis." J Biol Chem **280**(19): 18810-18821.

Gonzalez-Alegre, P., V. M. Miller, B. L. Davidson and H. L. Paulson (2003). "Toward therapy for DYT1 dystonia: allele-specific silencing of mutant TorsinA." Ann Neurol **53**(6): 781-787.

Gonzalez-Alegre, P. and H. L. Paulson (2004). "Aberrant cellular behavior of mutant torsinA implicates nuclear envelope dysfunction in DYT1 dystonia." J Neurosci **24**(11): 2593-2601.

Goodchild, R. E. and W. T. Dauer (2004). "Mislocalization to the nuclear envelope: an effect of the dystonia-causing torsinA mutation." Proc Natl Acad Sci U S A **101**(3): 847-852.

Goodchild, R. E. and W. T. Dauer (2005). "The AAA+ protein torsinA interacts with a conserved domain present in LAP1 and a novel ER protein." J Cell Biol **168**(6): 855-862.

Goodchild, R. E., C. E. Kim and W. T. Dauer (2005). "Loss of the dystonia-associated protein torsina selectively disrupts the neuronal nuclear envelope." Neuron **48**(6): 923-932.

Graeber, M. B. and U. Muller (1992). "The X-linked dystonia-parkinsonism syndrome (XDP): clinical and molecular genetic analysis." Brain Pathol **2**(4): 287-95.

Granata, A., R. Watson, L. M. Collinson, G. Schiavo and T. T. Warner (2008). "The dystonia-associated protein torsinA modulates synaptic vesicle recycling." J Biol Chem **283**(12): 7568-79.

Grundmann, K., B. Reischmann, G. Vanhoutte, J. Hubener, P. Teismann, T. K. Hauser, M. Bonin, J. Wilbertz, S. Horn, H. P. Nguyen, M. Kuhn, S. Chanarat, H. Wolburg, A. Van der Linden and O. Riess (2007). "Overexpression of human wildtype torsinA and human DeltaGAG torsinA in a transgenic mouse model causes phenotypic abnormalities." Neurobiol Dis **27**(2): 190-206.

Han, F., L. Racacho, A. E. Lang, D. E. Bulman and D. A. Grimes (2007). "Refinement of the DYT15 locus in myoclonus dystonia." Mov Disord **22**(6): 888-92.

Hanson, P. I. and S. W. Whiteheart (2005). "AAA+ proteins: have engine, will work." Nat Rev Mol Cell Biol **6**(7): 519-529.

Hernandez, M. C., P. J. Andres-Barquin, S. Martinez, A. Bulfone, J. L. Rubenstein and M. A. Israel (1997). "ENC-1: a novel mammalian kelch-related gene specifically

expressed in the nervous system encodes an actin-binding protein." J Neurosci **17**(9): 3038-51.

Hewett, J., C. Gonzalez-Agosti, D. Slater, P. Ziefer, S. Li, D. Bergeron, D. J. Jacoby, L. J. Ozelius, V. Ramesh and X. O. Breakefield (2000). "Mutant torsinA, responsible for early-onset torsion dystonia, forms membrane inclusions in cultured neural cells." Hum Mol Genet **9**(9): 1403-1413.

Hewett, J., P. Ziefer, D. Bergeron, T. Naismith, H. Boston, D. Slater, J. Wilbur, D. Schuback, C. Kamm, N. Smith, S. Camp, L. J. Ozelius, V. Ramesh, P. I. Hanson and X. O. Breakefield (2003). "TorsinA in PC12 cells: localization in the endoplasmic reticulum and response to stress." J Neurosci Res **72**(2): 158-68.

Hewett, J., Ziefer, P., Bergeron, D., Naismith, T., Boston, H., Slater, D., Wilbur, J., Schuback, D., Kamm, C., Smith, N., Camp, S., Ozelius, L. J., Ramesh, V., Hanson, P. I. and X. O. Breakefield (2003). "TorsinA in PC12 cells: localization in the endoplasmic reticulum and response to stress." J Neurosci Res **72**(2): 158-168.

Hewett, J. W., C. Kamm, H. Boston, R. Beauchamp, T. Naismith, L. Ozelius, P. I. Hanson, X. O. Breakefield and V. Ramesh (2004). "TorsinB--perinuclear location and association with torsinA." J Neurochem **89**(5): 1186-94.

Hewett, J. W., F. C. Nery, B. Niland, P. Ge, P. Tan, P. Hadwiger, B. A. Tannous, D. W. Sah and X. O. Breakefield (2008). "siRNA knock-down of mutant torsinA restores processing through secretory pathway in DYT1 dystonia cells." Hum Mol Genet **17**(10): 1436-45.

Hewett, J. W., B. Tannous, B. P. Niland, F. C. Nery, J. Zeng, Y. Li and X. O. Breakefield (2007). "Mutant torsinA interferes with protein processing through the secretory pathway in DYT1 dystonia cells." Proc Natl Acad Sci U S A **104**(17): 7271-6.

Hewett, J. W., J. Zeng, B. P. Niland, D. C. Bragg and X. O. Breakefield (2005). "Dystonia-causing mutant torsinA inhibits cell adhesion and neurite extension through interference with cytoskeletal dynamics." Neurobiol Dis.

Hewett, J. W., J. Zeng, B. P. Niland, D. C. Bragg and X. O. Breakefield (2006). "Dystonia-causing mutant torsinA inhibits cell adhesion and neurite extension through interference with cytoskeletal dynamics." Neurobiol Dis **22**(1): 98-111.

Huang, J. and D. J. Klionsky (2007). "Autophagy and human disease." Cell Cycle **6**(15): 1837-49.

Jarman, P. R., O. Bandmann, C. D. Marsden and N. W. Wood (1997). "GTP cyclohydrolase I mutations in patients with dystonia responsive to anticholinergic drugs." J Neurol Neurosurg Psychiatry **63**(3): 304-8.

Kamm, C., H. Boston, J. Hewett, J. Wilbur, D. P. Corey, P. I. Hanson, V. Ramesh and X. O. Breakefield (2004). "The early onset dystonia protein torsinA interacts with kinesin light chain 1." J Biol Chem **279**(19): 19882-19892.

Kikuchi, T., M. Nomura, H. Tomita, N. Harada, K. Kanai, T. Konishi, A. Yasuda, M. Matsuura, N. Kato, K. Yoshiura and N. Niikawa (2007). "Paroxysmal kinesigenic choreoathetosis (PKC): confirmation of linkage to 16p11-q21, but unsuccessful detection of mutations among 157 genes at the PKC-critical region in seven PKC families." J Hum Genet **52**(4): 334-41.

Kim, B. Y., J. A. Olzmann, G. S. Barsh, L. S. Chin and L. Li (2007). "Spongiform neurodegeneration-associated E3 ligase Mahogunin ubiquitylates TSG101 and regulates endosomal trafficking." Mol Biol Cell **18**(4): 1129-1142.

Kim, T. A., J. Lim, S. Ota, S. Raja, R. Rogers, B. Rivnay, H. Avraham and S. Avraham (1998). "NRP/B, a novel nuclear matrix protein, associates with p110(RB) and is involved in neuronal differentiation." J Cell Biol **141**(3): 553-66.

Kincaid, M. M. and A. A. Cooper (2007). "ERADicate ER stress or die trying." Antioxid Redox Signal **9**(12): 2373-87.

Kirk, E., L. S. Chin and L. Li (2006). "GRIF1 binds Hrs and is a new regulator of endosomal trafficking." J Cell Sci **119**(Pt 22): 4689-701.

Klein, C., L. Liu, D. Doheny, N. Kock, B. Muller, P. de Carvalho Aguiar, J. Leung, D. de Leon, S. B. Bressman, J. Silverman, C. Smith, F. Danisi, C. Morrison, R. H. Walker, M. Velickovic, E. Schwinger, P. L. Kramer, X. O. Breakefield, M. F. Brin and L. J. Ozelius (2002). "Epsilon-sarcoglycan mutations found in combination with other dystonia gene mutations." Ann Neurol **52**(5): 675-679.

Klein, C. and L. J. Ozelius (2002). "Dystonia: clinical features, genetics, and treatment." Curr Opin Neurol **15**(4): 491-7.

Kleizen, B. and I. Braakman (2004). "Protein folding and quality control in the endoplasmic reticulum." Curr Opin Cell Biol **16**(4): 343-9.

Kock, N., A. J. Allchorne, M. Sena-Esteves, C. J. Woolf and X. O. Breakefield (2005). "RNAi blocks DYT1 mutant torsinA inclusions in neurons." Neurosci Lett.

Kock, N., T. V. Naismith, H. E. Boston, L. J. Ozelius, D. P. Corey, X. O. Breakefield and P. I. Hanson (2006). "Effects of genetic variations in the dystonia protein torsinA:

identification of polymorphism at residue 216 as protein modifier." Hum Mol Genet **15**(8): 1355-1364.

Koh, Y. H., K. Rehfeld and B. Ganetzky (2004). "A Drosophila model of early onset torsion dystonia suggests impairment in TGF-{beta} signaling." Hum Mol Genet **13**(18): 2019-2030.

Konakova, M. and S. M. Pulst (2001). "Immunocytochemical characterization of torsin proteins in mouse brain." Brain Res **922**(1): 1-8.

Konakova, M. and S. M. Pulst (2005). "Dystonia-associated forms of torsinA are deficient in ATPase activity." J Mol Neurosci **25**(1): 105-117.

Kostova, Z., Y. C. Tsai and A. M. Weissman (2007). "Ubiquitin ligases, critical mediators of endoplasmic reticulum-associated degradation." Semin Cell Dev Biol **18**(6): 770-9.

Krek, W. (2003). "BTB proteins as henchmen of Cul3-based ubiquitin ligases." Nat Cell Biol **5**(11): 950-951.

Kuner, R., P. Teismann, A. Trutzel, J. Naim, A. Richter, N. Schmidt, O. von Ahsen, A. Bach, B. Ferger and A. Schneider (2003). "TorsinA protects against oxidative stress in COS-1 and PC12 cells." Neurosci Lett **350**(3): 153-156.

Kustedjo, K., M. H. Bracey and B. F. Cravatt (2000). "Torsin A and its torsion dystonia-associated mutant forms are lumenal glycoproteins that exhibit distinct subcellular localizations." J Biol Chem **275**(36): 27933-26939.

Kustedjo, K., S. Deechongkit, J. W. Kelly and B. F. Cravatt (2003). "Recombinant expression, purification, and comparative characterization of torsinA and its

torsion dystonia-associated variant Delta E-torsinA." Biochemistry **42**(51): 15333-15341.

Kvam, E. and D. S. Goldfarb (2006). "Nucleus-vacuole junctions in yeast: anatomy of a membrane contact site." Biochem Soc Trans **34**(Pt 3): 340-2.

Kwong, J., F. L. Roundabush, P. Hutton Moore, M. Montague, W. Oldham, Y. Li, L. S. Chin and L. Li (2000). "Hrs interacts with SNAP-25 and regulates Ca(2+)-dependent exocytosis." J Cell Sci **113 (Pt 12)**: 2273-84.

Lee, J. T., T. C. Wheeler, L. Li and L. S. Chin (2008). "Ubiquitination of alpha-synuclein by Siah-1 promotes alpha-synuclein aggregation and apoptotic cell death." Hum Mol Genet **17**(6): 906-17.

Leube, B., T. Hendgen, K. R. Kessler, M. Knapp, R. Benecke and G. Auburger (1997). "Evidence for DYT7 being a common cause of cervical dystonia (torticollis) in Central Europe." Am J Med Genet **74**(5): 529-32.

Leung, J. C., C. Klein, J. Friedman, P. Vieregge, H. Jacobs, D. Doheny, C. Kamm, D. DeLeon, P. P. Pramstaller, J. B. Penney, M. Eisengart, J. Jankovic, T. Gasser, S. B. Bressman, D. P. Corey, P. Kramer, M. F. Brin, L. J. Ozelius and X. O. Breakefield (2001). "Novel mutation in the TOR1A (DYT1) gene in atypical early onset dystonia and polymorphisms in dystonia and early onset parkinsonism." Neurogenetics **3**(3): 133-143.

Levine, B. and G. Kroemer (2008). "Autophagy in the pathogenesis of disease." Cell **132**(1): 27-42.

Li, Y., L. S. Chin, A. I. Levey and L. Li (2002). "Huntingtin-associated protein 1 interacts with hepatocyte growth factor-regulated tyrosine kinase substrate and functions in endosomal trafficking." J Biol Chem **277**(31): 28212-21.

Li, Y., L. S. Chin, C. Weigel and L. Li (2001). "Spring, a novel RING finger protein that regulates synaptic vesicle exocytosis." J Biol Chem **276**(44): 40824-33.

Liang, J., C. Yin, H. Doong, S. Fang, C. Peterhoff, R. A. Nixon and M. J. Monteiro (2006). "Characterization of erasin (UBXD2): a new ER protein that promotes ER-associated protein degradation." J Cell Sci **119**(Pt 19): 4011-24.

Liu, Z., A. Zolkiewska and M. Zolkiewski (2003). "Characterization of human torsinA and its dystonia-associated mutant form." Biochem J **374**(Pt 1): 117-122.

Lupas, A. N. and J. Martin (2002). "AAA proteins." Curr Opin Struct Biol **12**(6): 746-753.

Ma, Q., K. Kinneer, Y. Bi, J. Y. Chan and Y. W. Kan (2004). "Induction of murine NAD(P)H:quinone oxidoreductase by 2,3,7,8-tetrachlorodibenzo-p-dioxin requires the CNC (cap 'n' collar) basic leucine zipper transcription factor Nrf2 (nuclear factor erythroid 2-related factor 2): cross-interaction between AhR (aryl hydrocarbon receptor) and Nrf2 signal transduction." Biochem J **377**(Pt 1): 205-13.

Maurizi, M. R. and C. C. Li (2001). "AAA proteins: in search of a common molecular basis. International Meeting on Cellular Functions of AAA Proteins." EMBO Rep **2**(11): 980-985.

McBratney, S. and M. Winey (2002). "Mutant membrane protein of the budding yeast spindle pole body is targeted to the endoplasmic reticulum degradation pathway." Genetics **162**(2): 567-78.

McCray, B. A. and J. P. Taylor (2008). "The role of autophagy in age-related neurodegeneration." Neurosignals **16**(1): 75-84.

McLean, P. J., H. Kawamata, S. Shariff, J. Hewett, N. Sharma, K. Ueda, X. O. Breakefield and B. T. Hyman (2002). "TorsinA and heat shock proteins act as molecular chaperones: suppression of alpha-synuclein aggregation." J Neurochem **83**(4): 846-854.

McNaught, K. S., A. Kapustin, T. Jackson, T. A. Jengelley, R. Jnobaptiste, P. Shashidharan, D. P. Perl, P. Pasik and C. W. Olanow (2004). "Brainstem pathology in DYT1 primary torsion dystonia." Ann Neurol **56**(4): 540-547.

Meng, L., H. Yasumoto and R. Y. Tsai (2006). "Multiple controls regulate nucleostemin partitioning between nucleolus and nucleoplasm." J Cell Sci **119**(Pt 24): 5124-36.

Meusser, B., C. Hirsch, E. Jarosch and T. Sommer (2005). "ERAD: the long road to destruction." Nat Cell Biol **7**(8): 766-72.

Misbahuddin, A., M. R. Placzek, J. W. Taanman, S. Gschmeissner, G. Schiavo, J. M. Cooper and T. T. Warner (2005). "Mutant torsinA, which causes early-onset primary torsion dystonia, is redistributed to membranous structures enriched in vesicular monoamine transporter in cultured human SH-SY5Y cells." Mov Disord **20**(4): 432-440.

Mizushima, N., B. Levine, A. M. Cuervo and D. J. Klionsky (2008). "Autophagy fights disease through cellular self-digestion." Nature **451**(7182): 1069-75.

Muchir, A., C. Massart, B. G. van Engelen, M. Lammens, G. Bonne and H. J. Worman (2006). "Proteasome-mediated degradation of integral inner nuclear membrane protein emerin in fibroblasts lacking A-type lamins." Biochem Biophys Res Commun **351**(4): 1011-7.

Muraro, N. I. and K. G. Moffat (2006). "Down-regulation of torp4a, encoding the Drosophila homologue of torsinA, results in increased neuronal degeneration." J Neurobiol **66**(12): 1338-53.

Nagase, T., R. Kikuno, K. I. Ishikawa, M. Hirosawa and O. Ohara (2000). "Prediction of the coding sequences of unidentified human genes. XVI. The complete sequences of 150 new cDNA clones from brain which code for large proteins in vitro." DNA Res **7**(1): 65-73.

Naismith, T. V., J. E. Heuser, X. O. Breakefield and P. I. Hanson (2004). "TorsinA in the nuclear envelope." Proc Natl Acad Sci U S A **101**(20): 7612-7617.

Neuwald, A. F., L. Aravind, J. L. Spouge and E. V. Koonin (1999). "AAA+: A class of chaperone-like ATPases associated with the assembly, operation, and disassembly of protein complexes." Genome Res **9**(1): 27-43.

Nishikawa, S., J. L. Brodsky and K. Nakatsukasa (2005). "Roles of molecular chaperones in endoplasmic reticulum (ER) quality control and ER-associated degradation (ERAD)." J Biochem **137**(5): 551-5.

O'Farrell, C., D. G. Hernandez, C. Evey, A. B. Singleton and M. R. Cookson (2002). "Normal localization of deltaF323-Y328 mutant torsinA in transfected human cells." Neurosci Lett **327**(2): 75-78.

O'Farrell, C., P. J. Lockhart, S. Lincoln, M. De Lucia, A. B. Singleton, D. W. Dickson and M. R. Cookson (2004). "Biochemical characterization of torsinB." Brain Res Mol Brain Res **127**(1-2): 1-9.

Ogura, T. and A. J. Wilkinson (2001). "AAA+ superfamily ATPases: common structure--diverse function." Genes Cells **6**(7): 575-597.

Olzmann, J. A., K. Brown, K. D. Wilkinson, H. D. Rees, Q. Huai, H. Ke, A. I. Levey, L. Li and L. S. Chin (2004). "Familial Parkinson's disease-associated L166P mutation disrupts DJ-1 protein folding and function." J Biol Chem **279**(9): 8506-15.

Olzmann, J. A., K. Brown, K. D. Wilkinson, H. D. Rees, Q. Huai, H. Ke, A. I. Levey, L. Li and L. S. Chin (2004). "Familial Parkinson's disease-associated L166P mutation disrupts DJ-1 protein folding and function." J Biol Chem **279**(9): 8506-8515.

Olzmann, J. A., L. Li and L. S. Chin (2008). "Aggresome formation and neurodegenerative diseases: therapeutic implications." Curr Med Chem **15**(1): 47-60.

Olzmann, J. A., L. Li, M. V. Chudaev, J. Chen, F. A. Perez, R. D. Palmiter and L. S. Chin (2007). "Parkin-mediated K63-linked polyubiquitination targets misfolded DJ-1 to aggresomes via binding to HDAC6." J Cell Biol **178**(6): 1025-38.

Otsuka, M., Y. Ichiya, F. Shima, Y. Kuwabara, M. Sasaki, T. Fukumura, M. Kato, K. Masuda and I. Goto (1992). "Increased striatal 18F-dopa uptake and normal glucose metabolism in idiopathic dystonia syndrome." J Neurol Sci **111**(2): 195-9.

Ozelius, L. J., J. W. Hewett, C. E. Page, S. B. Bressman, P. L. Kramer, C. Shalish, D. de Leon, M. F. Brin, D. Raymond, D. P. Corey, S. Fahn, N. J. Risch, A. J. Buckler, J. F. Gusella and X. O. Breakefield (1997). "The early-onset torsion dystonia gene (DYT1) encodes an ATP-binding protein." Nat Genet **17**(1): 40-48.

Ozelius, L. J., J. W. Hewett, C. E. Page, S. B. Bressman, P. L. Kramer, C. Shalish, D. de Leon, M. F. Brin, D. Raymond, D. Jacoby, J. Penney, N. J. Risch, S. Fahn, J. F. Gusella and X. O. Breakefield (1998). "The gene (DYT1) for early-onset torsion dystonia encodes a novel protein related to the Clp protease/heat shock family." Adv Neurol **78**: 93-105.

Ozelius, L. J., Hewett, J. W., Page, C. E., Bressman, S. B., Kramer, P. L., Shalish, C., de Leon, D., Brin, M. F., Raymond, D., Jacoby, D., Penney, J., Risch, N. J., ahn, S., usella, J. F. and X. O. Breakefield (1998). "The gene (DYT1) for early-onset torsion dystonia encodes a novel protein related to the Clp protease/heat shock family." Adv Neurol **78**: 93-105.

Ozelius, L. J., C. E. Page, C. Klein, J. W. Hewett, M. Mineta, J. Leung, C. Shalish, S. B. Bressman, D. de Leon, M. F. Brin, S. Fahn, D. P. Corey and X. O. Breakefield (1999). "The TOR1A (DYT1) gene family and its role in early onset torsion dystonia." Genomics **62**(3): 377-84.

Parker, N. (1985). "Hereditary whispering dysphonia." J Neurol Neurosurg Psychiatry **48**(3): 218-24.

Patel, S. and M. Latterich (1998). "The AAA team: related ATPases with diverse functions." Trends Cell Biol **8**(2): 65-71.

Perez-Torrado, R., D. Yamada and P. A. Defossez (2006). "Born to bind: the BTB protein-protein interaction domain." Bioessays **28**(12): 1194-202.

Pham, P., K. P. Frei, W. Woo and D. D. Truong (2006). "Molecular defects of the dystonia-causing torsinA mutation." Neuroreport **17**(16): 1725-1728.

Pickart, C. M. (1997). "Targeting of substrates to the 26S proteasome." FASEB J **11**(13): 1055-66.

Pickart, C. M. and M. J. Eddins (2004). "Ubiquitin: structures, functions, mechanisms." Biochim Biophys Acta **1695**(1-3): 55-72.

Pickart, C. M. and D. Fushman (2004). "Polyubiquitin chains: polymeric protein signals." Curr Opin Chem Biol **8**(6): 610-6.

Prag, S. and J. C. Adams (2003). "Molecular phylogeny of the kelch-repeat superfamily reveals an expansion of BTB/kelch proteins in animals." BMC Bioinformatics **4**(1): 42.

Rainier, S., D. Thomas, D. Tokarz, L. Ming, M. Bui, E. Plein, X. Zhao, R. Lemons, R. Albin, C. Delaney, D. Alvarado and J. K. Fink (2004). "Myofibrillogenesis regulator 1 gene mutations cause paroxysmal dystonic choreoathetosis." Arch Neurol **61**(7): 1025-9.

Ramos, S., F. Khademi, B. P. Somesh and F. Rivero (2002). "Genomic organization and expression profile of the small GTPases of the RhoBTB family in human and mouse." Gene **298**(2): 147-57.

Rao, G. N. and E. Cotlier (1985). "The enzymatic activities of GTP cyclohydrolase, sepiapterin reductase, dihydropteridine reductase and dihydrofolate reductase; and

tetrahydrobiopterin content in mammalian ocular tissues and in human senile cataracts." Comp Biochem Physiol B **80**(1): 61-6.

Roberts, P., S. Moshitch-Moshkovitz, E. Kvam, E. O'Toole, M. Winey and D. S. Goldfarb (2003). "Piecemeal microautophagy of nucleus in Saccharomyces cerevisiae." Mol Biol Cell **14**(1): 129-41.

Robinson, D. N., K. Cant and L. Cooley (1994). "Morphogenesis of Drosophila ovarian ring canals." Development **120**(7): 2015-2025.

Robinson, D. N. and L. Cooley (1997). "Drosophila kelch is an oligomeric ring canal actin organizer." J Cell Biol **138**(4): 799-810.

Rogers, A., G. Schmuck, G. Scholz and D. C. Williams (2004). "c-fos mRNA expression in rat cortical neurons during glutamate-mediated excitotoxicity." Toxicol Sci **82**(2): 562-9.

Rostasy, K., S. J. Augood, J. W. Hewett, J. C. Leung, H. Sasaki, L. J. Ozelius, V. Ramesh, D. G. Standaert, X. O. Breakefield and J. C. Hedreen (2003). "TorsinA protein and neuropathology in early onset generalized dystonia with GAG deletion." Neurobiol Dis **12**(1): 11-24.

Rubinsztein, D. C. (2006). "The roles of intracellular protein-degradation pathways in neurodegeneration." Nature **443**(7113): 780-6.

Sambrook, J., E. F. Fritsch and T. Maniatis (1989). Molecular Cloning: A Laboratory Manual. Colspring Harbor, NY, Cold Spring Harbor Laboratory.

Seglen, P. O. and P. B. Gordon (1982). "3-Methyladenine: specific inhibitor of autophagic/lysosomal protein degradation in isolated rat hepatocytes." Proc Natl Acad Sci U S A **79**(6): 1889-92.

Sharma, N., M. G. Baxter, J. Petravicz, D. C. Bragg, A. Schienda, D. G. Standaert and X. O. Breakefield (2005). "Impaired motor learning in mice expressing torsinA with the DYT1 dystonia mutation." J Neurosci **25**(22): 5351-5355.

Sharma, N., J. Hewett, L. J. Ozelius, V. Ramesh, P. J. McLean, X. O. Breakefield and B. T. Hyman (2001). "A close association of torsinA and alpha-synuclein in Lewy bodies: a fluorescence resonance energy transfer study." Am J Pathol **159**(1): 339-344.

Shashidharan, P., P. F. Good, A. Hsu, D. P. Perl, M. F. Brin and C. W. Olanow (2000). "TorsinA accumulation in Lewy bodies in sporadic Parkinson's disease." Brain Res **877**(2): 379-381.

Shashidharan, P., B. C. Kramer, R. H. Walker, C. W. Olanow and M. F. Brin (2000). "Immunohistochemical localization and distribution of torsinA in normal human and rat brain." Brain Res **853**(2): 197-206.

Shashidharan, P., N. Paris, D. Sandu, L. Karthikeyan, K. S. McNaught, R. H. Walker and C. W. Olanow (2004). "Overexpression of torsinA in PC12 cells protects against toxicity." J Neurochem **88**(4): 1019-1025.

Shashidharan, P., D. Sandu, U. Potla, I. A. Armata, R. H. Walker, K. S. McNaught, D. Weisz, T. Sreenath, M. F. Brin and C. W. Olanow (2005). "Transgenic mouse model of early-onset DYT1 dystonia." Hum Mol Genet **14**(1): 125-133.

Shen, X., K. Zhang and R. J. Kaufman (2004). "The unfolded protein response--a stress signaling pathway of the endoplasmic reticulum." J Chem Neuroanat **28**(1-2): 79-92.

Soltysik-Espanola, M., R. A. Rogers, S. Jiang, T. A. Kim, R. Gaedigk, R. A. White, H. Avraham and S. Avraham (1999). "Characterization of Mayven, a novel actin-binding protein predominantly expressed in brain." Mol Biol Cell **10**(7): 2361-2375.

Stogios, P. J., G. S. Downs, J. J. Jauhal, S. K. Nandra and G. G. Prive (2005). "Sequence and structural analysis of BTB domain proteins." Genome Biol **6**(10): R82.

Stogios, P. J. and G. G. Prive (2004). "The BACK domain in BTB-kelch proteins." Trends Biochem Sci **29**(12): 634-7.

Toninelli, G. F., P. Spano and M. Memo (2003). "TorsinA, microtubules and cell polarity." Funct Neurol **18**(1): 7-10.

Torres, G. E., A. L. Sweeney, J. M. Beaulieu, P. Shashidharan and M. G. Caron (2004). "Effect of torsinA on membrane proteins reveals a loss of function and a dominant-negative phenotype of the dystonia-associated {Delta}E-torsinA mutant." Proc Natl Acad Sci U S A **101**(44): 15650-15655.

Vale, R. D. (2000). "AAA proteins. Lords of the ring." J Cell Biol **150**(1): F13-F19.

Valente, E. M., A. R. Bentivoglio, E. Cassetta, P. H. Dixon, M. B. Davis, A. Ferraris, T. Ialongo, M. Frontali, N. W. Wood and A. Albanese (2001). "DYT13, a novel primary torsion dystonia locus, maps to chromosome 1p36.13--36.32 in an Italian family with cranial-cervical or upper limb onset." Ann Neurol **49**(3): 362-6.

Vasudevan, A., X. O. Breakefield and P. G. Bhide (2006). "Developmental patterns of torsinA and torsinB expression." Brain Res **1073-1074**: 139-45.

Volpicelli, L. A., J. J. Lah, G. Fang, J. R. Goldenring and A. I. Levey (2002). "Rab11a and myosin Vb regulate recycling of the M4 muscarinic acetylcholine receptor." J Neurosci **22**(22): 9776-84.

Volpicelli, L. A., J. J. Lah and A. I. Levey (2001). "Rab5-dependent trafficking of the m4 muscarinic acetylcholine receptor to the plasma membrane, early endosomes, and multivesicular bodies." J Biol Chem **276**(50): 47590-47598.

von Bulow, M., H. Heid, H. Hess and W. W. Franke (1995). "Molecular nature of calicin, a major basic protein of the mammalian sperm head cytoskeleton." Exp Cell Res **219**(2): 407-413.

Walker, R. H., M. F. Brin, D. Sandu, P. F. Good and P. Shashidharan (2002). "TorsinA immunoreactivity in brains of patients with DYT1 and non-DYT1 dystonia." Neurology **58**(1): 120-124.

Walker, R. H., M. F. Brin, D. Sandu, P. Gujjari, P. R. Hof, C. Warren Olanow and P. Shashidharan (2001). "Distribution and immunohistochemical characterization of torsinA immunoreactivity in rat brain." Brain Res **900**(2): 348-354.

Walker, R. H., P. F. Good and P. Shashidharan (2003). "TorsinA immunoreactivity in inclusion bodies in trinucleotide repeat diseases." Mov Disord **18**(9): 1041-1044.

Wang, C. W. and D. J. Klionsky (2003). "The molecular mechanism of autophagy." Mol Med **9**(3-4): 65-76.

Way, M., M. Sanders, C. Garcia, J. Sakai and P. Matsudaira (1995). "Sequence and domain organization of scruin, an actin-cross-linking protein in the acrosomal process of Limulus sperm." J Cell Biol **128**(1-2): 51-60.

Webber, E., L. Li and L. S. Chin (2008). "Hypertonia-associated protein Trak1 is a novel regulator of endosome-to-lysosome trafficking." J Mol Biol **382**(3): 638-51.

Welch, W. J. (2004). "Role of quality control pathways in human diseases involving protein misfolding." Semin Cell Dev Biol **15**(1): 31-38.

Wheeler, T. C., L. S. Chin, Y. Li, F. L. Roudabush and L. Li (2002). "Regulation of synaptophysin degradation by mammalian homologues of seven in absentia." J Biol Chem **277**(12): 10273-10282.

Wider, C., S. Melquist, M. Hauf, A. Solida, S. A. Cobb, J. M. Kachergus, J. Gass, K. D. Coon, M. Baker, A. Cannon, D. A. Stephan, D. F. Schorderet, J. Ghika, P. R. Burkhard, G. Kapatos, M. Hutton, M. J. Farrer, Z. K. Wszolek and F. J. Vingerhoets (2008). "Study of a Swiss dopa-responsive dystonia family with a deletion in GCH1: redefining DYT14 as DYT5." Neurology **70**(16 Pt 2): 1377-83.

Wilkins, A., Q. Ping and C. L. Carpenter (2004). "RhoBTB2 is a substrate of the mammalian Cul3 ubiquitin ligase complex." Genes Dev **18**(8): 856-61.

Wilkinson, K. D. (1999). "Ubiquitin-dependent signaling: the role of ubiquitination in the response of cells to their environment." J Nutr **129**(11): 1933-6.

Wilkinson, K. D. (2000). "Ubiquitination and deubiquitination: targeting of proteins for degradation by the proteasome." Semin Cell Dev Biol **11**(3): 141-8.

Williams, S. K., H. J. Spence, R. R. Rodgers, B. W. Ozanne, U. Fitzgerald and S. C. Barnett (2005). "Role of Mayven, a kelch-related protein in oligodendrocyte process formation." J Neurosci Res **81**(5): 622-31.

Xiao, J., S. Gong, Y. Zhao and M. S. LeDoux (2004). "Developmental expression of rat torsinA transcript and protein." Brain Res Dev Brain Res **152**(1): 47-60.

Xie, Z. and D. J. Klionsky (2007). "Autophagosome formation: core machinery and adaptations." Nat Cell Biol **9**(10): 1102-9.

Xu, L., Y. Wei, J. Reboul, P. Vaglio, T. H. Shin, M. Vidal, S. J. Elledge and J. W. Harper (2003). "BTB proteins are substrate-specific adaptors in an SCF-like modular ubiquitin ligase containing CUL-3." Nature **425**(6955): 316-21.

Yang, Y., E. Allen, J. Ding and W. Wang (2007). "Giant axonal neuropathy." Cell Mol Life Sci **64**(5): 601-9.

Yang, Y. P., Z. Q. Liang, Z. L. Gu and Z. H. Qin (2005). "Molecular mechanism and regulation of autophagy." Acta Pharmacol Sin **26**(12): 1421-34.

Yorimitsu, T. and D. J. Klionsky (2005). "Autophagy: molecular machinery for self-eating." Cell Death Differ **12 Suppl 2**: 1542-52.

Yorimitsu, T. and D. J. Klionsky (2007). "Eating the endoplasmic reticulum: quality control by autophagy." Trends Cell Biol **17**(6): 279-85.

Yorimitsu, T. and D. J. Klionsky (2007). "Endoplasmic reticulum stress: a new pathway to induce autophagy." Autophagy **3**(2): 160-2.

Zhang, K. and R. J. Kaufman (2004). "Signaling the unfolded protein response from the endoplasmic reticulum." J Biol Chem **279**(25): 25935-8.

Zhao, Y., M. DeCuypere and M. S. LeDoux (2008). "Abnormal motor function and dopamine neurotransmission in DYT1 DeltaGAG transgenic mice." Exp Neurol **210**(2): 719-30.

Zhu, L., J. O. Wrabl, A. P. Hayashi, L. S. Rose and P. J. Thomas (2008). "The Torsin-family AAA+ Protein OOC-5 Contains a Critical Disulfide Adjacent to Sensor-II that Couples Redox State to Nucleotide Binding." Mol Biol Cell.

Zimprich, A., M. Grabowski, F. Asmus, M. Naumann, D. Berg, M. Bertram, K. Scheidtmann, P. Kern, J. Winkelmann, B. Muller-Myhsok, L. Riedel, M. Bauer, T. Muller, M. Castro, T. Meitinger, T. M. Strom and T. Gasser (2001). "Mutations in the gene encoding epsilon-sarcoglycan cause myoclonus-dystonia syndrome." Nat Genet **29**(1): 66-9.